



FACULTY OF GRADUATE STUDIES

Kinase Inhibitors as Potential Drugs: A Molecular Dynamics Simulation Study

This thesis is submitted in partial fulfillment of the requirements for the
Master's Degree in

Applied Chemistry from the Faculty of Graduate Studies at Birzeit
University, Palestine

Iman Hammad

Supervisor: Dr. Mazen Hamed

2017

Kinase Inhibitors as Potential Drugs: A Molecular Dynamics Simulation Study

By Iman Esam Hammad

Accepted by the Faculty of Graduate studies, Birzeit University, in partial fulfillment of the requirements of the degree of Master of Applied Chemistry

Committee Members

Signature

Mazen Hamed, Ph. D (Principal Advisor)

.....

Wael Karain, Ph. D (Member)

.....

Abdallah Sayyed-Ahmad, Ph. D (Member)

.....

ACKNOWLEDGEMENTS

I would like to extend my sincere appreciation to my supervisor Dr. Mazen Hamed for his support, guidance and motivation throughout the project. I would also like to express my gratitude to my family and husband for providing me with veracious support and continuous motivation throughout this project and my years of study.

TABLE OF CONTENTS

ACKNOWLEDGMENTS	I
TABLE OF CONTENTS	II
ABSTRACT	IV
LIST OF FIGURES	VI
LIST OF TABLES	XI
ملخص	XII
1.INTRODUCTION.....	1
1.1 Computer aided drug design.....	2
1.2 Protein Kinases.....	5
1.3 Role of the kinase enzymes in cancer	5
1.4 3-Phosphoinositide dependent kinase-1 (PDK-1).....	7
1.5 Identification of residues in the ATP pocket	10
1.6 Inhibition of PDK-1 Kinase enzyme.....	13
1.7 Known potent drugs for cancer diseases.....	15
1.8 Classification of inhibitors.....	20
1.9 Drug design and drug properties.....	21
1.10 Computational approach for binding free energy calculation using MM- GBSA (or MM-PBSA).....	23
1.10.1 Binding free energy of ligand-protein complex using MM-GBSA.....	23
2. Computational methods	28
2.1 Protein- Inhibitor structures.....	28
2.2 Equilibration of the solvated system.....	29
2.3 Production step of the solvated system.....	31
2.4 Calculating the binding free energy of the protein-inhibitor complex.....	31
2.5 Calculating the entropic contribution.....	31

3. Results and discussion.....	32
3.1 Analysis of simulations.....	32
3.2 Study of binding energies of kinase – inhibitors.....	37
3.2.1 Binding free energies of protein-inhibitor complexes: MM-PBSA versus MM-GBSA	37
3.3 Analysis of binding mode of inhibitor (1)-PDK-1 complex.....	42
3.4 Analysis of binding mode of inhibitor (2)-PDK-1 complex.....	45
3.5 Analysis of binding mode of inhibitor (3)-PDK-1 complex.....	51
3.6 Analysis of binding mode of inhibitor (4)-PDK-1 complex.....	56
3.7 Analysis of binding mode of inhibitor (5)-PDK-1 complex.....	64
3.8 Effect of thermodynamic parameters on the protein-inhibitor complexes.....	74
3.9 Correlation between IC ₅₀ and binding free energy.....	78
3.10 Energies calculated by MM-GBSA and contributing energies	81
3.11 Classification of inhibitors studied	84
3.12 Analysis of the inhibitors according to Lipinski’s Rule of five, Veber Rule and MDDR Rule.....	85
3.13 Potency and selectivity of Inhibitor (5).....	90
4. Conclusion	91
References.....	94
APPENDICES	100
Appendix A: SEP non-standard residue and inhibitor files.....	100
Appendix B: Input files for simulation.....	103
Appendix C: Output files.....	114

ABSTRACT

Molecular dynamics simulation and binding free energy (ΔG_{bind}) calculations were done to inspect the interaction between five inhibitors and PDK-1 kinase. The free energy (ΔG_{bind}) values were computed using MM-GBSA and MM-PBSA free energy calculation methods.

The entropic contribution of the binding free energy ΔS was computed using normal mode (NMODE) method. The change of enthalpy (ΔH) was calculated using the equation $\Delta G = \Delta H - T \cdot \Delta S$.

There is a noticeable difference in the values of ΔG depending on the calculation method whether MM-PBSA or MM-GBSA, and this is due to the calculation different approach in each case.

PDK-1 kinase is a well validated anticancer target. The results gave the binding modes between PDK-1 kinase and the five inhibitors, which can be used in the future in the drug design processes for cancer treatment. The placement of water molecules in the binding sites are known. This can be used to design better inhibitors through adding substituents to the inhibitor to replace a water molecule that binds kinase in the active site based on the creation of an inhibitor that includes a structural water mimic.

Through Molecular dynamics simulation, we identify potency PDK-1 inhibitor (5) that have unique binding to the inactive kinase conformation (DFG-out). On the other hand, inhibitors (1-4) are consider as classical ATP-competitive kinase inhibitors (Type I) which are bind to the active conformation DFG-in.

It was reported that **type I kinase inhibitors** form water-mediated hydrogen bond networks (both water molecules W1 and W2 are commonly observed) and the ligand does not extend to the water-filled cavity. These two features distinguish type I from type II inhibitors and these two features were obvious in our study in the binding modes of inhibitors (1-4) with the PDK-1 kinase.

LIST OF FIGURES

Figure 1.1: Structure of PDK-1 kinase domain with ATP molecule. The C-terminal lobe (in blue), the C-helix in green, the N-terminal lobe (in green), and the pSer241 in the T-loop (in purple/red spheres).....	8
Figure 1.2: PIF-binding pocket of PDK-1 kinase.....	9
Figure 1.3: ATP binding pocket region: phosphate region (in magenta); sugar region (in green); Adenine region (in cyan); buried region (in violet) and solvent accessible region in (yellow).....	11
Figure 1.4: Context of target cells determined target specificities of inhibitors.....	15
Figure 1.5: Example on potent inhibitors of PDK-1: BX-795, BX-912 and BX-320, respectively.....	16
Figure 1.6: Structure of BX-320 bound to the ATP binding pocket of PDK-1.....	16
Figure 1.7: The five PDK-1 inhibitors that used in this investigation.....	19
Figure 1.8: Thermodynamic cycles for binding affinity calculations for a complex solvated systems (in blue boxes), whereas systems in the gas phase in (white boxes)...	24
Figure 3.1: Density of protein-inhibitor (1) complex system during equilibration.....	32
Figure 3.2: Temperature of protein-inhibitor (1) complex system during equilibration.....	33
Figure 3.3: Pressure of protein-inhibitor (1) complex system during equilibration.....	34
Figure 3.4: Total, kinetic and potential energy of protein-inhibitor (1) complex system during equilibration runs. The kientic energy (in red line); the potential energy (in black line); the total energy (in green line) which is the sum of kinteic and potential energy.....	35

Figure 3.5: RMSD of protein backbone during unrestrained equilibration run of protein-inhibitor (1) complex	36
Figure 3.6: Correlation between ΔG calculated by MM-GBSA and ΔG experimental values.....	37
Figure 3.7: Correlation between ΔG calculated by MM-PBSA and ΔG experimental Values.....	38
Figure 3.8: (a) Graphical representation of inhibitor (1), (b) inhibitor (1)-PDK-1 complex and (c) other weak interactions between inhibitor (1) and kinase.....	43
Figure 3.9: (a) Graphical representation of inhibitor (2), (b) inhibitor (2)-PDK-1 complex and (c) other weak interactions between inhibitor (2) and kinase.....	47
Figure 3.10: (a) Graphical representation of inhibitor (3), (b) inhibitor (3)-PDK-1 complex and (c) other weak interactions between inhibitor (3) and kinase.....	53
Figure 3.11:(a) Graphical representation of inhibitor (4), (b) inhibitor (4)-PDK-1 complex and (c) other weak interactions between inhibitor (4) and kinase.....	57
Figure 3.12: The distribution of hydrogen bond lengths for 180 ATP-binding site ligand-W1 hydrogen bonds.....	58
Figure 3.13: Example of inhibitor that includes a structural water mimic in the active site of HIV-1.....	63
Figure 3.14: (a) Graphical representation of inhibitor (5), (b) inhibitor (5)-PDK-1 complex and (c) other weak interactions between inhibitor (5) and kinase.....	66
Figure 3.15: The PIF pocket regions of active PDK-1 kinase (PDB ID: 3HRF, grey) and inactive PDK-1 kinase (PDB ID: 3NAX, orange).....	73

Figure 3.16: Relationship between the difference of Gibbs free energy (ΔG) and the entropic contribution ($T\Delta S$).....	74
Figure 3.17: Relationship between the difference of Gibbs free energy (ΔG) and the difference of enthalpy (ΔH).....	75
Figure 3.18: Correlation between the IC_{50} values and binding free energies that calculated by MM-GBSA.....	79
Figure 3.19: Correlation between the IC_{50} values and binding free energies that calculated by MM-PBSA.....	80
Figure 3.20: Correlation between the IC_{50} values and the experimental binding free energies.....	80
Figure 3.21: Contributions of electrostatic energy and van der Waals energies to the difference of Gibbs free energy (ΔG) of different inhibitor-PDK-1 kinase complexes.....	81
Figure 3.22: Relationship between the difference of Gibbs free energy (ΔG) and the Van der Waals energy.....	83
Figure 3.23: Relationship between the difference of Gibbs free energy (ΔG) and the electrostatic energy.....	83
Figure 3.24: Analysis of the inhibitors according to Lipinski's Rule of five, Veber and MDDR Rules.....	86
Figure 3.25: Relationship between the difference of Gibbs free energy (ΔG) calculated by MM-GBSA and the molecular weight.....	88

Figure 3.26: Relationship between the difference of Gibbs free energy (ΔG) calculated by MM-GBSA and log P.....89

Figure 3.27: Relationship between the difference of Gibbs free energy (ΔG) calculated by MM-GBSA and PSA.....89

LIST OF TABLES

Table 1.1: Molecular docking analysis of Myricetin.....	18
Table 3.1: Binding free energies (kcal/0mol) calculated at T= 300 K and P= 1 atm for PDK-1 binding with the five inhibitors	39
Table 3.2: Hydrogen bond analysis of inhibitor (1) in 62O-PDK-1complex.....	44
Table 3.3: Hydrogen bond analysis of inhibitor (2) in 63L-PDK-1complex.....	48
Table 3.4: Hydrogen bond analysis of inhibitor (3) in MOL-PDK-1complex.....	54
Table 3.5: Hydrogen bond analysis of inhibitor (4) in 61Y-PDK-1complex.....	59
Table 3.6: Hydrogen bond analysis of inhibitor (5) in MOL-PDK-1complex.....	67
Table 3.7: Thermodynamic parameters of the five protein-inhibitor complexes that calculated at T= 300 K and P= 1 atm	77
Table 3.8: Total binding free energy (ΔG_{total}), van der Waals energy (VDW), electrostatic energy (ELE), solvation free energy (ΔG_{sol}), and binding affinity of inhibitor-protein complex (ΔG_{bind}) that calculated by MM-GBSA. All energies are in unit kcal/mol.....	82
Table 3.9: Analysis of the inhibitors according to Lipinski's Rule of five, Veber and MDDR Rules.....	87

ملخص

في هذه الدراسة قمنا باستخدام التمثيل الجزيئي من أجل حساب قيم طاقة الربط لخمس مثبطات لانزيم الكاينيز PDK

1- باستخدام الطريقتين (Molecular Mechanics/Generlized-Born surface area)

(Molecular Mechanics/Poisson Boltzmann surface area) . وتم حساب قيم مساهمة الفوضى $T.\Delta S$ باستخدام

طريقة (Nmode) وتم حساب التغير في الطاقة $H\Delta$ باستخدام هذه المعادلة $\Delta G = \Delta H - T.\Delta S$.

هناك فرق ملحوظ في قيم التغير في طاقة الربط اعتمادا على طريقة الحساب سواء باستخدام (MM-PBSA or MM-GBSA)

بحيث كانت نتائج MM-GBSA افضل من نتائج MM-PBSA وهذا يرجع الي الاختلاف في طريقة الحساب التي يتم اعتمادها من قبل

.MM-PBSA and MM-GBSA

كذلك وضحت نتائج هذه الدراسة كيفية ارتباط هذه المثبطات بانزيم الكاينيز PDK-1 والتي يمكن استخدامها لعلاج السرطان.

بحيث أن موقع جزيئات الماء كانت موجودة في مواقع الربط ويمكن استخدام هذه النتائج في تصميم مثبطات أفضل من خلال إضافة

ذرات مثل الأوكسجين والهيدروجين للمثبط لكي يكون قادرا على تكوين روابط هيدروجينية لكي يحل مكان جزيئات الماء التي كانت

موجودة في مواقع الربط من خلال الاستناد على مبدأ تكوين مثبطات جديدة محاكية لجزيئات الماء.

من خلال محاكاة الديناميات الجزيئية قمنا بتحديد مثبط (المركب 5) والذي يرتبط بشكل فريد بأنزيم الكاينيز PDK-1 لتكوين

كاينيز غير نشيط على نقيض المركبات الأخرى (4-1) والتي يتم اعتبارها مثبطات كاينيز كلاسيكية منافسة ل ATP . ومن الجدير بالذكر

ان المثبط (المركب 5) هو دواء فعال وذلك بسبب قيمة طاقة الربط الكبيرة $\Delta G = -52.3 \text{ Kcal/mol}$, هذه القيمة الكبيرة ناتجة من

تكوين خمس روابط هيدروجينية قوية بين هذا المثبط وأنزيم الكاينيز PDK-1.

وفقا لما ذكرته التقارير فان النوع الأول من مثبطات الكاينيز (مثبطات كلاسيكية منافسة ل ATP) تتميز عن النوع الثاني من المثبطات من خلال تشكيل شبكات من الروابط الهيدروجينية بواسطة جزيئين من الماء وهذا يتوافق مع نتائج هذه الدراسة بحيث انه تم ملاحظة هذه الميزة في المثبطات (المركب4) و (المركب 3).

Chapter 1

1. INTRODUCTION

In this work, structure-based drug design that employs molecular dynamics, binding free energy calculations is used to investigate anti-cancer inhibitors of 3-phosphoinositide dependent kinase-1 (PDK-1)¹. This computational drug design approach has been successfully applied to both lead optimization and hit identification against PDK-1¹.

Fast expansion in this area has been made possible by advances in software and hardware computational power and sophistication, identification of molecular targets, and an increasing database of publicly available target protein structures. CADD is being utilized to identify hits (active drug candidates), select leads (most likely candidates for further evaluation), and optimize leads i.e. transform biologically active compounds into suitable drugs by improving their physicochemical, pharmaceutical, ADMET/PK (pharmacokinetic) properties.²

The purpose of usages of computational tools as we hope to improve effectiveness and efficiency of drug discovery and development process, decrease use of animals, and increase predictability.²

1.1 Computer-aided drug design

A general strategy for drug discovery efforts can be summarized by the following steps: Identifying a target, screening for inhibitors, isolating hits, optimization and selection of a candidate molecule for clinical studies¹. Drug discovery is a very long and expensive process in which twelve to twenty-four years are needed to discover and develop a new drug. In addition, the average cost to develop a new drug into markets is more than \$1 billion¹.

Historically, Paul Ehrlich³ was the first person to postulate on the existence of chemoreceptors that can be exploited therapeutically. It was reported that initial stages in chemotherapy was focused on the isolation and purification of active ingredients from natural products such as plants. This was followed by rational approach which was based on understanding the mechanisms of action and the drug-receptor interactions³. Despite using the newer approach, it was reported that only 18 new chemical entities (NCE) were approved in the year 2005 and 2006⁴. For this reason, a newer approach was developed to increase the efficiency of drug discovery process.

Computer-aided drug design (CADD) is an example on the newer approaches that is using computer based techniques to analyze molecules and molecular systems to predict their biological properties.⁵ This approach helps in the identification and optimization of new potential drugs⁵. Computational drug design has played an

important role in the successful development of marketed drugs such as saquinavir, ritonavir, and indinavir were utilized in the treatment of human immunodeficiency virus (HIV)⁶.

There are two broad strategies in computational drug design:⁵

1. Using Ligands for drug design
2. Receptor-based drug design Related to structure

The first strategy is a ligand-based drug design (LBDD) that is usually applied if a number of biologically active compounds are characterized and the target 3D structure is unknown⁵. By analyzing the physico-chemical properties of these active molecules, LBDD aims at predicting new chemical structures that are likely to have better biological properties⁶. There are many methods that use active known molecules to predict new ligands including Quantitative structure-activity relationship, Pharmacophore modeling and shape-based screening methods⁷. For example, Quantitative structure-activity relationship (QSAR) method is based on the regression analysis of relationship between biological activity of set of homologous compounds and their various physico-chemical descriptors such as hydrophobic properties, electrostatic properties, steric factors, donor-acceptor⁵.

Another example is the Pharmacophore modeling which based on accounting for direct protein–ligand binding, and ignores other interactions outside the pharmacophore region⁷. A Pharmacophore is defined as the three-dimensional representation of active chemical features of active compounds⁷.

The second strategy is Structure-based drug design methods are usually used when the X-ray crystal/NMR structure of the target protein is available⁵. The core strategy of this approach is based on analyzing the active ligand interaction with the binding site on the target protein. This means that ligands that exhibit similar interactions to the active ones will have similar biological effects⁶.

Ligand Docking and de novo drug design are two examples on the SBDD methods. Docking methods require the structure of the target protein to estimate the binding energy of a number of ligands and rank them according to their estimated binding free energies. In comparison, De novo drug design require the structure of the active site as starting point⁵.

1.2 Protein Kinases

There are more than 500 protein kinases known in the human genome. They are the second largest group of currently investigated drug targets^{8,9}. Protein kinases main biological function is to catalyze the transfer of phosphoryl group of ATP to a hydroxyl group of threonine, tyrosine or serine residues¹⁰. Signal-transduction

pathways are activated by the phosphorylation of certain proteins which are responsible for the transition of cellular signals throughout the cells and to the nucleus¹⁰.

The deregulation of phosphorylation reaction due to mutations in kinase genes are known to cause 218 diseases. For this reason, protein kinases are considered as an important therapeutic target in different diseases and viral infections. Therefore, the protein kinases are considered as important effectors in human pathology¹⁰ and thereby a highly attractive therapeutic target in drug discovery⁹.

1.3 Role of the kinase enzymes in cancer

It was reported that abnormality in protein kinases can lead to the development of several reported disorders and major diseases such as, endocrine disorders, cardiovascular disease are due to malfunction of phosphorylation process¹¹.

There are 500 genes that encode kinases are involved in cancer, while other oncogenes activate kinases or are phosphorylated by other kinases. This what makes kinases as potential targets for drug development¹¹.

There are three specific sites in protein kinase that are involved in phosphorylation: an ATP binding site, a domain catalyzing the transfer of phosphoryl group from ATP (phosphate pocket) and a substrate- binding site (PIF-pocket).¹²

Perturbed signal transduction provokes deregulation of different processes in cell migration, which can lead to malignant phenotype. 50% or more of receptor tyrosine kinase (RTK) and several serine/threonine kinases have been perturbed in different human malignancies. Irregular activity of a protein kinase which occur by genomic rearrangements result in hybrid proteins with catalytic domains of a protein kinase and another unrelated protein.¹² A second mechanism that damages the normal function of protein kinases is the mutations responsible for kinase constitutive activity. The third mechanism is explained by increasing expression of protein kinases. Finally, deregulation of kinase activity by activation of oncogenes can also contribute to tumorigenesis.

The chemotherapy treatment of breast cancer by using cyclophosphamide causes weight gain, ovarian failure, cardiac toxicity and Probability of developing a second cancers¹³. Studies estimated that in 2050 the global cancer will increase to 27million new cases¹⁴. Therefore, there are urgent need to discover a potent and selective cancer drug with no side effects.

1.4 3-Phosphoinositide dependent kinase-1 (PDK-1)

PDK-1 is a 556 amino acids serine/threonine kinase that belongs to the AGC protein kinase family. It plays an important role in the phosphorylation and activation of a number of proteins such as protein kinase B (PKB), protein kinase

C isoforms, the p70 ribosomal S6 kinase and serum and glucocorticoid-induced kinase¹⁵.

Structure of PDK-1 is consisting of two lobes: C-terminal lobe and N-terminal lobe and is similar in overall structure to PKA¹⁶. C-terminal pleckstrin homology domain (PH) is essential for interaction of PDK-1 with the cell membrane because it binds with phosphoinositide lipids of the plasma membrane¹⁵.

PDK-1 residues Val124, Val127 on the α -helix, Lys115, Ile119, Ile118 on the B-helix, and Leu155 on B-sheet form a hydrophobic pocket (PIF) pocket (Fig 1.1)¹⁶. Since Leu155 is presented at the center of this pocket, whereas the other residues form a lining of the inside wall of the pocket¹⁷.

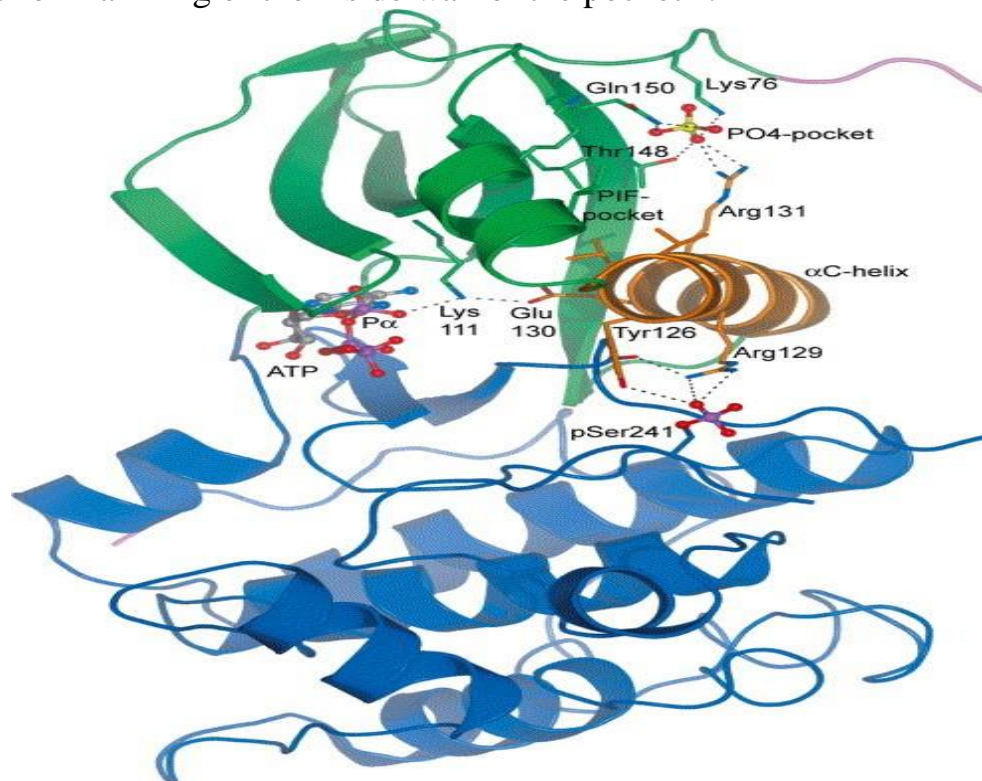


Figure 1.1: Structure of PDK-1 kinase domain with ATP molecule. The C-terminal lobe (in blue), the C-helix in green, the N-terminal lobe (in green), and the pSer241 in the T-loop (in purple/red spheres)¹⁶

S6K1 substrate interacts with the PIF-pocket of PDK-1 with higher affinity when it is phosphorylated at its hydrophobic motif. This indicated that the phosphate-binding site may be located close to the PIF-pocket.¹⁷

It was reported that the mutation of Leu155 to Glu canceled the ability of PDK-1 to interact with a peptide (PIFtide) substrates such as PRK2, S6K1 and SGK1.¹⁷ Whereas mutation of Ile119, Lys115, Leu155, and Glu150 to Ala decreased the affinity of PDK-1 to PIFtide binding substrates but did not abolish the ability of PDK-1 for phosphorylation and activation of PIFtide substrates such as S6K1 and SGK1.¹⁷

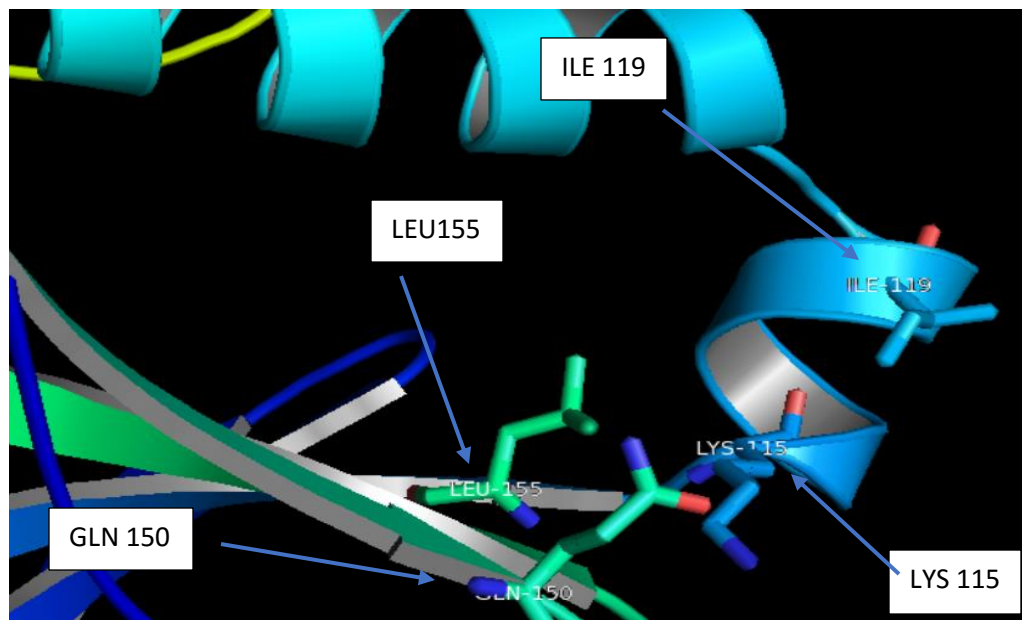


Figure 1.2: PIF-binding pocket of PDK-1 kinase

Phosphate-docking site is another small pocket lined with basic residues. This pocket is located in close vicinity to the PIF pocket (Fig 1.2). In the crystal structure

shown in figure 1.1, this pocket was occupied by a sulfate-anion that interacts with four residues lining the phosphate pocket, namely Gln150, Arg131, Lys76, and Thr148.^{16,17}

The α C-helix (residues 129–131) is an important element in the core of PDK-1 structure formed from residues 124–136. It links both the N-terminal lobe and the C-terminal lobe with the active site as well as the phosphopeptide pocket with the phosphoserine in the T-loop. In particular, Val127 and Val124 are involved in formation of the hydrophobic pocket (PIF-pocket).

Arg129 and Arg131 form two hydrogen bonds with the phosphorylated Ser241 and sulfate in the phosphate pocket, respectively (Fig. 1.1). In addition, each of Glu130 and Lys111 forms a hydrogen bond with the phosphate of bound ATP that are crucial for kinase activation. Finally, Tyr126 forms a hydrogen bond with the phosphorylated Ser241.¹⁶

1.5 Identification of residues in the ATP pocket

The ATP binding pocket as described in Figure 1.3 consists of multiple regions¹⁸ as described below:

- 1) The Adenine region which is a conserved hydrophobic region. It is made up of residues at positions P2 (residue 88), P10 (residue 96), P13 (residue 109), P17 (residue142), P35 (residue 212). The adenine ring of ATP makes hydrophobic contacts with these five residues. In addition, it makes two hydrogen bonds with the

backbone of the hinge region residues (P20-P27). A third hydrogen bond occurs between two C-H groups of pyrimidene ring with the carbonyl group of P23. The adenine-binding region is not characterized by large variability of amino acids, as a result of this it is not a good site for high degree of specificity.¹⁸

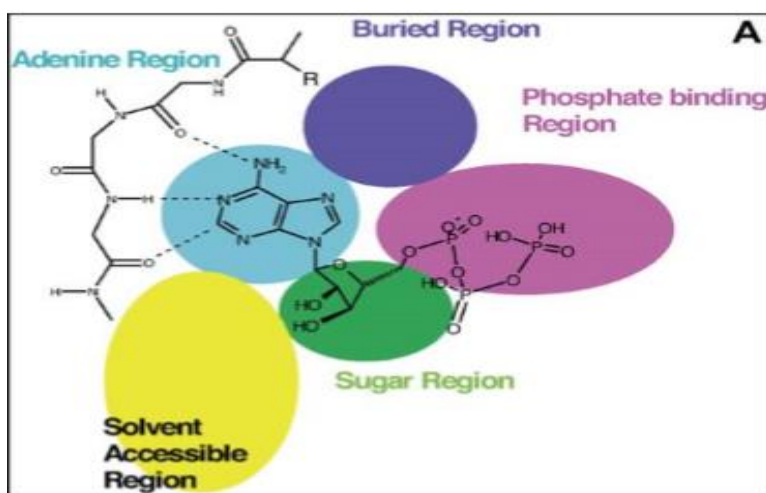


Figure 1.3: ATP binding pocket region: phosphate region (in magenta); sugar region (in green); Adenine region (in cyan); buried region (in violet) and solvent accessible region in (yellow)¹⁸

and P27 (residue 164).¹⁸ In 80.7% of protein kinases P27 residue is a serine, a glutamate, an aspartate or glutamine. The variability in P27 allows for the development of selective and potent inhibitors as demonstrated in the EGFR family of kinases where a unique cysteine placed in P27 position.¹⁸

3) Phosphate region which contains many highly polar residues and it consists of two parts: (a) glycine-rich loop (GXGXXGXV: P3 -P10) lies on the N-terminal lobe. It is the only one that shows significant conformational flexibility.¹⁸

(b) alpha-helix which consists an essential and conserved residues: which is made up of residues at position P14 (residue 111), P15 (residue 129), P33 (residue 209), P37 (residue 223) and P38 (residue 225).¹ P15 (residue 129) with three-dimensional location that makes an essential indicator of the active state of any kinase. P37 (residue 223) and P38 (residue 225) are conserved in all protein kinases and these are essential for the transfer of phosphate group from ATP to the substrate. This part gives an indication whether the kinases are in their active or inactive conformations.¹⁸

4) Buried region: the largest sequence diversity in the ATP pocket residues are found in this region, this region is not occupied by ATP, which is made up of residues at position P16 (residue 133), P17(residue 142), P18 (residue 144), P19 (residue 156), P20 (residue 158), P36 (residue 222).¹⁸ The residue in position P20 is important in determining the size of this specific region in the ATP binding pocket. P20 is often a bulky amino acid (40% methionine, 15% phenylalanine). It acts as a “molecular gate” to the buried ATP binding region. The introduction of a group to the buried region increases potency and, increases selectivity compared to that of kinases when this region is smaller.¹⁸

5) Solvent accessible regions: this region is important in exploited to increasing the binding affinity and to modulate ADME (toxicity) properties of ligands. The major difference in shape of solvent accessible area is contributed to the presence or

absence of glycine residue in position P26. Often the NH of glycine forms intramolecular hydrogen bond with the carbonyl of P23 residue.¹⁸

1.6 Inhibition of PDK-1 Kinase enzyme

It was reported that overexpression of PDK-1 resulted in vitro and the PDK-1 phosphorylation was reported to suffer a high elevated levels in vivo breast cancers.¹⁹ This explained that there are a strong relationship between PDK-1 and malignant phenotype.

The main strategy of developing kinase inhibitors is to reduce ATP binding and/ or inhibit kinase activity¹². ATP and PDK-1 inhibitors compete in binding to the PDK-1 active site. When the PDK-1 inhibitors bind to PDK-1 active site they act to stop the transmission of phosphoryl group from ATP to different amino acids. As a result, PDK-1 signal transduction is blocked. Development of PDK-1 inhibitors could lead to development of better treatment options for cancer.

specificity would not be a challenge if the target protein has unique catalytic functions and active site structures.²⁰ All 500 protein kinases encoded in the human genome have similar ATP-binding site structure.²¹ In the last decade, more than 50 patents of PDK-1 inhibitors were published in which the ATP-pocket within the kinase domain was the target.²²

Therefore, it is easy to establish the reason of kinase inhibitors being very specific and why the off-target effects are inevitable.²⁰ Nonetheless, Off-target effects are sometimes advantageous in clinical drugs. For example, Gleevec (Imatinib) was developed for treatment of chronic leukemia as an oral inhibitor of BCR-Abl. Currently, it has been approved for treatment of gastrointestinal stromal tumor (GIST).²⁰ This work demonstrates that the context of cells determine specificities of chemical inhibitors in vivo conditions.

Figure 1.4 shows that the specificities of inhibitors depend on cellular context. For example, in vitro standardized conditions were employed for enzyme-substrate and ATP concentrations, in addition to ‘standard temperature and pressure’ in physical chemistry. These conditions do not reflect the situation in living cells.²⁰ This reflect the facts that even we discovered the excellent drug in vitro condition, it may be not become an excellent one in vivo condition.

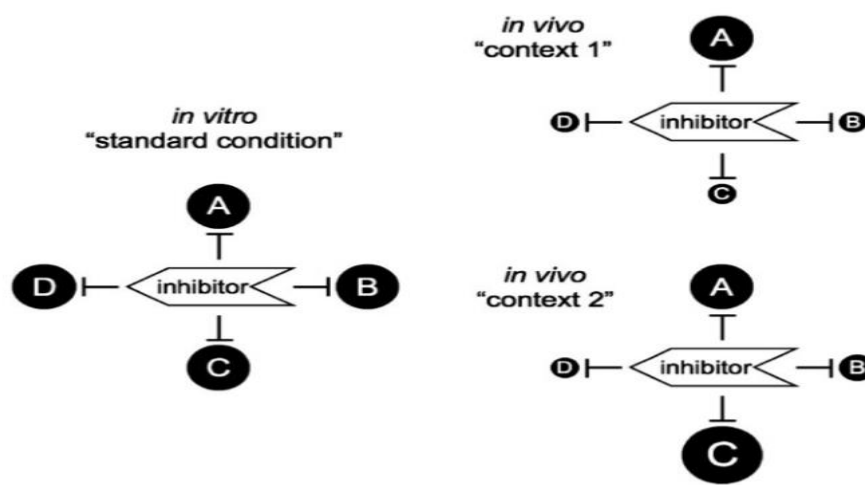


Figure 1.4: Context of target cells determined target specificities of inhibitors²⁰

1.7 Known potent drugs for cancer diseases

BX-320, BX-795 and BX-912 (Figure 1.5) are considered as potent and selective competitive inhibitors of PDK-1 enzyme activity with respect to its substrate (ATP). BX-320 which inhibit the PDK-1 signaling pathway in different cancer cell lines including MDA-453 (breast), U87-MG (glioblastoma), PC-3 (prostate), HCT-116 (colon), MiaPaCa (pancreatic) and LOX (melanoma) cells. BX-795 and BX-912 potently inhibited the growth of PC-3, U87-MG and MDA-453 cancer cell lines only.²³

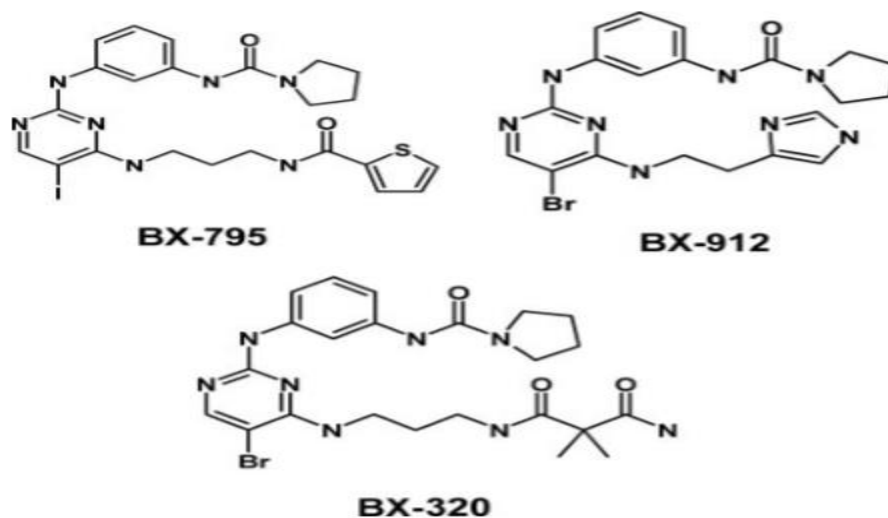


Figure 1.5: Example on potent inhibitors of PDK-1: BX-795, BX-912 and BX-320, respectively²³

The high potency and selectivity of BX-320 is due to the formation of two hydrogen bonds between two nitrogens of amino-pyrimidine group with Ala162, which lies in the hinge region of the PDK-1 (Figure 1.6) .²³

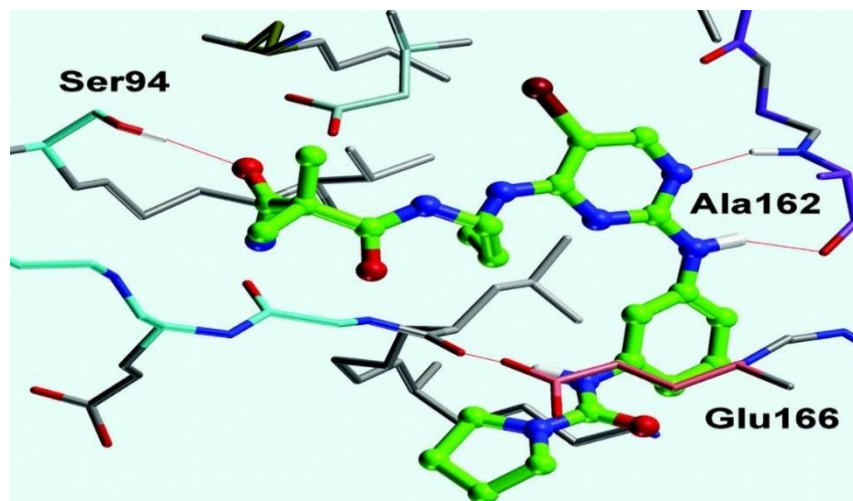
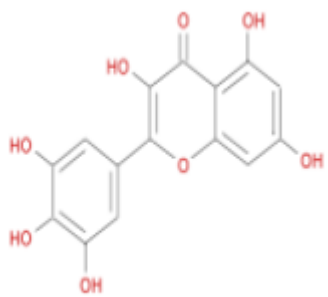


Figure 1.6: Structure of BX-320 bound to the ATP binding pocket of PDK-1²³

Singh et al²⁴ reported using molecular docking that myricetin (3,5,7-Trihydroxy-2-(3,4,5-trihydroxyphenyl)-4-chromenone) acts as a probable anti-cancer agent. Myricetin is naturally occurring flavanol and it is a polyphenolic compound.²⁴

Myricetin is considered as a potent PDK-1 inhibitor because of: (1) negative Docking energy of Myricetin-PDK-1 complex (-41 Kcal/mol), which indicates a favorable binding of Myricetin at the binding site of the PDK-1 kinase. (2) Formation of the most essential type of interaction between PDK-1 receptor and myricetin molecule (hydrogen bonding). The residues involved in formation of hydrogen bonds were Thr 222, Ala 162, Lys111, Asp 223, Ser 160, and Glu 130. Ala 162 and Ser 160 among these amino acid residues lie in the Hinge of PDK-1 protein. This type of interaction confirms that Myricetin fits into the active pocket of PDK-1receptor tightly (Table 1.1).²

Table 1.1: Molecular docking analysis of Myricetin²⁴

Myricetin	Docking energy (Kcal/mol)	Hydrogen bonding residues	Hydrogen bond distances (Å)
	-41	O5: H-Lys ¹¹¹	2.44
		O5: H-Lys ¹¹¹	2.19
		O8: H-Ala ¹⁶²	2.34
		H28: O-Glu ¹³⁰	2.31
		H30: O-Asp ²²³	2.09
		H23: O-Ser ¹⁶²	2.14
		H33: O-Ser ¹⁶²	1.98

Ong et al²⁵ reported that Myricetin possesses both antioxidant properties and prooxidant properties, it also has a therapeutic potential in cancer treatment, cardiovascular diseases and diabetes mellitus. Benzo(a)-pyrenes cause cancer of the skin and lungs. Myricetin reduces the risk of skin cancer caused by polycyclic aromatic hydrocarbons.²⁵ Polycyclic aromatic hydrocarbons when metabolized produce carcinogenic metabolites.²⁵ Myricetin was found to inhibit the hydroxylation of benzo(a)pyrene in the human liver microsomes.²⁵

Virtual screening, NMR-based fragment screening, and ultrahigh throughput screening (UHTS) led to the identification of diverse chemicals as PDK-1 inhibitors which bind the PDK-1 kinase in the ATP-site with at least one H-bond towards the

hinge region. The first four inhibitors that are used in this investigation were identified using a combined screening method (HTS and virtual screening).²²

The inhibitors studied in this work are 6-methoxy-2-(1H-pyrazol-5-yl)-1H-benzimidazole (inhibitor 1), 4-dicarboxylic acid diamide (inhibitor 2), 4-butyl-6-(1H-pyrrolo[2,3-b]pyridin-3-yl)pyrimidin-2-amine (inhibitor 3), 4-ethyl-6-[5-(1H-pyrazol-4-yl)-1H-pyrrolo[2,3-b]pyridin-3-yl]pyrimidin-2-amine (inhibitor 4)²² and 1-(3,4-difluorobenzyl)-2-oxo-N-((1R)-2-[(2-oxo-2,3-dihydro-1H-benzimidazol-5-yl)oxy]-1-phenylethyl)-1,2-dihydropyridine-3-carboxamide (inhibitor 5) which are shown in figure 1.7.

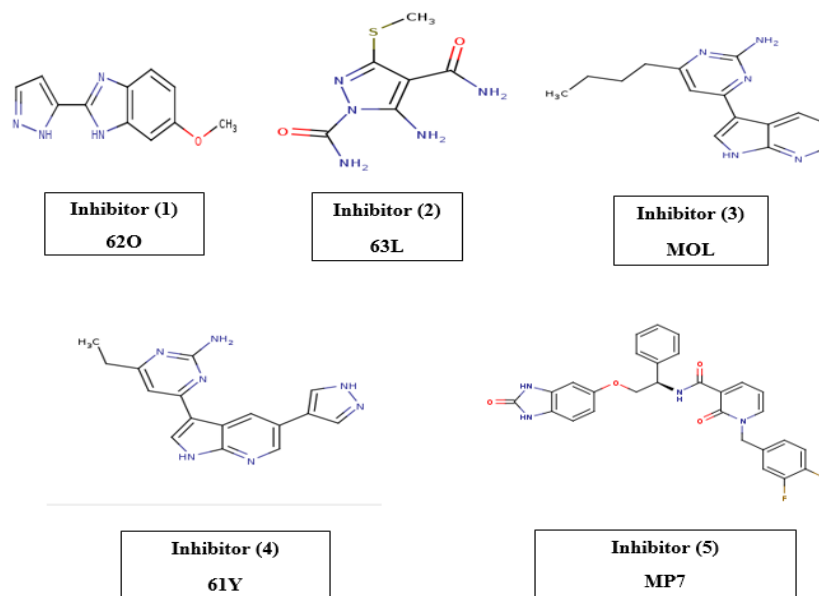


Figure 1.7: The five PDK-1 inhibitors that used in this investigation²²

Inhibitor (5) is an example of pyridinonyl-based PDK-1 inhibitors described by Sunesis and Biogen Idec.²⁶ The concept of these inhibitors is mainly dependent on

the presence of a flexible linker to a hinge binding moiety (HBM) bearing neighboring H bond donor (HD) and H bond acceptor (HA) groups.²⁶

1.8 Classification of inhibitors

Protein kinase inhibitors are classified according to their binding modes as follows:

Type I inhibitors: which are classical ATP-competitive and bind the ATP-binding site when the protein kinase is an activated state. They bind the hinge region with at least one hydrogen bond. FDA recently approved Type I anticancer kinase inhibitors: gefitinib, dasatinib, sunitinib, lapatinib, ruxolitinib, pazopanib, vemurafenib, crizotinib, erlotinib, and bosutinib.²⁷

Type II inhibitors: are also ATP-competitive with binding to the extended ATP-binding site of protein kinase in an inactive state. If a significant change in the protein conformation occurs, it means that the inhibitor belongs to type II. Conformational changes in the protein kinase structure open a new hydrophobic pocket in the back of the protein that is called the *Deep Pocket* (also called the Phe pocket or allosteric pocket). These inhibitors, usually are hydrogen bonded to the hinge region but this is not a requirement for their action.²⁸

Type III inhibitors (Allosteric binders): are ligands that target allosteric binding sites of protein kinase, therefore they are non-ATP-competitive. As

allosteric binding sites are highly specific for a protein kinase, this means a high degree of selectivity can be achieved. A specific feature that characterized this type of inhibitors no hydrogen bond in the hinge region. At present no drug on the market belongs to this type.²⁸ Traxler has developed a pharmacophore model for ATP-competitive inhibitors (type I) that identifies five different regions within the ATP-binding site.²⁸

1.9 Drug design and drug properties

The drug-likeness of oral small molecules were evaluated by several guidelines. Up to 2015, a total of 28 small molecule kinase inhibitors SMKIs are FDA approved for the treatment of human cancer. Lipinski's Rule of Five (ROF) has been used as a rule of thumb to evaluate their absorption, permeability and solubility of drugs. The Veber Rules (Number of rotatable bonds (NRB) ≤ 10 and polar surface area (PSA) $\leq 140 \text{ \AA}^2$) to evaluate oral bioavailability. Analysis of the number of rings (NOR) as included in the MDDR Rule (NOR ≥ 3).²⁹

The physicochemical properties of more than 2,000 drugs and candidate drugs in clinical trials were analyzed by Lipinski: A compound has drug-like properties if it matches the following criteria (The Lipinski rule of five).³⁰

- Its molecular weight (M.W) < 500 .

- The lipophilicity property of compound (logP) which is the logarithm of the partition coefficient between 1-octanol and water³¹ ≤ 5 .
- The number of atoms in the molecule that donate hydrogen atoms to form hydrogen bonds (OH & NH) ≤ 5
- The number of atoms that can accept hydrogen atoms to form hydrogen bonds (O & N) ≤ 10

Poor absorption or permeability is possible when the compound properties not obey the rule of five.³²

Analysis of 28 FDA approved SMKIs revealed that 28 SMKIs were fitted well with ROF (HBD ≤ 5 and HBA ≤ 10) and the molecular weight of 28 SMKIs is in the range 400 to 600. It is worth noting that with the exception of exitinib all inhibitors have at least six HBAs this reflect the fact that nitrogen and oxygen atoms are beneficial for kinase inhibitors. The Veber Rule³³ are abided by all inhibitors except dabrafenib. The analysis of number of rings as included in MDDR Rule³⁴ showed good adherence, NOR was no more than five for all SMKIs.²⁹

1.10 Computational approach for binding free energy calculation using MM-GBSA (or MM-PBSA)

Several computational methods are available for calculating the binding free energy of protein-protein interactions, protein-DNA interactions and ligand-protein

interactions.³⁵ Some methods are more accurate but computationally intensive such as the thermodynamic integration (TI) and the free energy perturbation (FEP) methods.³⁶ On the other hand, less accurate methods such as molecular mechanics/Poisson Boltzmann surface area (MM/PBSA) and molecular mechanics/Generalized Born surface area (MM/GBSA) are less time-consuming methods.³⁷ MM/PBSA and MM/GBSA methods are end point methods because they calculate the binding affinity through simulations of only two end states (unbound and bound states of a ligand and its protein target).³⁷

1.10.1 Binding free energy of ligand-protein complex using MM-GBSA

In the MM-GBSA formulation, the binding free energy of a ligand to a protein is calculated as the difference between the free energy of protein-ligand complex and the sum of the free energies of protein and ligand separately as follows.³⁸

$$\Delta G^0_{\text{binding, solvated}} = G^0_{\text{complex, solvated}} - [G^0_{\text{receptor, solvated}} + G^0_{\text{ligand, solvated}}] \quad (1.1)$$

From the thermodynamic cycle shown in Figure 1.8. The binding free energy calculated as illustrated in equation (1.2).

$$\Delta G^0_{\text{binding, solvated}} = \Delta G^0_{\text{binding, vacuum}} + \Delta G^0_{\text{solv, complex}} - (\Delta G^0_{\text{solv, receptor}} + \Delta G^0_{\text{solv, ligand}}) \quad (1.2)$$

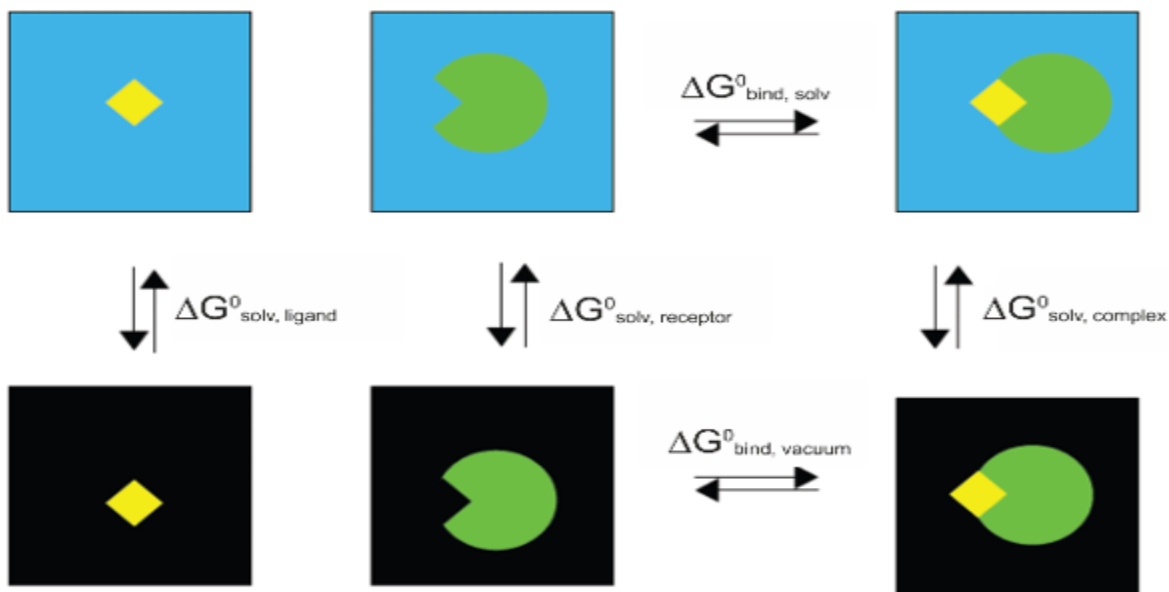


Figure 1.8: Thermodynamic cycles for binding free energy calculations for complex solvated systems (in blue boxes), whereas systems in the gas phase (in white boxes)

In the calculation of the solvation free energy term polar and nonpolar contributions are considered. For the polar contribution, the change in the free energy resulting from transfer of a charged molecule from gas-phase (modeled as a homogeneous medium with dielectric constant=1) to solvent (modeled as a homogeneous medium with=80), equation (1.4) γ and β values are constants dependent on the applied method.^{39,40}

$$\Delta G_{sol}^0 = \Delta G_{polar}^0 + \Delta G^0 \quad (1.3)$$

$$\Delta G_{sol(nonpolar)}^0 = \gamma(SASA) + \beta \quad (1.4)$$

$$\Delta G_{sol(polar)}^0 = G_{electrostatic, \epsilon=80}^0 - G_{electrostatic, \epsilon=1}^0 \quad (1.5)$$

The approximation formula of the electrostatic contribution appears in equation (1.6), but extended Generalized Born model consists of a set of radii (a_i) and charges contributions from Equation 1.7 for each particle.⁴¹

$$\Delta G_{elec} = -\frac{q^2}{2a} \left(1 - \frac{1}{\epsilon}\right) \quad (1.6)$$

$$\Delta G_{elec} = -\left(1 - \frac{1}{\epsilon}\right) \sum_{i=1}^N \sum_{j=i+1}^N \frac{q_i q_j}{r_{ij}} - \frac{1}{2} \left(1 - \frac{1}{\epsilon}\right) \sum_{i=1}^N \frac{q_i^2}{a_i} \quad (1.7)$$

$$\Delta G^0_{bind, vacuum} = \Delta E^0_{MM} - T \cdot \Delta S^0_{Nmode} \quad (1.8)$$

$$E_{MM} = E_{bond} + E_{Angle} + E_{Torsion} + E_{Van\ der\ Waals} + E_{electrostatic} \quad (1.9)$$

Protein -inhibitor average binding energy estimated by in the gas phase by molecular mechanics. Two types of energy are involved: first are non-covalent energies consisting of van der Waals energy and electrostatic energy. The second type are the covalent energies represented by bonds, angles and dihedral energies.³⁹

Another way to calculate binding affinity is by molecular mechanics-Poisson Boltzmann surface area(MM-PBSA). Both MM-GBSA and MM-PBSA use the same previous equations to calculate the binding free energy, but the difference in the calculation of the electrostatic solvation energy G_{sol} (polar contribution).⁴²

$$\Delta G_{sol} = \Delta G_{PB/GB} + \Delta G_{SA} \quad (1.10)$$

Where ΔG_{sol} is the sum of electrostatic solvation energy (polar contribution), $\Delta G_{\text{PB/GB}}$, and the nonelectrostatic solvation component (nonpolar contribution), ΔG_{SA} .⁴² The electrostatic energy (ΔG_{PB}) is calculated by solving the Poisson-Boltzmann numerically. By combining Poisson's equation (1.11) for the electrostatic potential with Boltzmann's equation (1.12) that gives the charge distribution, you end up with the Poisson-Boltzmann equation (1.13).⁴¹

$$\nabla^2 \phi(\mathbf{r}) = -\frac{4\pi\rho(\mathbf{r})}{\epsilon} \quad (1.11)$$

$$n(\mathbf{r}) = Ne^{-\frac{V(\mathbf{r})}{k_bT}} \quad (1.12)$$

$$\Delta G_{\text{sol}} = \frac{1}{2} \sum_i q_i (\phi_i^{\epsilon=80} - \phi_i^{\epsilon=1}) \quad (1.13)$$

Chapter 2

Computational Methods

2.1 Protein- Inhibitor structures

The crystal structure of PDK-1 complex with five inhibitors were taken from the Brookhaven Protein Data Bank. The PDB codes of the PDK-1 with inhibitors 6-methoxy-2-(1H-pyrazol-5-yl)-1H-benzimidazole (inhibitor 1), 4-dicarboxylic acid diamide (inhibitor 2), 4-butyl-6-(1H-pyrrolo[2,3-b]pyridin-3-yl)pyrimidin-2-amine (inhibitor 3), 4-ethyl-6-[5-(1H-pyrazol-4-yl)-1H-pyrrolo[2,3-b]pyridin-3-yl]pyrimidin-2-amine (inhibitor 4), and 1-(3,4-difluorobenzyl)-2-oxo-N-[(1R)-2-[(2-oxo-2,3-dihydro-1H-benzimidazol-5-yl)oxy]-1-phenylethyl]-1,2-dihydropyridine-3-carboxamide (inhibitor 5) are 5HNG, 5HO7, 5HO8, 5HKM, and 3NAX respectively. Water molecules and two sulfate groups were removed from the PDB files.

It was reported that part of N-terminal lobe of PDK-1 (residues 1-50) interact with Ralguanine nucleotide exchange factors. This region was not present in the PDB file of PDK-1 structure, because this region assumed a unique conformation in PDK-1.¹⁷ PDK-1 protein consists of 556 amino acids, the Phosphoserine residue (SEP) is in position 241 is linking L-peptide ($C_3H_8NO_6P$).

It was reported that 3-Phosphoinositide-dependent protein kinase-1 (PDK-1) expressed in 293 cells was phosphorylated at Ser25, Ser241, Ser393, Ser396 and Ser410. Mutation of Ser241 to Ala canceled PDK-1 activity, whereas mutation of the other phosphorylation sites individually to Ala did not affect PDK-1 activity. Also it was reported that PDK-1 can phosphorylate itself at Ser241, leading to its own activation.⁴³ The pdb files of PDK-1 structure in inhibitors (1-4) show a phosphorylated T-loop in Ser241 therefore, it is in an active state.¹⁷

2.2 Equilibration of the solvated system

Four steps were used to equilibrate the system: minimization, heating, density equilibration and unrestrained equilibration.

(a) Relaxation of the solvated system.

We used *sander* to minimize our system in order to remove any bad contacts as a result of the hydrogenation steps in *xLeap*. Minimization (imin=1) was done in two steps: The first step involves the relaxation of water molecules only, whereas protein and inhibitor atoms were fixed by using a harmonic restraint (restraint_wt=2.0). The second step involves the minimization of the whole system using Sander. The input file min.in was used to perform the first step and min_all.in was used to perform the second step of minimization (see Appendix B). Minimization was performed using 500 steps of the steepest descent method, then

switching to conjugate gradient algorithm for the remaining steps (maxcyc=1000, nyc=500). Constant volume periodicity was applied (ntb=1).

(b) Heating the solvated system.

The system was then heated (imin=0) using langevin thermostat (ntt=3) to maintain the temperature of our system to 300K, with a collision frequency 2 ps^{-1} . This method is more efficient than Berendsen method (ntt=1) due to hot solvent, cold solute phenomena.⁴⁴ The file titled heat.in (see Appendix B) was used to perform the heating process.

(c) Density equilibration.

The file titled density.in (see Appendix B) was used to perform this step. The system was equilibrated at 300 K with constant pressure periodic boundary (ntp=1) using Particle mesh Ewald (PME) method and positional restrains of $2 \text{ Kcal/mol. \AA}^2$ was applied.

(d) Unrestrained equilibration

The file titled equil.in (see Appendix B) was used to perform this step. The unrestrained system was equilibrated at 300 K with constant pressure periodic boundary (ntp=1). The *SHAKE* method⁴⁵ was applied (ntc=2, ntf=2) to hold all covalent bonds containing hydrogen atoms.

2.3 Production step of the solvated system

The production simulation time is 2ns that run using the same conditions as in the final phase of equilibration to prevent any sudden jump in the potential energy due to a change in simulation conditions. The production run was carried out over four sequential steps using the input file prod.in (see Appendix B). During all the MD simulations, the Particle Mesh Ewald (PME) method was utilized with 10Å cutoff for long-range interactions.

2.4 Calculating the binding free energy of the protein-inhibitor complex

We carried out the binding free energy calculation using both the MM-GBSA method and the MM-PBSA method for comparison. This is achieved using input file for mmpbsa.in (see Appendix B).

2.5 Calculating the entropic contribution

Normal Mode Analysis (*Nmode*) was used to calculate the entropic contribution.⁴⁶

The file titled mmpbsa_nm.in (see Appendix B) was used to do this step.

Chapter 3

Results and discussion

3.1 Analysis of simulations

The system reached state of equilibrium after different stages of simulation. This was checked by monitoring of different properties during the simulation. The system properties were extracted from the output files, and were plotted versus time. Figures 3.1 to 3.4 show plots for inhibitor 1-protein complex.

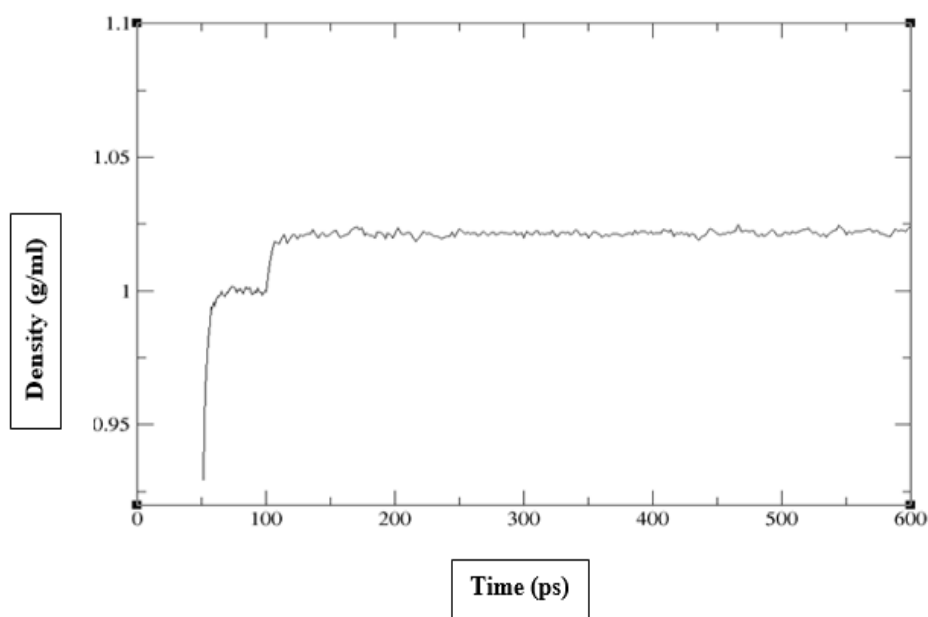


Figure 3.1: Density of protein-inhibitor (1) complex system during equilibration

As shown in Figure 3.1, the first 50 ps of the simulation represents the heating stage. There was no density data recorded due to the constant volume condition that took place until 50 ps. After that the density increased up to 1.02 g/ml and stayed around this number until the last 550 ps. This is reasonable because the density of pure water at 300 K is 1.00 g/ml, so adding inhibitor 1-protein complex lead to a rise in density of the system by 4%.⁴⁷

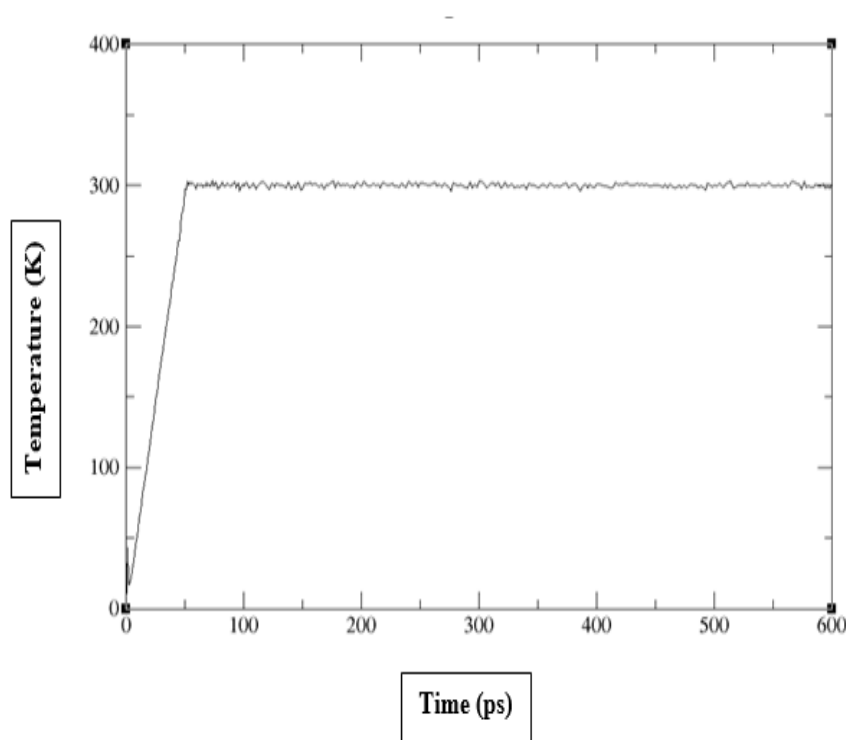


Figure 3.2: Temperature of protein-inhibitor (1) complex system during equilibration runs

In Figure 3.2, the temperature rises regularly from 0 K to 300 K. After that the temperature of the system reached an equilibrium value of 300 K over the last

stage of simulations, indicating that Langenvin dynamics applied successfully in this case.⁴⁷

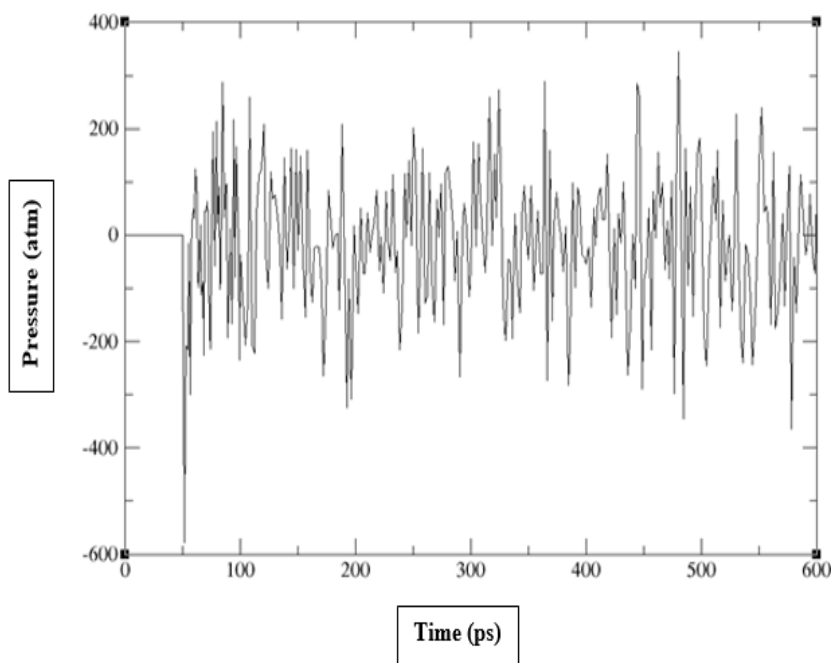


Figure 3.3: Pressure of protein-inhibitor (1) complex system during equilibration

In the pressure versus time plot (Figure 3.3). It shows that in the time interval between 0-50 ps the pressure was zero, because it was running at constant volume. At 50 ps the system changed to constant pressure, the volume of the box changed and the pressure dropped sharply becoming negative.⁴⁸ Positive values of pressure reflect a force trying to make the water box larger, whereas negative pressure values reflect a force trying to reduce the volume of the water box.⁴⁷ While the pressure plot shows that the pressure fluctuated during the simulation, pressure stabilized at 1 atm, this indicates a successful equilibration.

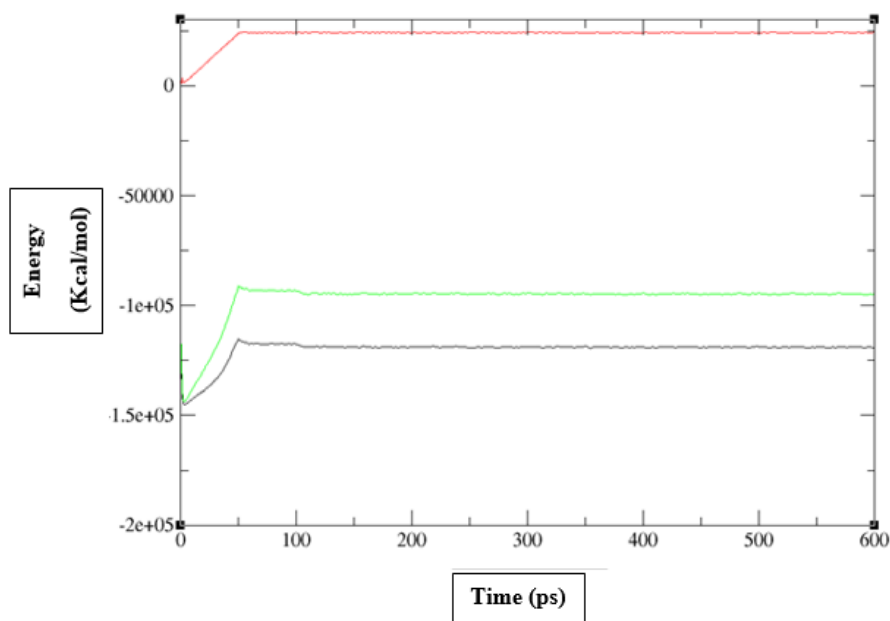


Figure 3.4: Total, kinetic and potential energy of protein-inhibitor (1) complex system during equilibration runs. The kinetic energy (in red line); the potential energy (in black line); the total energy (in green line) which is the sum of kinetic and potential energy

According to the energy plot versus time (Figure 3.4) the first 50 ps of simulation there was an increase in all energies corresponding to heating from 0 K to 300 K. The kinetic energy remained constant in the last stages indicating a successful performance of temperature thermostat.⁴⁷

The potential energy and the total energy initially increased, then during the constant volume stage (0 to 20 ps) there was a plateau, then at 20 to 40 ps there was a decrease in the energy values because, at this stage we switched off the protein-ligand restraints and moved to constant pressure. After that the potential energy

leveled off for the remainder of our simulation indicating stability and a relaxed system.⁴⁷

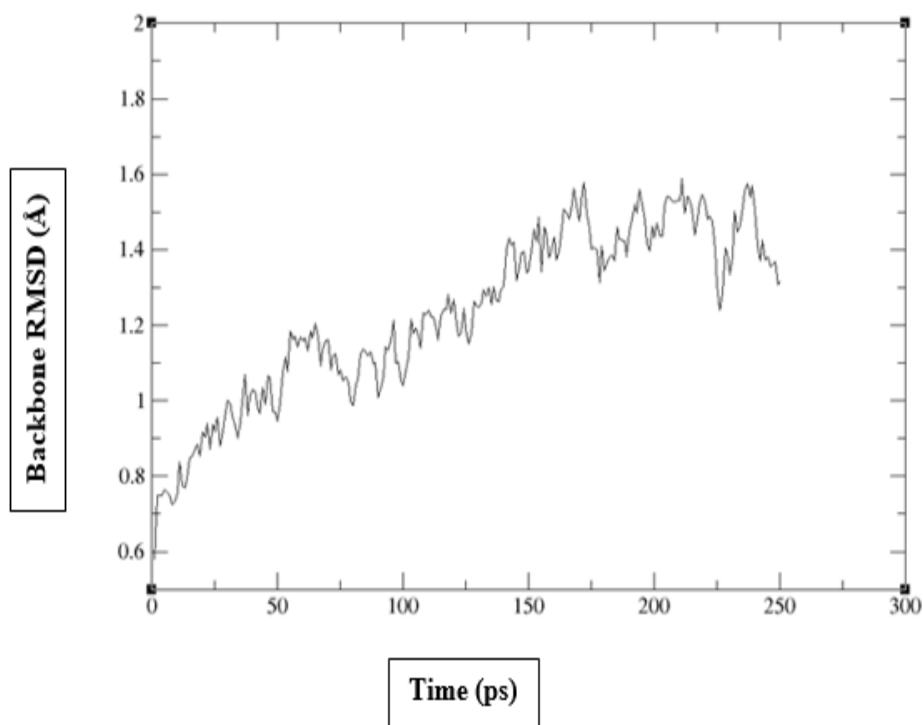


Figure 3.5: RMSD of protein backbone during unrestrained equilibration run of protein-inhibitor (1) complex

In order to quantify the similarity between a native inhibitor1-protein complex (com_wat.inpcrd) and a generated inhibitor1-protein complex (equil.mdcrd), the mass weighted RMSD (Root-mean square deviation) can be calculated between these two structures. Figure 3.5 shows that the root mean square deviation (RMSD) values increased rapidly in the first 75 ps, then it fluctuated around a value of 1.4 Å until the last 250 ps, which is an acceptable value. RMSD

values were around 1.4 Å, this reflects an acceptable conformational changes in the protein backbone .

3.2 Study of binding energies of kinase – inhibitors

3.2.1 Binding free energies of protein-inhibitor complexes: MM-PBSA versus MM-GBSA

MM-PBSA and MM-GBSA are direct methods for the quantitative prediction of binding free energy of ligand-protein complex.⁴⁹

Both methods are used in this work to calculate the binding free energy of PDK-1 kinase with five inhibitors (Table 3.1). As shown in Figure 3.6 there is a good correlation between binding free energies were calculated by MM-GBSA, and experimental values of binding free energies which are derived from the experimental reported IC₅₀ values ($R^2 = 0.54$).

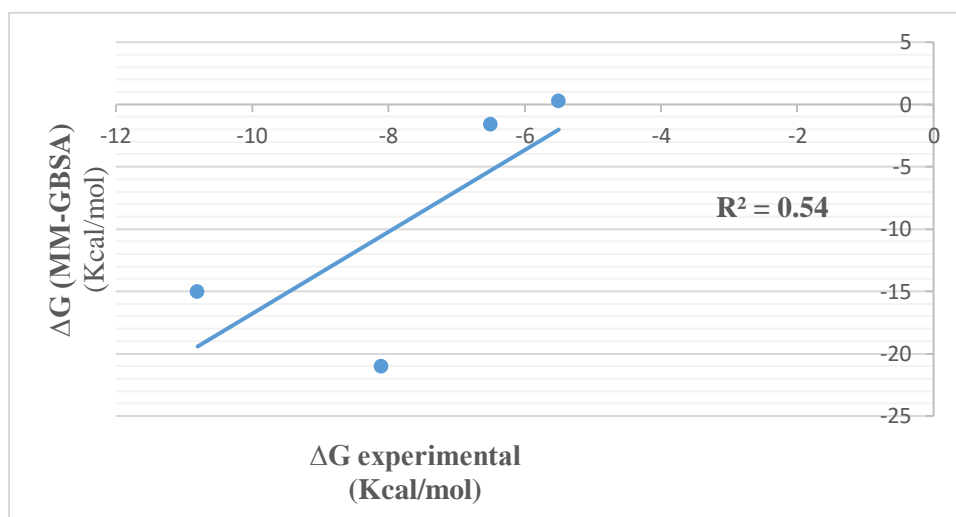


Figure 3.6: Correlation between ΔG calculated by MM-GBSA and ΔG experimental values

To the contrary, the correlation between the binding free energies were calculated by MM-PBSA and experimental values of binding affinity (Fig 3.7) which are derived from the experimental reported IC₅₀ values is weaker ($R^2 = 0.06$).

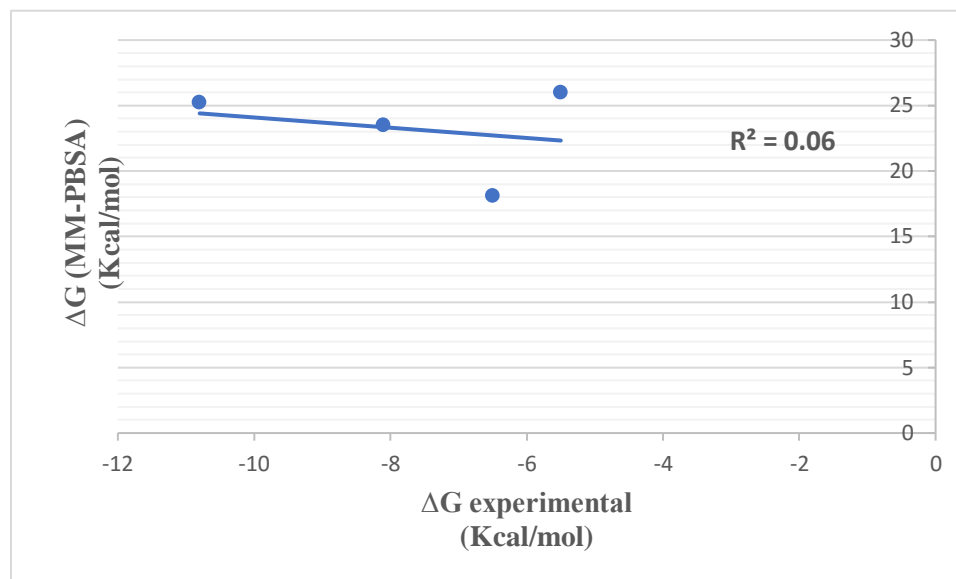
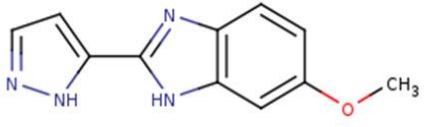
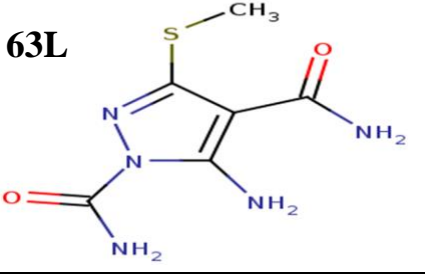
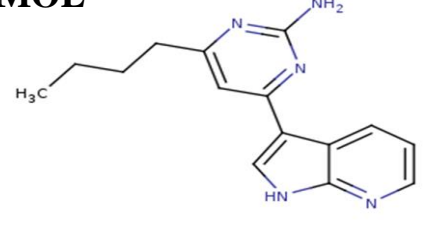
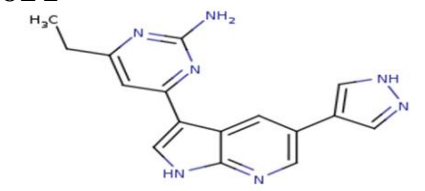
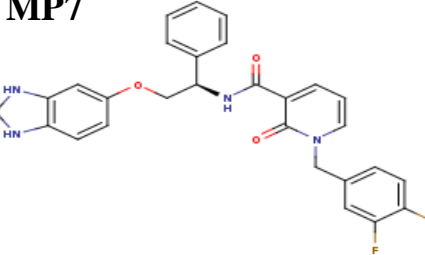


Figure 3.7: Correlation between ΔG calculated by MM-PBSA and ΔG experimental values

It is observed that the calculated binding free energies using MM-GBSA method were closer to the experimental values than those calculated using MM-PBSA method. In principle, PB is more theoretically rigorous than GB, but it does not mean that MM/PBSA can give better predictions than MM/GBSA.⁵⁰ Our result agrees with some of the reports that MM-GBSA based on GB^{OBCI} is considered a better approach than the MM-PBSA in calculating the binding free energies when heterocyclic and aromatic system is present.⁵¹

Table 3.1: Binding free energies (kcal/mol) calculated at T= 300 K and P= 1 atm for PDK-1 binding with the four inhibitors

Inhibitor	Experimental		Calculated	
	IC ₅₀ (μ M)	$\Delta G_{\text{exp}}^{22}$ (Kcal/mole)	ΔG_{calc} (MM-GBSA) (Kcal/mole)	ΔG_{calc} (MM-PBSA) (Kcal/mole)
62O 	93	-5.5	0.3 \pm 1.6	26.0 \pm 1.7
63L 	17	-6.5	-1.6 \pm 2.0	18.1 \pm 2.0
MOL 	1.1	-8.1	-21.0 \pm 1.5	23.5 \pm 2.3
61Y 	0.013	-10.8	-15.0 \pm 1.8	25.2 \pm 2.6
MP7 	-	-	-52.3 \pm 2.8	-11.4 \pm 3.0

The experimental binding free energies (ΔG_{bind}) were calculated from the experimental values of IC_{50} , by using this equation:

$$\Delta G_{\text{bind}} = RT \ln K_D = RT \ln IC_{50} \quad (3.1)$$

The reported IC_{50} values are concentrations at which the PDK-1 kinase activity is inhibited by 50% of the initial concentration.⁵² The kinetic study of enzyme-inhibitor reaction in the absence of inhibitor follows a simple Michaelis-Menten equation (3.2).⁵³ The following equation assumes that the concentration of enzyme is sufficiently low (neglected).

$$V_0 = \frac{V_{\text{max}} S}{K_m + S} \quad (3.2)$$

$$V_I = \frac{V_{\text{max}} S}{K_m \left(1 + \frac{I}{K_I}\right) + S} \quad (3.3)$$

Where, V_{max} = maximum velocity; V_0 = velocity in the absence of the inhibitor; K_m = Michaelis constant of the substrate; V_I = velocity in the presence of inhibitor; I = concentration of inhibitor; S = substrate concentration; K_I = dissociation constant of enzyme-inhibitor complex (EI).

When $I = I_{50}$, $V_0 = 2V_I$ then⁵³

$$\frac{2 V_{max} S}{K_m \left(1 + \frac{I_{50}}{K_I}\right) + S} = \frac{V_{max} S}{K_m + S} \quad (3.4)$$

By rearranging equation 3.4:

$$I_{50} = K_I \left(1 + \frac{S}{K_m}\right) \quad (3.5)$$

In the case of a competitive inhibitor, $S \ll K_m$, then $K_i \sim IC_{50}$.

3. 3 Analysis of the binding mode of inhibitor (1)-PDK-1 complex

In this section we discussed the binding mode of inhibitor (1) with PDK-1 kinase complex (Figure 3.8(a) and (b)). The non-covalent interaction of inhibitor to the proteins is governed by different interactions including van der Waal and hydrogen bond interaction.²⁴

Inhibitor (1) makes two strong hydrogen bond interactions with the backbone oxygen atom of Ser⁹⁰ in the adenine region of the kinase with a distance of 2.1 Å and 1.8 Å (Table 3.2). The benzimidazole ring is in a buried region. It is surrounded by residue Thr¹⁵² (4.6 Å not considered as hydrogen bond).

Other weak interactions were formed between the inhibitor (1) and the PDK-1 (Figure 3.8(c)), C-H π interaction⁵⁴ between carbon hydrogen atom of Leu¹⁸ and the center of benzimidazole ring of inhibitor (3.1 Å is the average distance from the hydrogen atom to the center of ring). The same type of interaction was made by Ala⁹² in the hinge region, but the average distance is 3.9 Å.

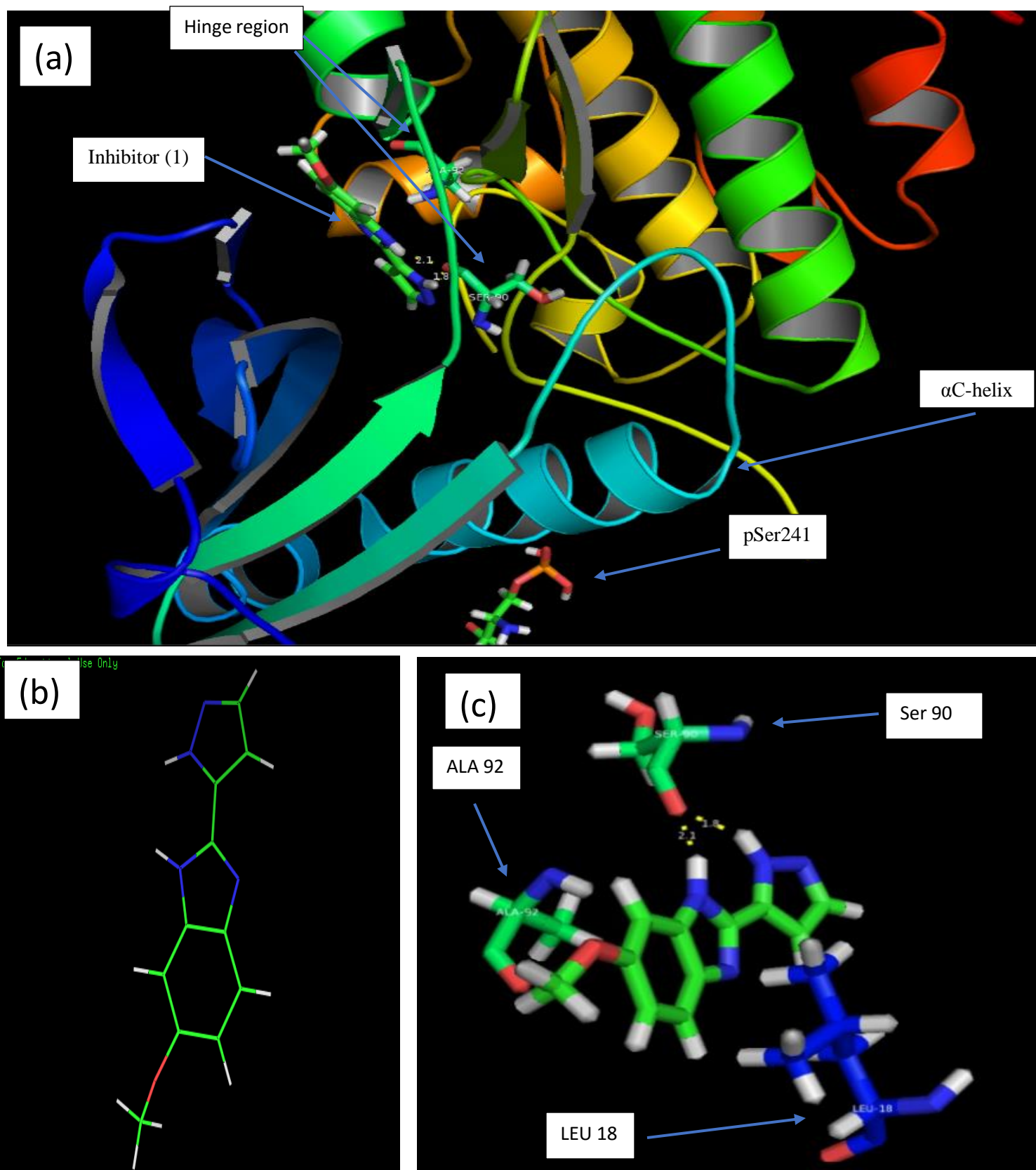
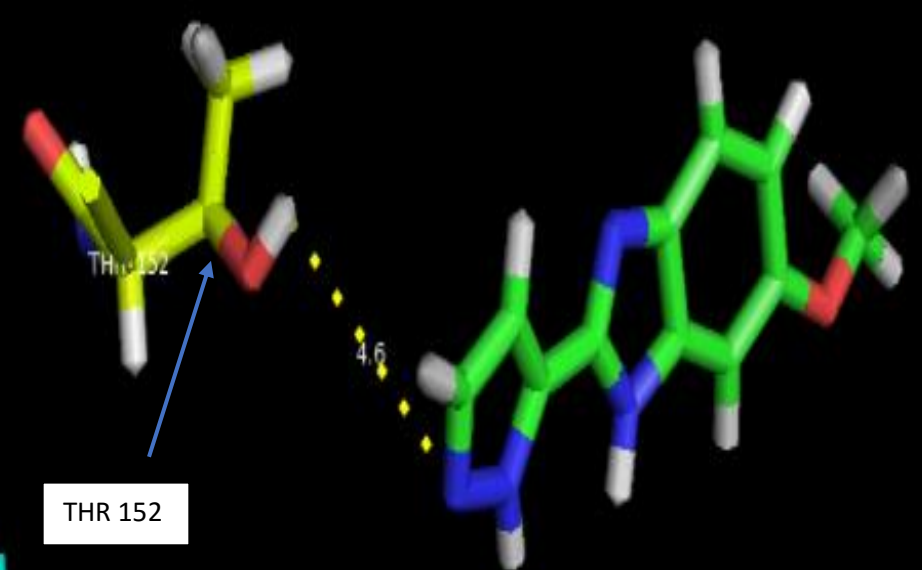
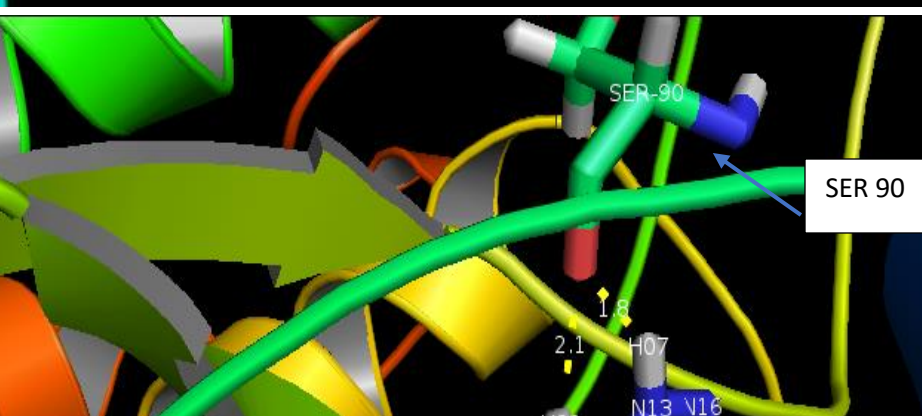
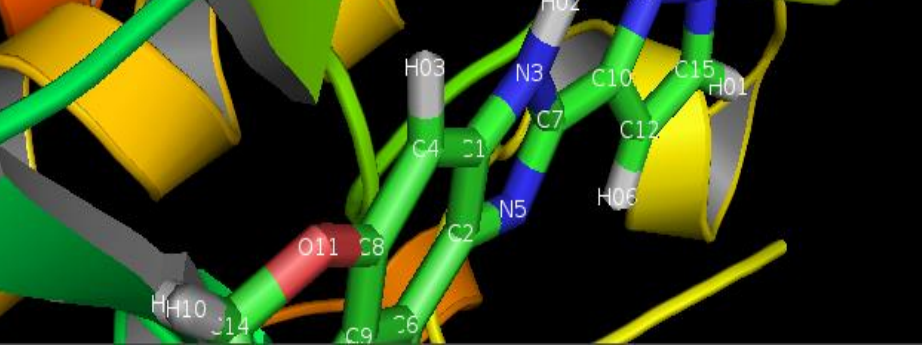


Figure 3.8: (a) Inhibitor (1)-PDK-1 complex, (b) graphical representation of inhibitor (1) and (c) other weak interactions between inhibitor (1) and kinase

Table 3.2: Hydrogen bond analysis of inhibitor (1) in 6Z0-PDK-1complex

Atom of inhibitor	Atom of protein/H ₂ O	Comment
N16	H-Thr ¹⁵² no considerable hydrogen bonds	
HO2	O-Ser ⁹⁰	
HO7	O-Ser ⁹⁰	

3.4 Analysis of the binding mode of inhibitor (2)-PDK-1 complex

In this section we discussed the binding mode of inhibitor (2) with PDK-1 kinase complex (Figure 3.9(a) and (b)). Inhibitor (2) has hydrogen bond interaction with the backbone carbonyl group of Ser⁹⁰ with 2.1 Å distance, and another two hydrogen bonds are formed with Ala⁹² at 3.2 Å and 2.1 Å distances in the hydrophobic adenine pocket (Table 3.3).

A strong hydrogen bond interaction with the carbonyl group of Thr¹⁵² in the buried region (length = 1.8 Å). It is worth noting that this inhibitor has an intramolecular hydrogen bond between hydrogen atom of amino group (HO2) and oxygen of carbonyl group (O14) as shown in table 3.3.

The highest frequency of intramolecular hydrogen bonds for planer, six membered rings stabilized by conjugation with a π -system. The formation of an intramolecular hydrogen bond result in an increased lipophilicity and membrane permeability accompanied by reduced aqueous solubility. These are due to the removal of one donor and one acceptor function from the surface of a molecule.⁵⁵

Replacing real rings by such pseudo rings to form pseudo six-membered ring is a new and non-conventional strategy and the new classes of kinase inhibitors follow this approach.⁵⁶

We noted that inhibitor (2) interacts with the active site in water-mediated hydrogen bonds with active-site residues. A water-mediated network of hydrogen bonds is formed by 2 water molecules to inhibitor (2) as shown in table 3.3.

In addition to all of these interactions, other weak interactions were formed between inhibitor (2) and PDK-1 (Figure 3.11(c)), C-H.....C=O interaction⁵⁴ between hydrogen atom of Tyr⁹¹ and the carbonyl group of inhibitor (2.6 Å).

Another weak interaction was formed of the type C-H..... π interaction⁵⁴ between carbon hydrogen atom of Val²⁶ with the center of pyrazole ring (3.7 Å is average distance between the center of the pyrazole ring and the hydrogen atom) as shown in figure 3.9(c).

It is worth noting that Leu¹⁸ is close to inhibitor due to the C-H.....C=O weak interaction between hydrogen atom of Leu¹⁸ and the carbonyl group of Val²⁶ (2.1 Å) as shown in figure 3.9(c).

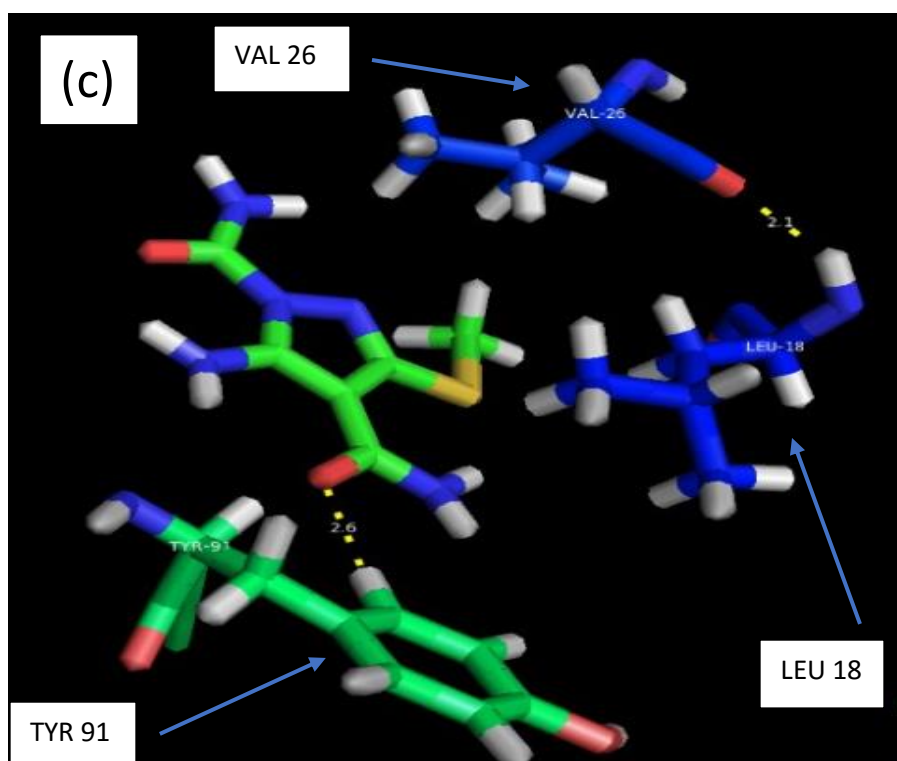
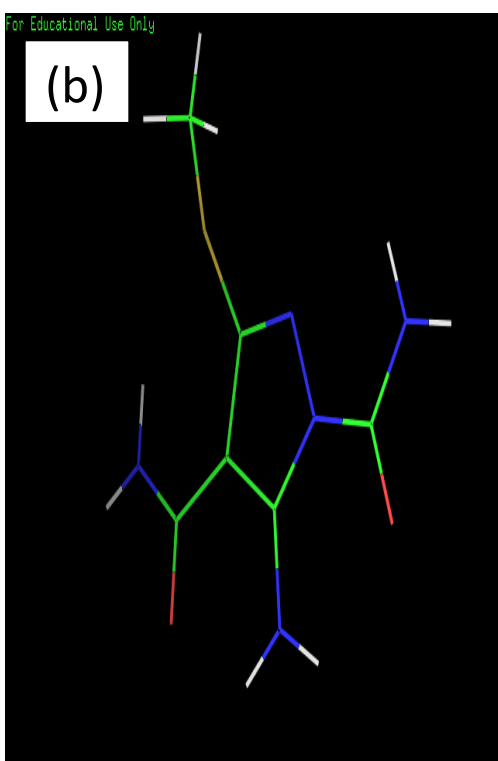
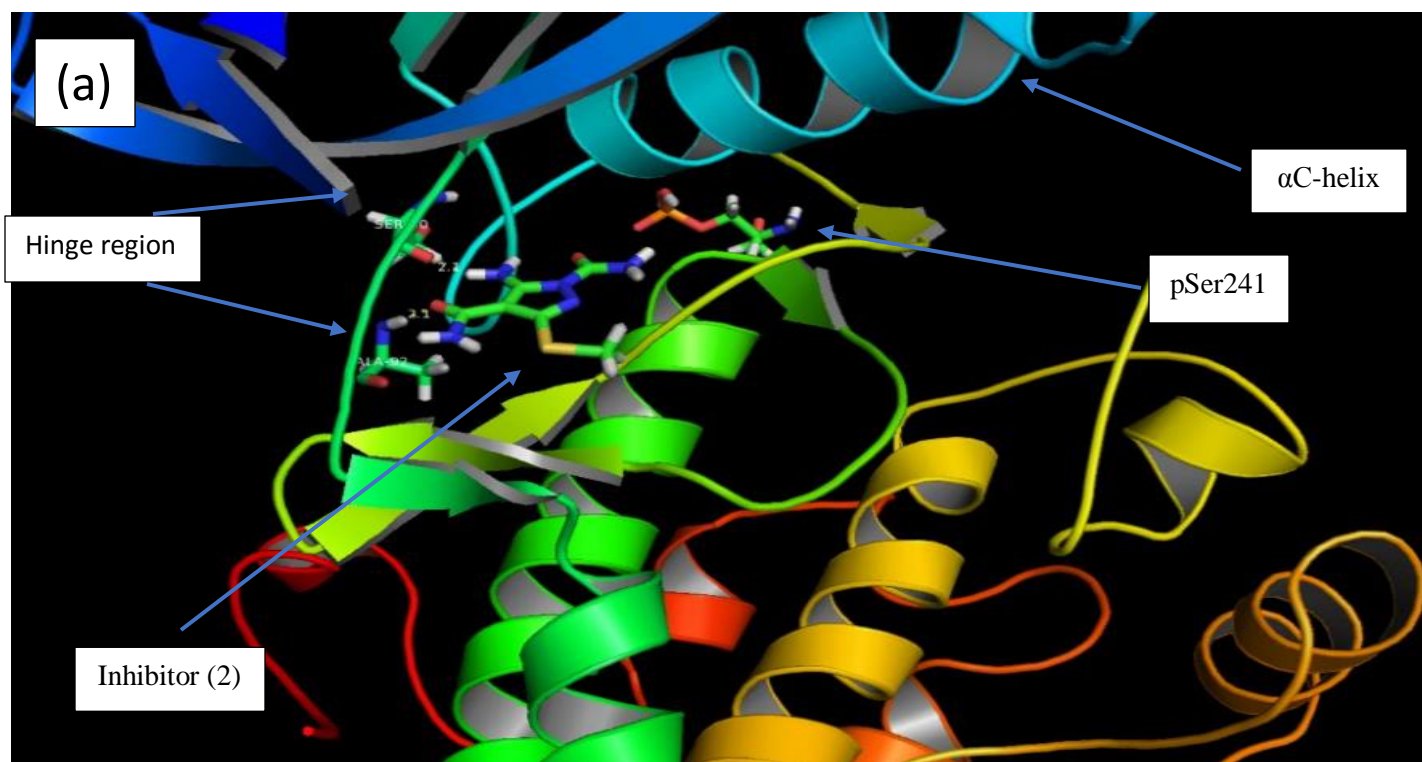


Figure 3.9: (a) Inhibitor (2)-PDK-1 complex, (b) graphical representation of inhibitor (2) and (c) other weak interactions between inhibitor (2) and kinase

Table 3.3: Hydrogen bond analysis of inhibitor (2) in 63L-PDK-1complex

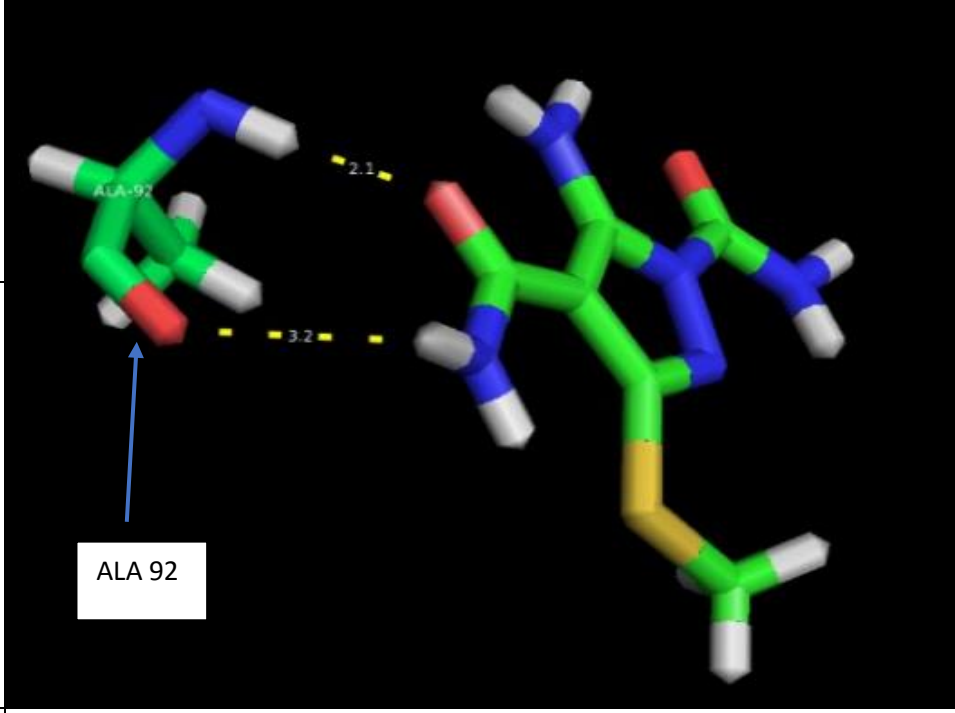
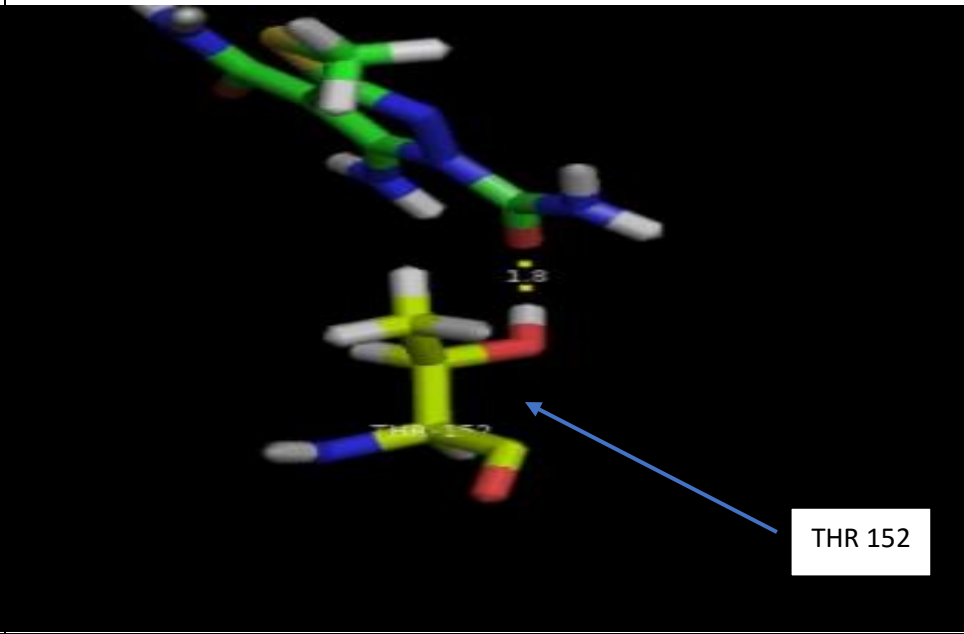
Atom of inhibitor	Atom of protein/H ₂ O	Comment
O10	H-Ala ⁹²	
HO7	O-Ala ⁹²	
O14	H-Thr ¹⁵²	
		

Table 3.3: Hydrogen bond analysis of inhibitor (2) in 63L-PDK-1complex

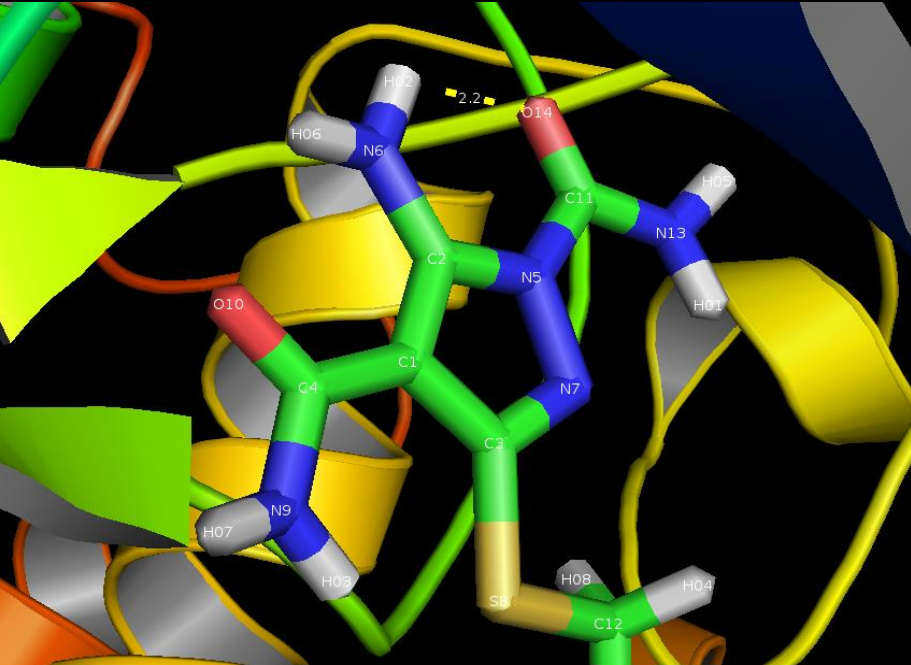
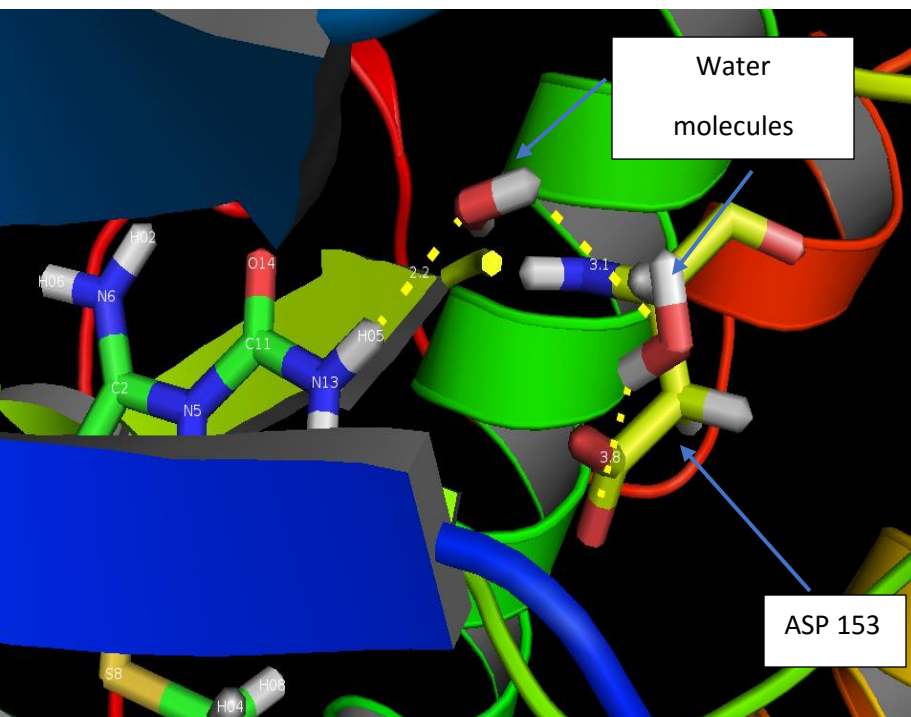
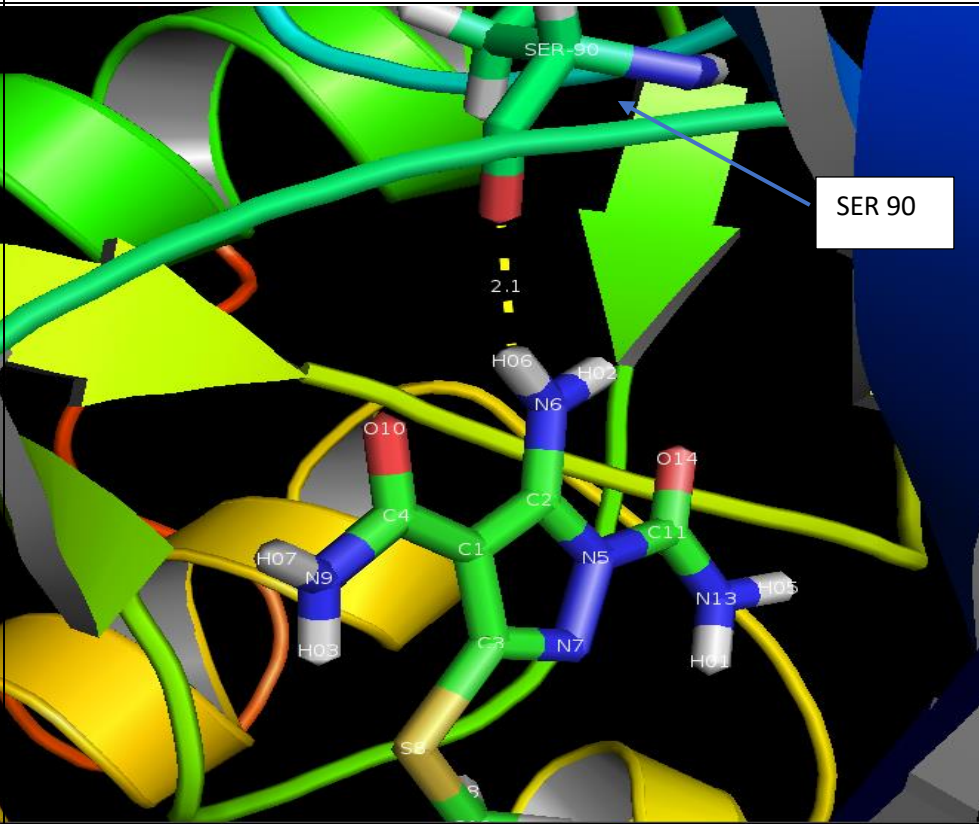
Atom of inhibitor	Atom of protein/H ₂ O	Comment
O14	H-63L ²⁸² (Intramolecular hydrogen bond)	
HO5	O-Asp ¹⁵³ (Water mediated)	

Table 3.3: Hydrogen bond analysis of inhibitor (2) in 63L-PDK-1complex

Atom of inhibitor	Atom of protein/H ₂ O	Comment
HO6	O-Ser ⁹⁰	 <p>The image shows a 3D molecular model of the inhibitor (2) in the 63L-PDK-1 complex. The inhibitor is represented by a stick model with green carbon atoms, blue nitrogen atoms, and red oxygen atoms. The protein backbone is shown as a yellow and green ribbon. A specific hydrogen bond is highlighted between the inhibitor atom HO6 and the protein atom O-Ser⁹⁰. The distance between these two atoms is indicated as 2.1 Å. A callout box labeled 'SER 90' points to the corresponding residue in the protein structure.</p>

3.5 Analysis of the binding mode of inhibitor (3)-PDK-1 complex

In this section we discussed the binding mode of inhibitor (3) with PDK-1 kinase complex (Figure 3.10(a) and (b)). Inhibitor (3) is located in the ATP-binding site (which lies between the N-terminal and C-terminal lobes of kinases).⁵⁷ The 7-azaindole ring mimics the interactions of the adenine base in ATP with the protein backbone, where two conserved hydrogen bonds are formed between the 7-azaindole nitrogen N3 in inhibitor (3) and the backbone-hydrogen of Ala⁹², and the 7-azaindole hydrogen HO5 and the backbone-oxygen of Ser⁹⁰ as shown in table 3.4.

In addition to the presence of direct hydrogen bonds, there are water-mediated hydrogen bond interactions. The water mediated hydrogen bond interaction occur between inhibitor (3) and Lys⁴¹ in the phosphate region, and Thr¹⁵² in the buried region as shown in table 3.4.

It was reported that the discovery of aminoindazole ring and the addition of one heterocyclic ring which is involved by using its nitrogen atoms in the hydrogen bond interaction with inhibitor. This is critical for binding. Overall cumulative data confirm that each nitrogen in the aminoindazole positively contributes to PDK-1 binding and inhibition activity.⁵⁸

Other weak interactions were formed between inhibitor (3) and the PDK-1,

C-H... π interaction⁵⁴ between carbon hydrogen atom of Leu¹⁸ and the center of 7-azaindole ring (3.3 Å is average distance between the hydrogen atom and the center of the ring) as shown in figure 3.10(c).

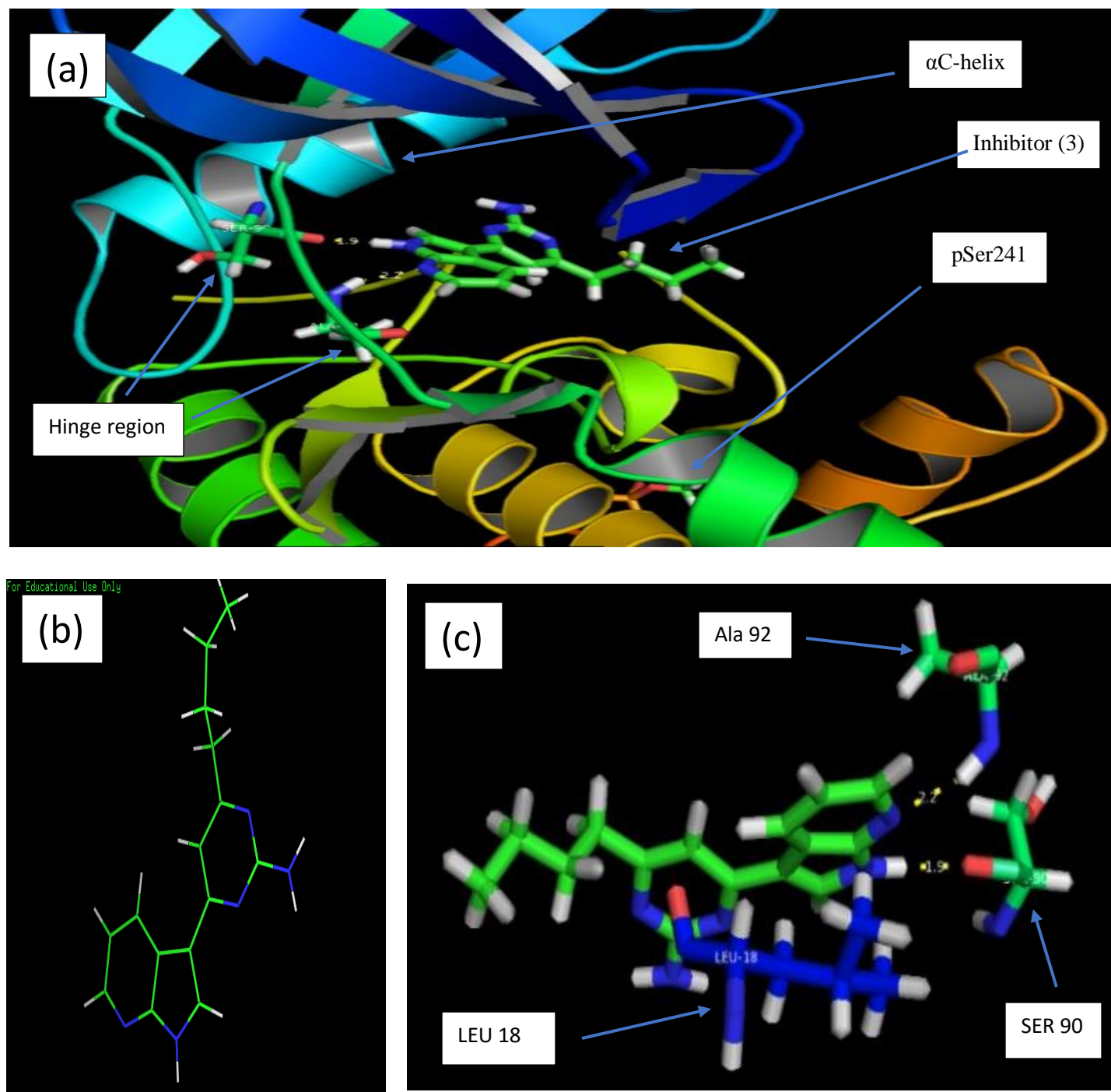
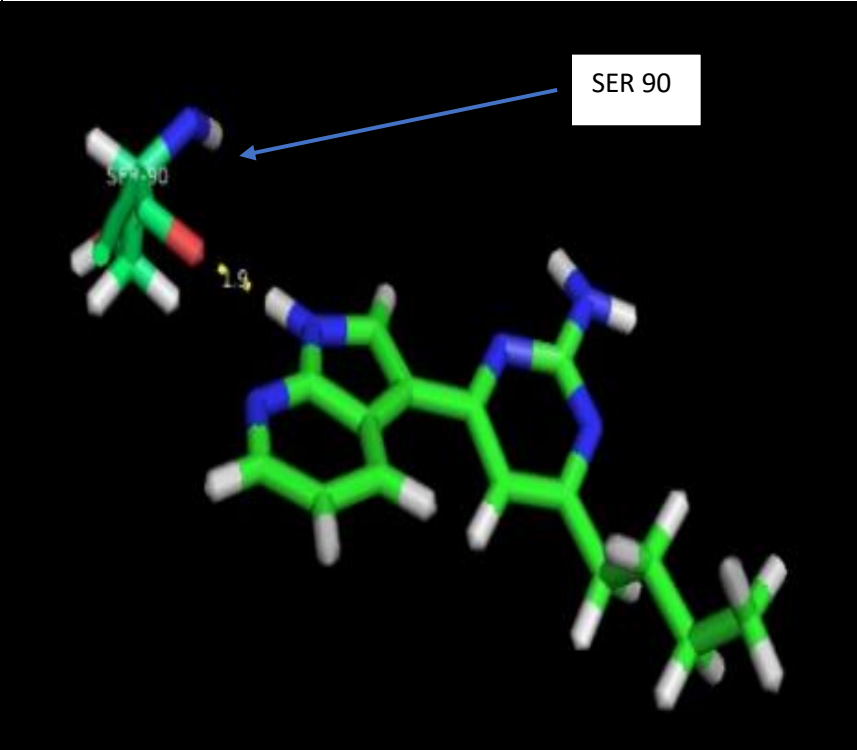
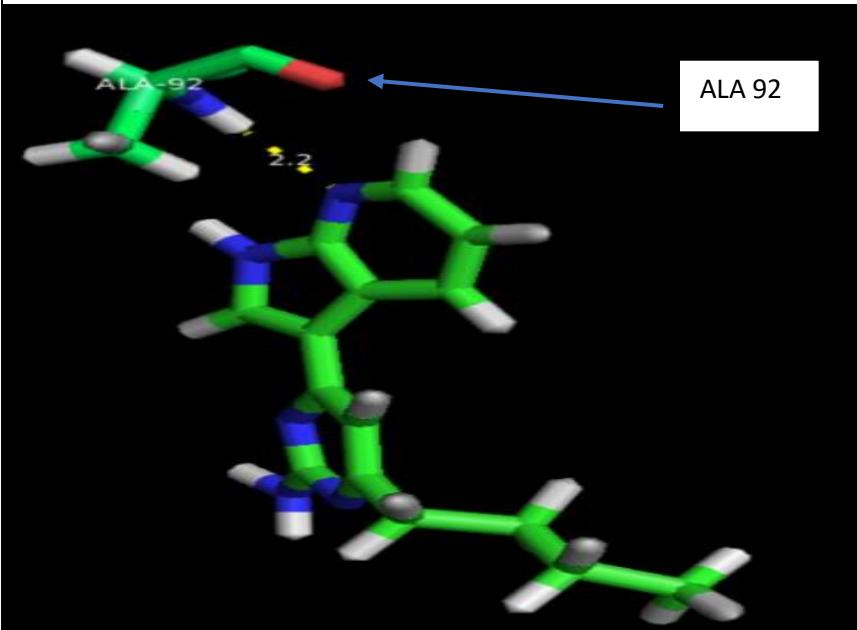


Figure 3.10: (a) Inhibitor (3)-PDK-1 complex, (b) graphical representation of inhibitor (3) and (c) other weak interactions between inhibitor (3) and kinase

Table 3.4: Hydrogen bond analysis of inhibitor (3) in MOL-PDK-1complex

Atom of inhibitor	Atom of protein/H ₂ O	Comment
N16	H-Lys ⁴¹ (Water mediated)	
N16	H-Lys ⁴¹	
N15	H-Thr ¹⁵²	
HO8	O-Thr ¹⁵² (Water mediated)	

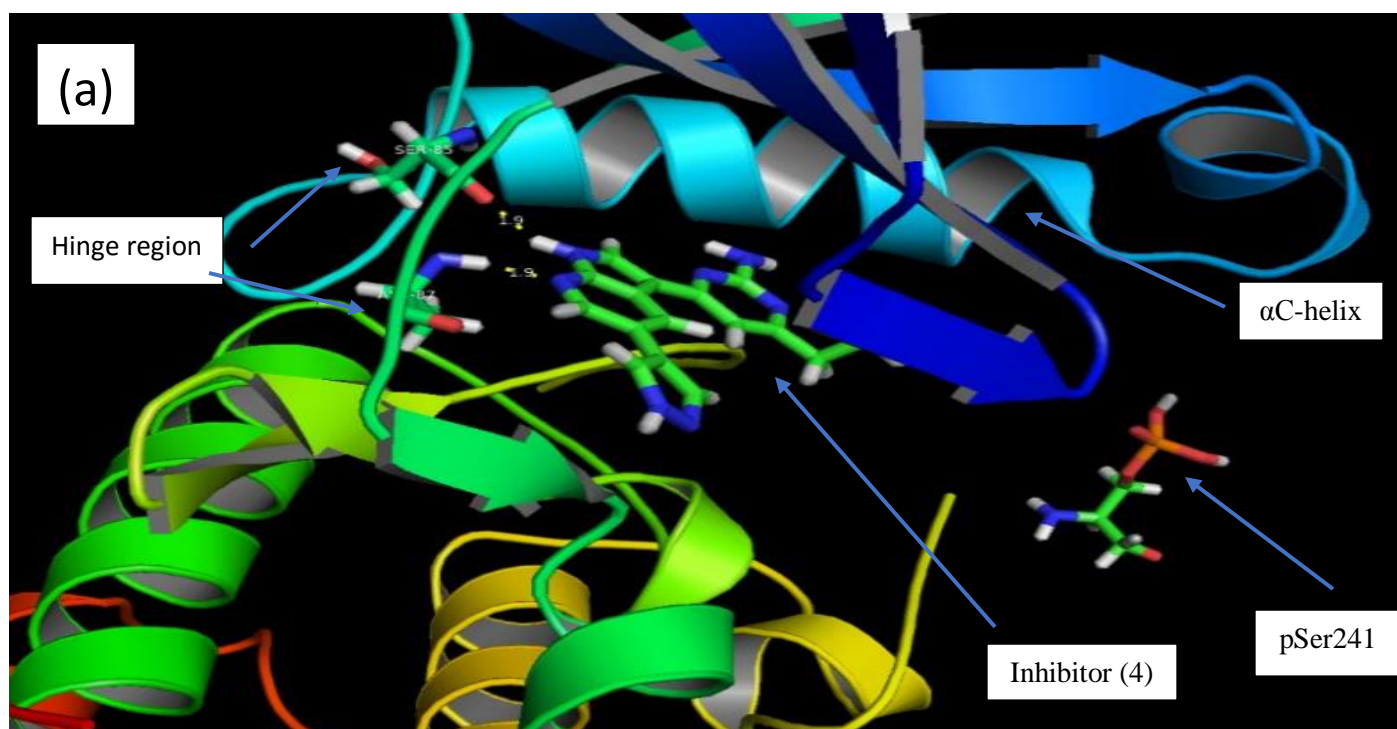
Table 3.4: Hydrogen bond analysis of inhibitor (3) in MOL-PDK-1complex

Atom of inhibitor	Atom of protein/H ₂ O	Comment
HO5	O-Ser ⁹⁰	 <p>A 3D ball-and-stick model of the inhibitor (green and blue) and a Serine residue (Ser90, green and blue) from the protein. A blue arrow points from a white box labeled 'SER 90' to the oxygen atom of the Ser90 residue. A yellow double-headed arrow indicates a hydrogen bond between the HO5 atom of the inhibitor and the oxygen atom of Ser90, with a distance of 1.9 Å. The Ser90 residue is also labeled '579-90'.</p>
N3	H-Ala ⁹²	 <p>A 3D ball-and-stick model of the inhibitor (green and blue) and an Alanine residue (Ala92, green and blue) from the protein. A blue arrow points from a white box labeled 'ALA 92' to the hydrogen atom of the Ala92 residue. A yellow double-headed arrow indicates a hydrogen bond between the N3 atom of the inhibitor and the hydrogen atom of Ala92, with a distance of 2.2 Å. The Ala92 residue is also labeled 'ALA-92'.</p>

3.6 Analysis of the binding mode of inhibitor (4)-PDK-1 complex

In this section we discussed the binding mode of inhibitor (4) with PDK-1 kinase complex (Figure 3.11(a) and (b)). Inhibitor (4) forms four hydrogen bonds with the protein. The N12 atom binds the hydroxyl group hydrogen of Thr¹⁴⁷ in the buried region, N4 atom binds hydroxyl group hydrogen of Ala⁸⁷ in the adenine region, N23 atom binds the hydrogen atom of Lys⁹⁴, N23 atom binds hydroxyl group hydrogen atom of Glu⁹¹ in the sugar region and HO5 hydrogen atom binds to the backbone carbonyl group of Ser⁸⁵ in the adenine region (Table 3.5).

Other weak interaction was formed between inhibitor (4) and the PDK-1, C-H... π interaction⁵⁴ between carbon hydrogen atom of Leu¹³ and the center of 7-azaindole ring as shown in figure 3.11(c).



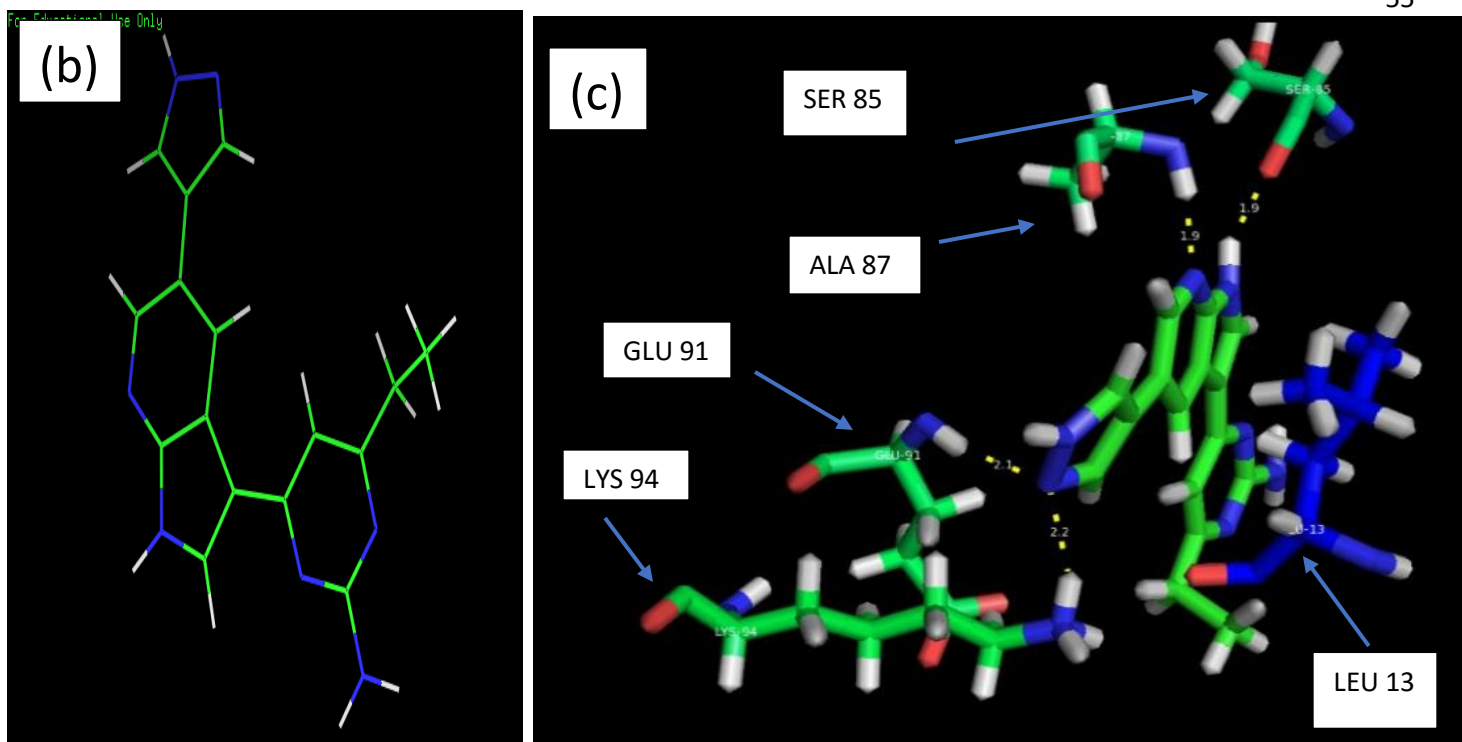


Figure 3.11: (a) Inhibitor (4)-PDK-1 complex, (b) graphical representation of inhibitor (4) and (c) other weak interactions between inhibitor (4) and kinase

It was reported that **type I kinase inhibitors** form water-mediated hydrogen bond networks (both water molecules W1 and W2 are commonly observed) and the ligand does not extend to the water-filled cavity. These two features distinguish type I from type II inhibitors.⁵⁹

Figure 3.12 illustrates the typical distribution of ligand-W1 hydrogen bond distances for 180 ATP-binding site ligands.⁵⁹ According to inhibitor (4), the ligand-W1 hydrogen bonds was 3.0 Å which is agree with the typical distribution of hydrogen bonds.

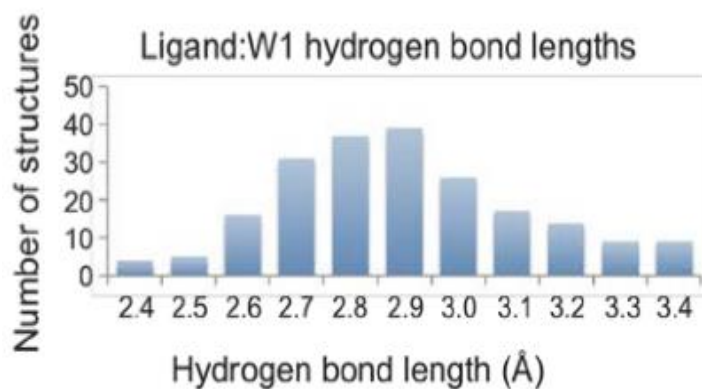


Figure 3.12: The distribution of hydrogen bond lengths for 180 ATP-binding site ligand-W1 hydrogen bonds⁵⁹

Table 3.5: Hydrogen bond analysis of inhibitor (4) in 61Y-PDK-1complex

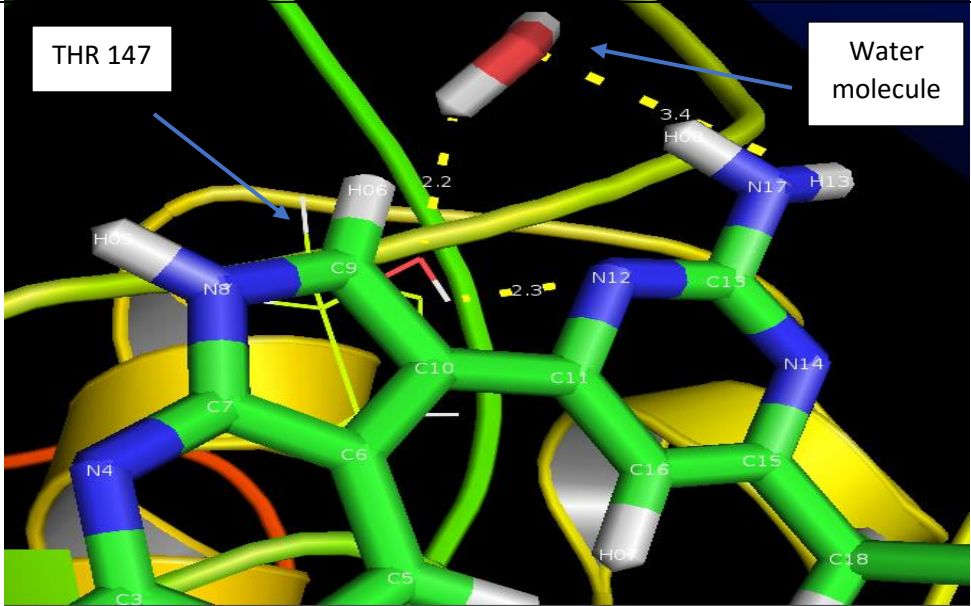
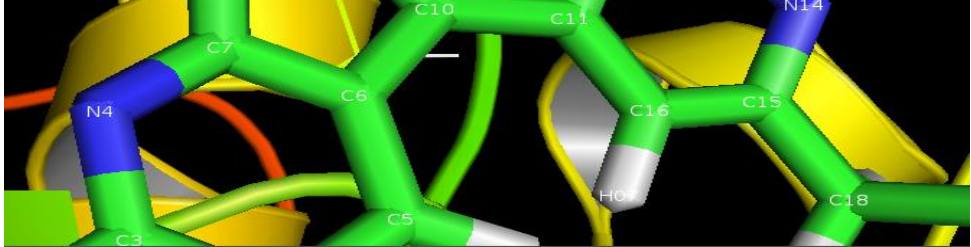
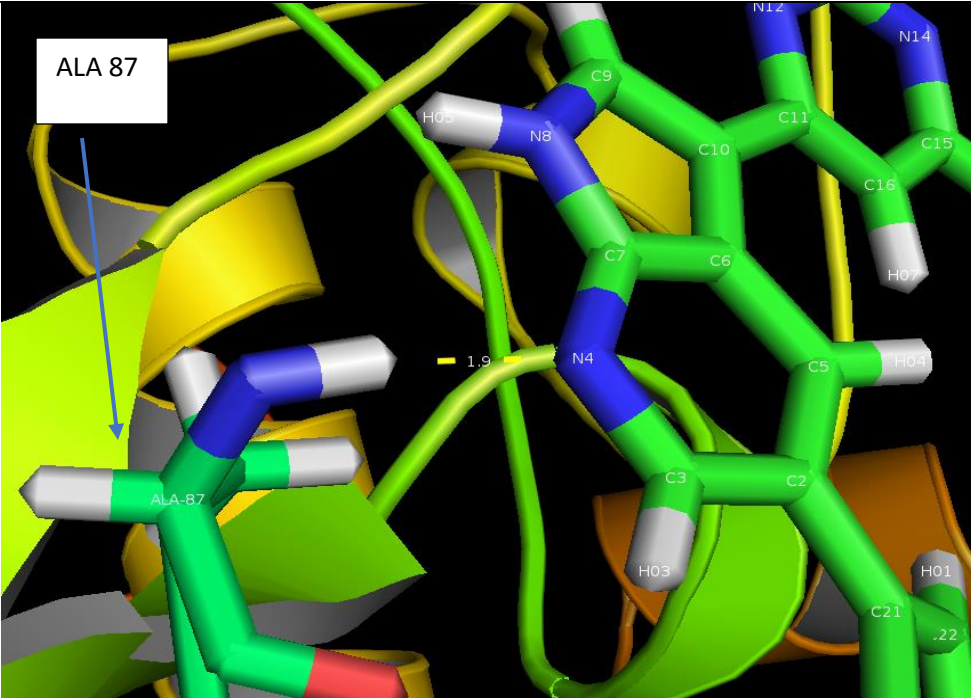
Atom of inhibitor	Atom of protein/H ₂ O	Comment
N12	H-Thr ¹⁴⁷	
H13	O-Thr ¹⁴⁷ (Water mediated)	
N4	H-Ala ⁸⁷	

Table 3.5: Hydrogen bond analysis of inhibitor (4) in 61Y-PDK-1complex

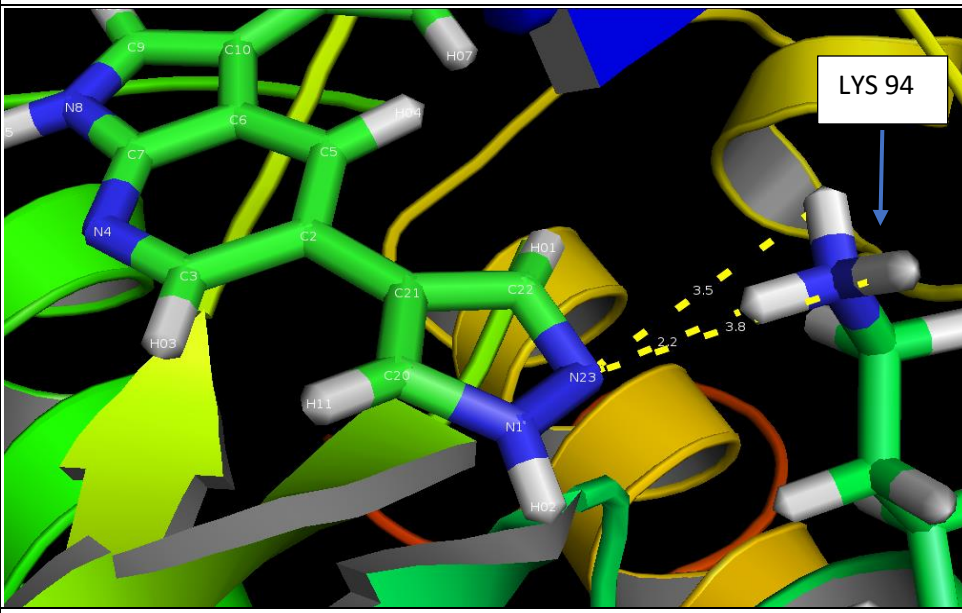
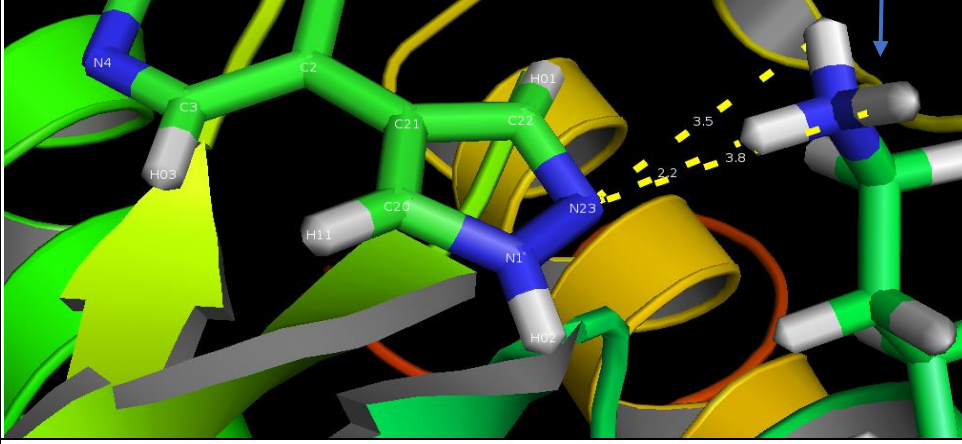
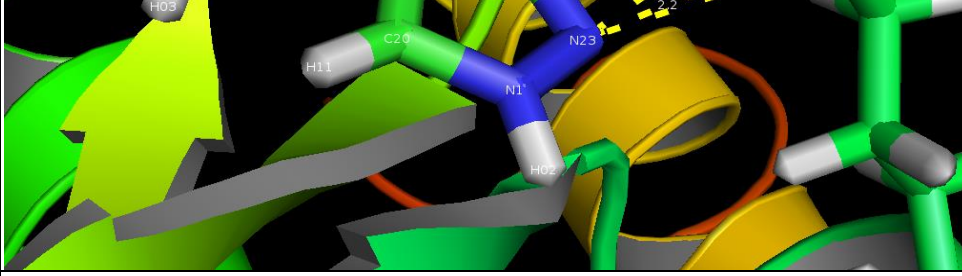
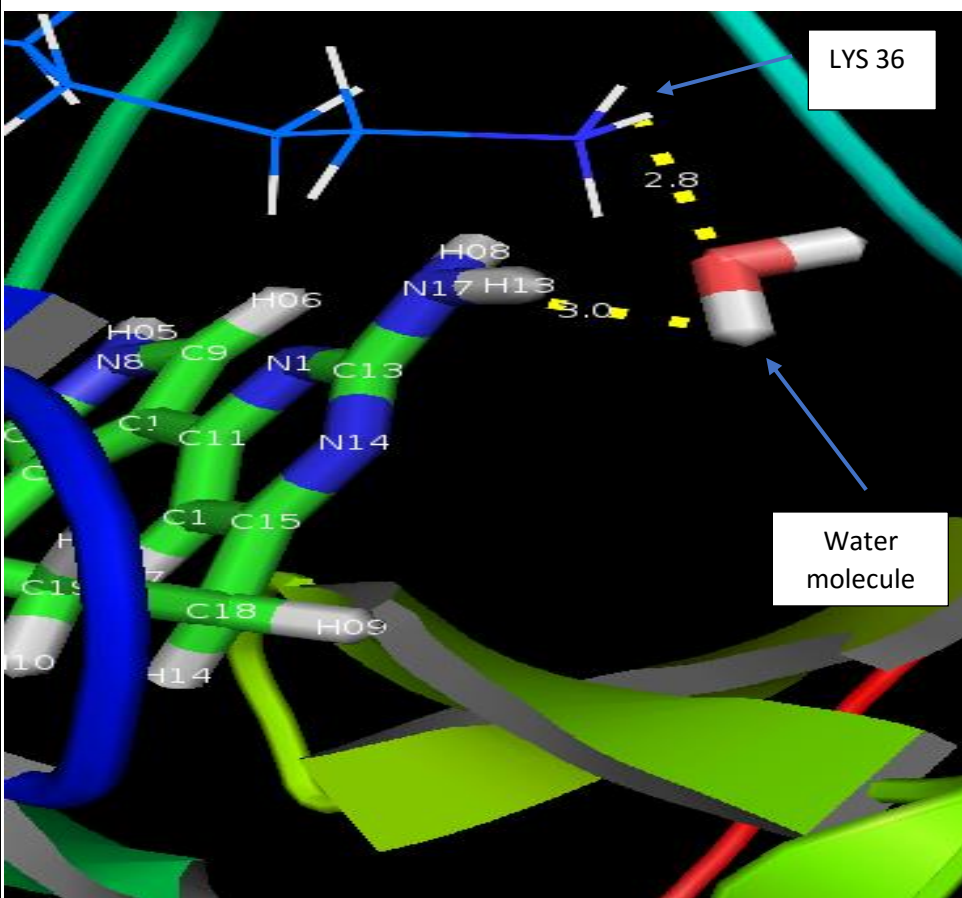
Atom of inhibitor	Atom of protein/H ₂ O	Comment
N23	H-Lys ⁹⁴	
N23	H-Lys ⁹⁴	
N23	H-Lys ⁹⁴	
N17	H-Lys ³⁶ (Water mediated)	

Table 3.5: Hydrogen bond analysis of inhibitor (4) in 61Y-PDK-1complex

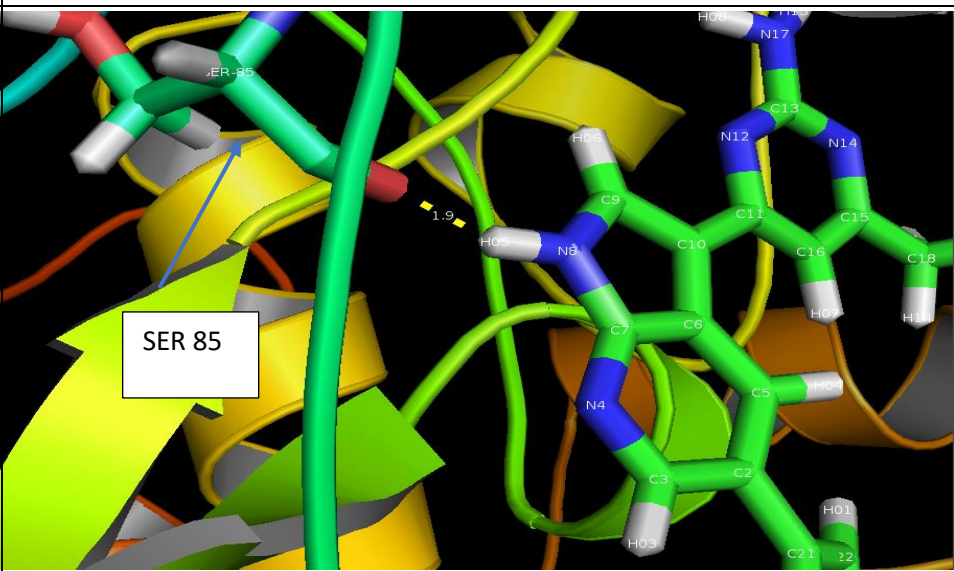
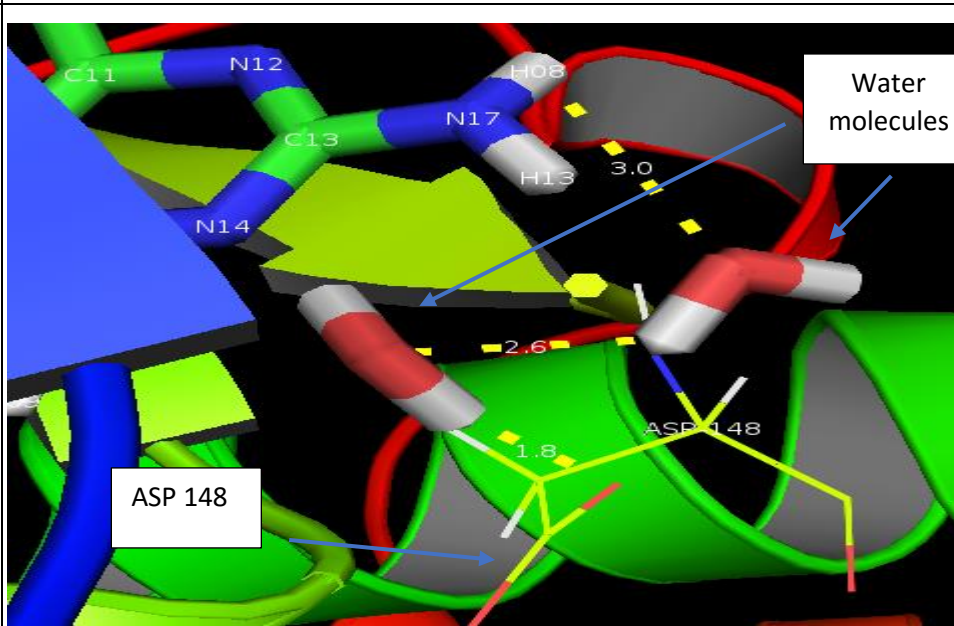
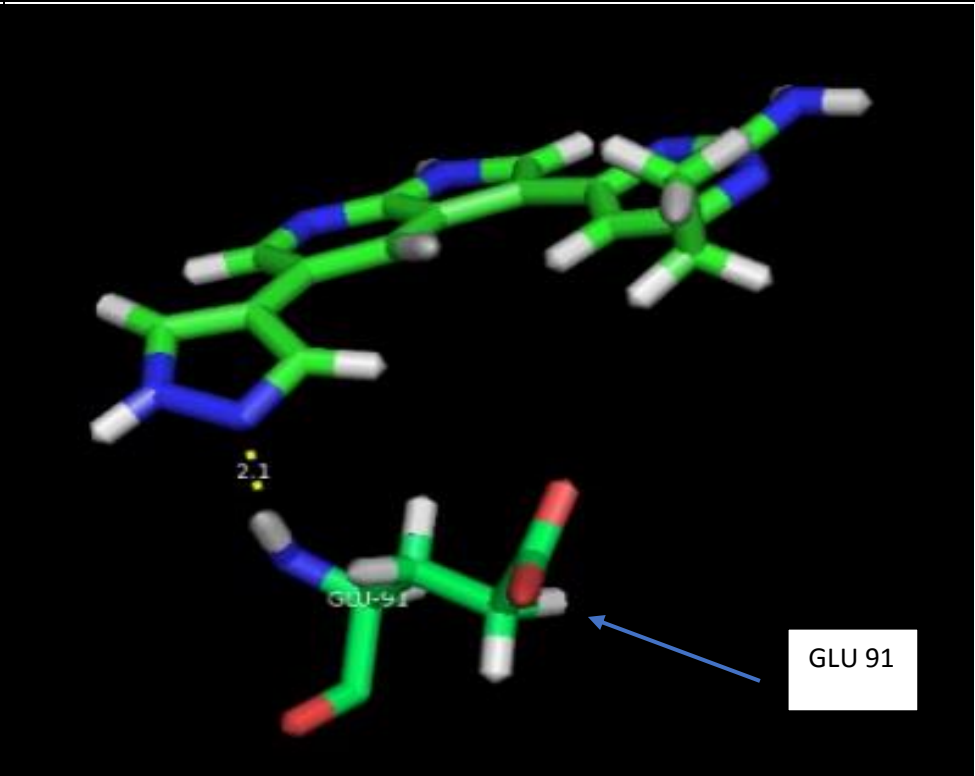
Atom of inhibitor	Atom of protein/H ₂ O	Comment
HO5	O-Ser ⁸⁵	
HO8	O-Asp ¹⁴⁸ (Water mediated)	

Table 3.5: Hydrogen bond analysis of inhibitor (4) in 61Y-PDK-1complex

Atom of inhibitor	Atom of protein/H ₂ O	Comment
N23	H-Glu ⁹¹	

Dunitz et. al⁶⁰ reported that the entropic gain of releasing a bound water molecule from the binding site of protein can be 7 cal/mol. K, corresponding to an energy gain of 2.1 kcal/mol at 300 K.⁶⁰ The entropic contribution to binding affinity is observed upon removing water molecules from the binding sites of protein molecules, and is an essential part which cannot be ignored in drug design.⁶¹

The position of water molecules in the binding sites can be used to design better inhibitors in which the principle lies in the fact that a substituent is added to the inhibitor that replaced a water molecule that bounded to kinase (design inhibitor that includes a structural water mimic).⁶²

An increase in ligand affinity can result if the contribution of substituent is greater than free energy cost which results from displacing solvent molecules. This is an easy process because the ligand already has paid the energy cost as translational and rotational entropy.⁶¹

3.7 Analysis of the binding mode of inhibitor (5)-PDK-1 complex

In this section we discussed the binding mode of inhibitor (5) with PDK-1 kinase complex (Figure 3.13(a) and (b)). Inhibitor (5) occupied allosteric site of the protein kinase PDK-1 called the PDK1 -interacting fragment (PIF)ide-binding site, or PIF pocket. This inhibitor was occupied PIF/Phosphate pocket which was determined by Lys115, Ile118, Ile119, Val124, Leu155 residues.

Inhibitor (5) binds to the inactive kinase conformation (DFG-out) in the PIF/Phosphate pocket of PDK-1 kinase, so this inhibitor considered as Type II (Deep pocket binder) inhibitor. It is worth noting that this is the first reported example of Type II (DFG-out) kinase inhibitor for AGC kinase.⁶³

Inhibitor (5) consists three molecular fragments: a hinge binding group, a linker, and a hydrophobic moiety.⁶³ The hydrophobic moiety interacts with the phosphate pocket through four strong hydrogen bond interactions. Three hydrogen bonds are formed between O34 atom and hydrogen atoms (HZ1, HZ2, and HZ3) of the amino group of Lys³⁶. The fourth strong hydrogen bond is formed between the carbonyl group of inhibitor and the amino group hydrogen atom of Asp¹⁴⁸ as shown in table 3.6.

This inhibitor interacts with the hinge region through Ser⁸⁵, and Ala⁸⁷. The first interaction is between H22 amino group hydrogen atom of inhibitor and the

carbonyl group of Ser⁸⁵. The second interaction is between carbonyl group of inhibitor and amino group hydrogen atom of backbone Ala⁸⁷ (Table 3.6).

It is worth noting that a strong intramolecular hydrogen bond interaction is present. This intramolecular interaction is between the carbonyl group and the amino group hydrogen atom (HO1). This type of interaction is like inhibitor (2) between hydrogen atom of amino group (HO2) and oxygen of carbonyl group (O14) as shown in table 3.6.

As previously stated: replacing real rings by pseudo rings to form pseudo six-membered ring is a new and non-conventional strategy and the new classes of kinase inhibitors follow this approach.⁵⁶

In addition to the strong interactions, other weak interactions were formed between inhibitor (5) and the PDK-1 (Figure 3.13(c)), C-H...C=O interaction⁵⁴ between the carbonyl group of Phe¹⁴⁹ and the carbon hydrogen atom of inhibitor (3.0 Å distance), between the carbon hydrogen atom of Leu⁸⁴ and the carbonyl group of inhibitor (3.0 Å distance) and between the carbon hydrogen atom of Tyr⁸⁶ and the carbonyl group of inhibitor (3.0 Å distance) as shown in figure 3.14(c).

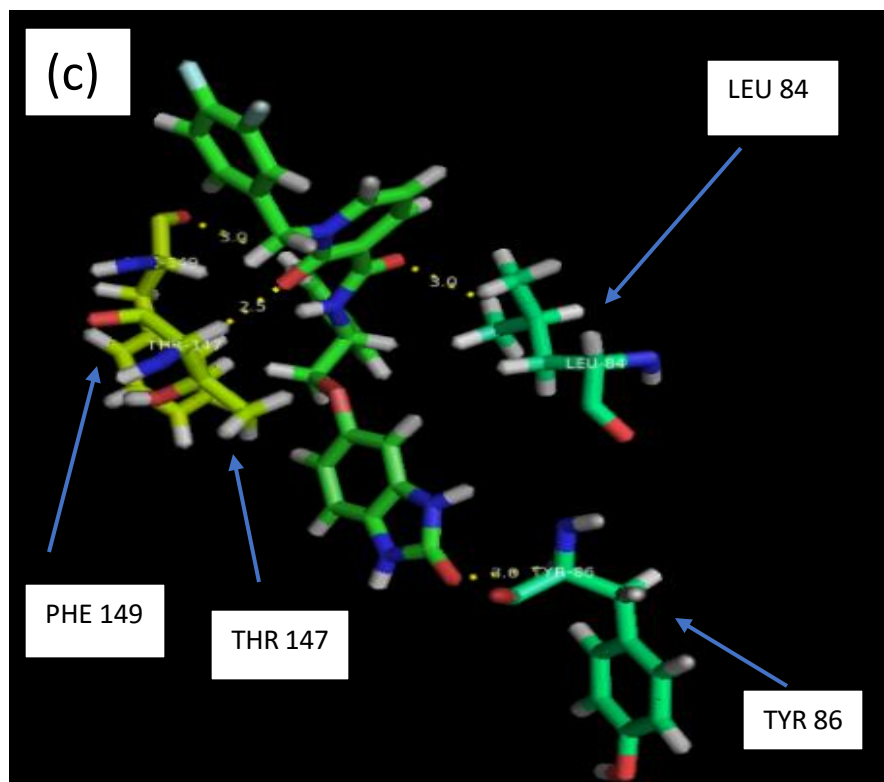
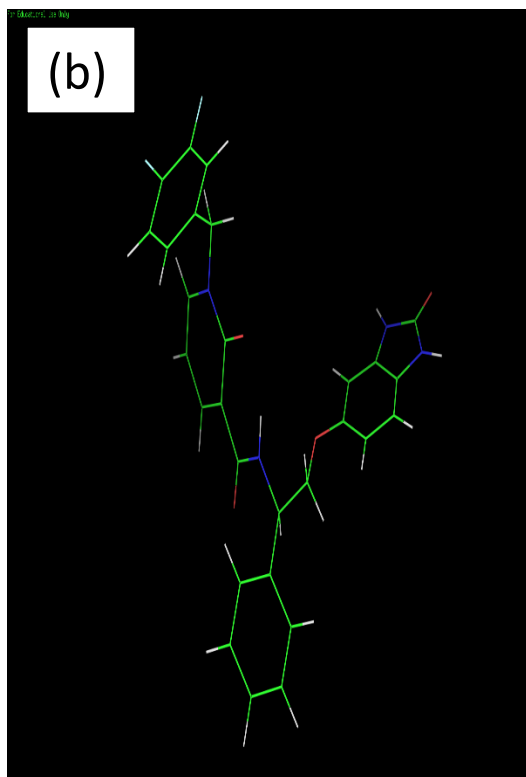
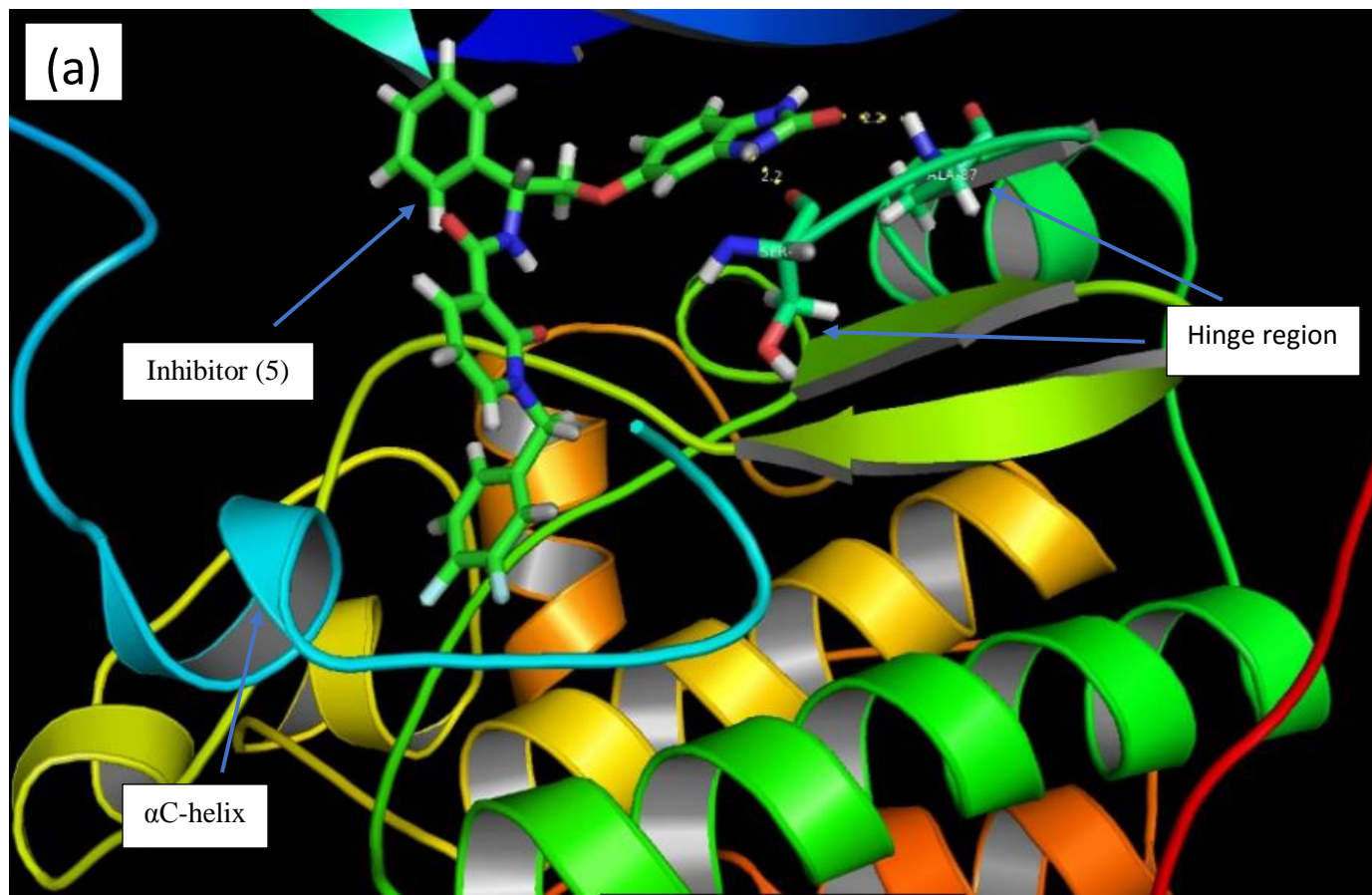


Figure 3.13: (a) Inhibitor (5)-PDK-1 complex, (b) graphical representation of inhibitor (5) and (c) other weak interactions between inhibitor (5) and kinase

Table 3.6: Hydrogen bond analysis of inhibitor (5) in MP7-PDK-1complex

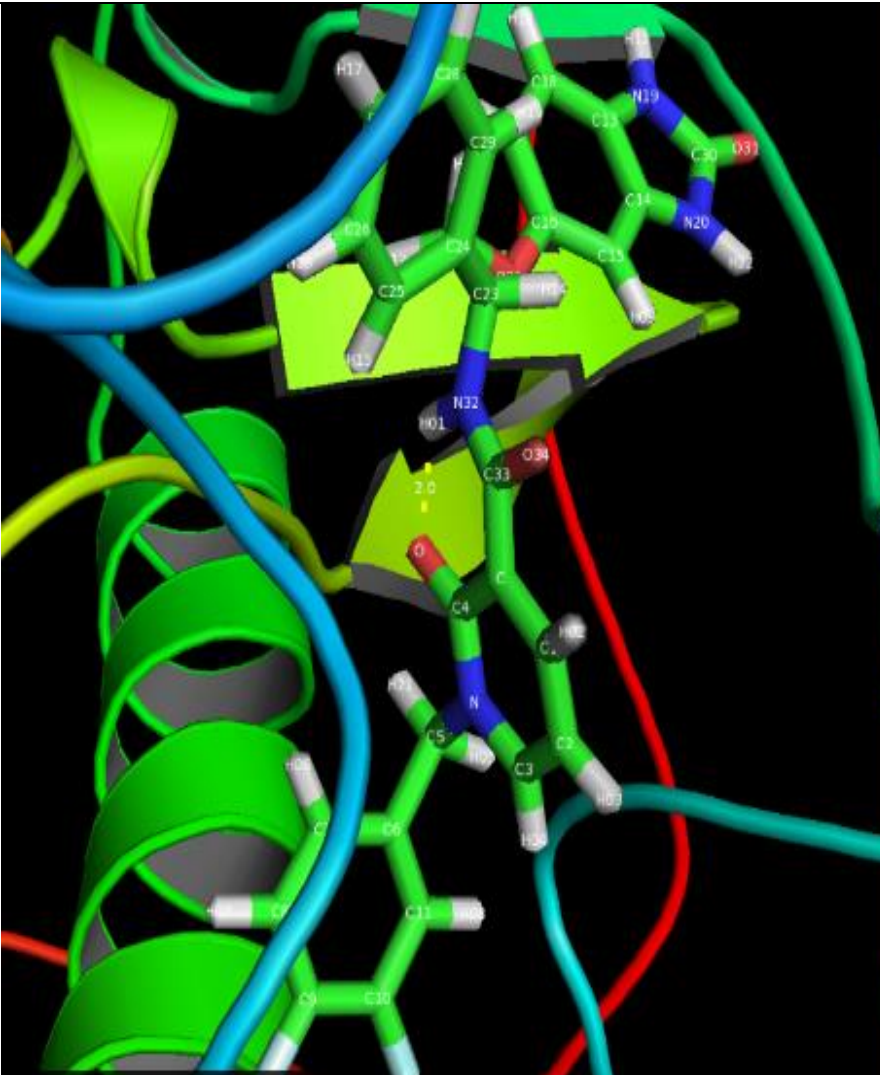
Atom of inhibitor	Atom of protein/H ₂ O	Comment
O	H-MP7 ²⁷⁹ (Intramolecular hydrogen bond)	

Table 3.6: Hydrogen bond analysis of inhibitor (5) in MP7-PDK-1complex

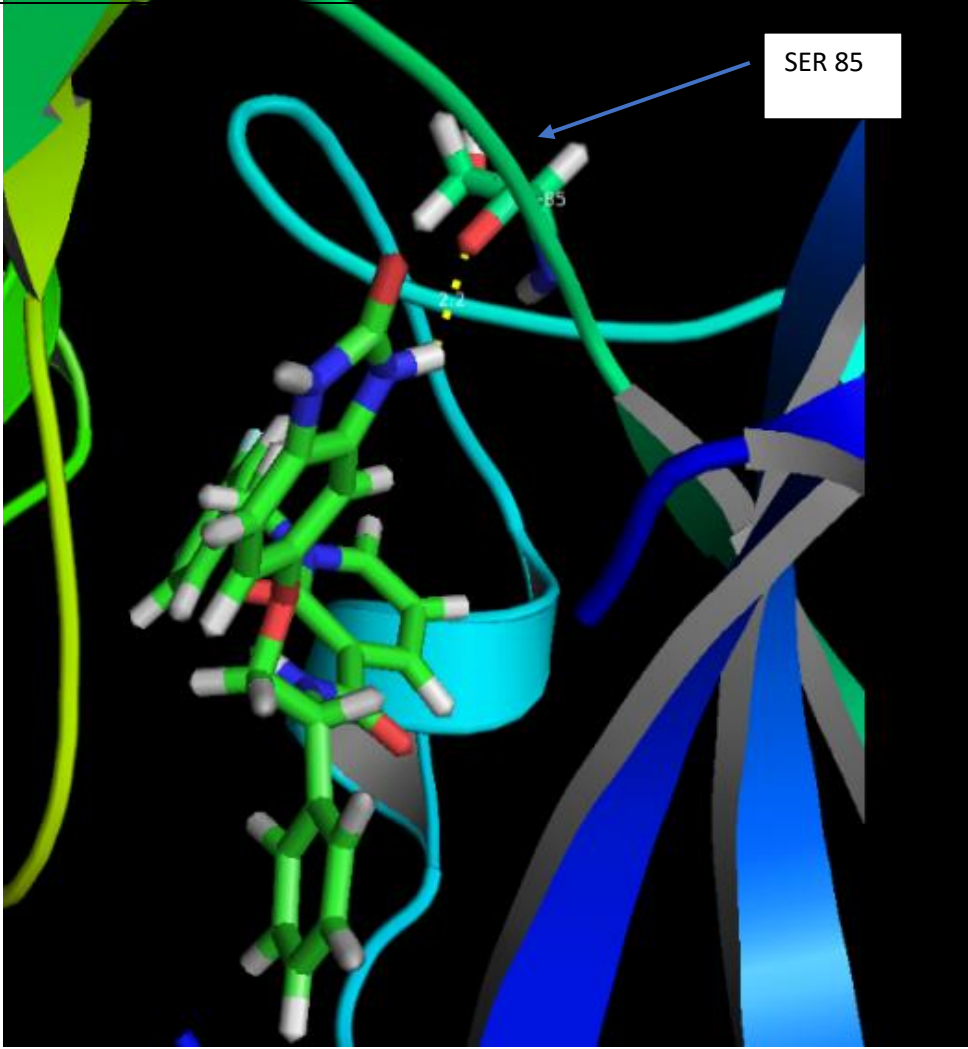
Atom of inhibitor	Atom of protein/H ₂ O	Comment
H22	O-Ser ⁸⁵	

Table 3.6: Hydrogen bond analysis of inhibitor (5) in MP7-PDK-1complex

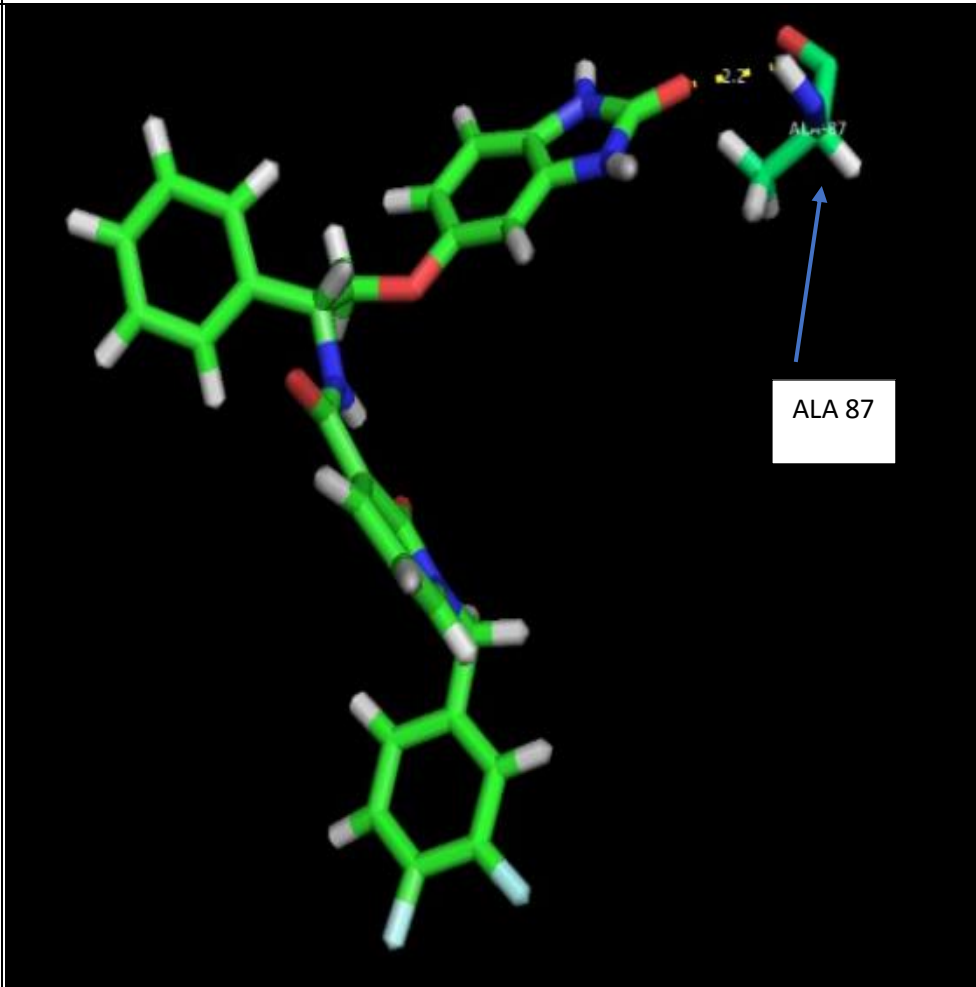
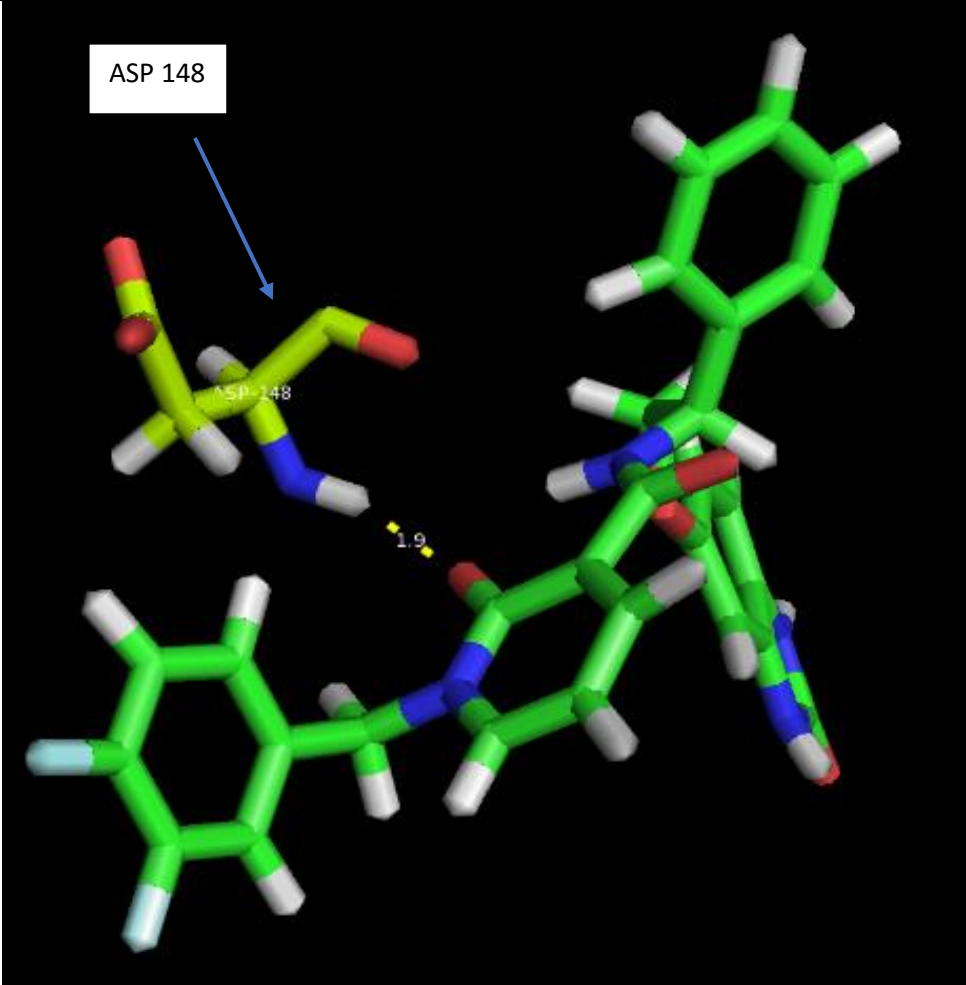
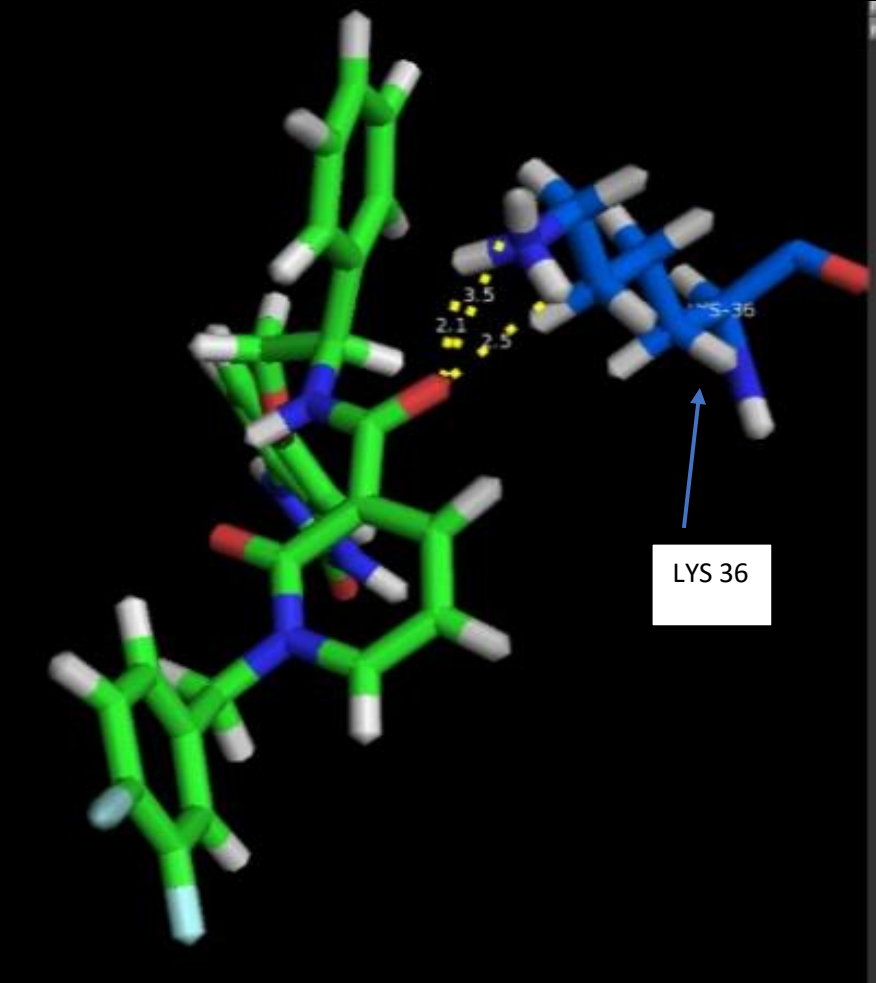
Atom of inhibitor	Atom of protein/H ₂ O	Comment
O31	H-Ala ⁸⁷	

Table 3.6: Hydrogen bond analysis of inhibitor (5) in MP7-PDK-1complex

Atom of inhibitor	Atom of protein/H ₂ O	Comment
O	H-Asp ¹⁴⁸	

Atom of inhibitor	Atom of protein/H ₂ O	Comment
O	H-Lys ³⁶	 A 3D molecular model showing the interaction between an inhibitor (green sticks) and a lysine residue (blue sticks) labeled LYS 36. The inhibitor is shown in a conformation that interacts with the lysine side chain. Distances are marked as 3.5, 2.1, and 2.5. A blue arrow points to the lysine residue, which is labeled LYS 36 in a white box.

A significant difference between the classical ATP-competitive inhibitors and Type II (Deep pocket binder) inhibitors were firstly, α C-helix of PDK-1 kinase was distorted. The conformational change in this helix is due to displacing of Glu-130 residue from the active site⁶⁰, this disruption was observed in our study.⁶⁴

Secondly, there was a hydrogen bond interaction between Arg¹³¹ with PS⁴⁸ in the classical ATP-competitive inhibitors, but this is replaced by Arg¹³¹ with Glu¹³⁰ in the inactive conformation.⁶⁴ This is consistent with our results.

It was reported that the distortion of DFG motif is the most obvious in Type II (Deep pocket binder) inhibitor. Rotation about ϕ main chain torsion angle of Asp³⁸¹, as a result of this rotation, Phe³⁸² removed from ATP pocket and Asp³⁸¹ becomes to the back pocket⁶⁵.

This conformational change creates an inactive state of the kinase because the flipped-out phenylalanine blocks ATP-binding site.⁶⁵ This distortion was not observed in our study because Asp³⁸¹ and Phe³⁸² residues were not present in the original PDB files of inhibitor-protein complex.

3.8 Effect of Thermodynamic parameters on the protein-inhibitor complexes

The unfavorable interactions between studied inhibitors (1-5) and PDK-1 is reflected in the negative value of entropic contribution ($T\Delta S$). This is due to the release of the ordered H₂O molecules in addition to the conformational change, which is typically negative as the association of a ligand with its target results in the loss of conformational freedom for one or both molecules.⁶⁶

In other words, the negative entropic contribution resulted from “freezing out” of translational, rotational and internal degrees of freedom of the ligand on

binding.⁶⁷ As illustrates in figure 3.14, the coefficient of determination value is $R^2 = 0.12$. This reflects that entropic contribution is not a driving force of binding affinity. Whereas, as appears in figure 3.15. The difference of enthalpy is considered as a driving force of binding free energy, due to the high value of coefficient of determination ($R^2 = 0.98$).

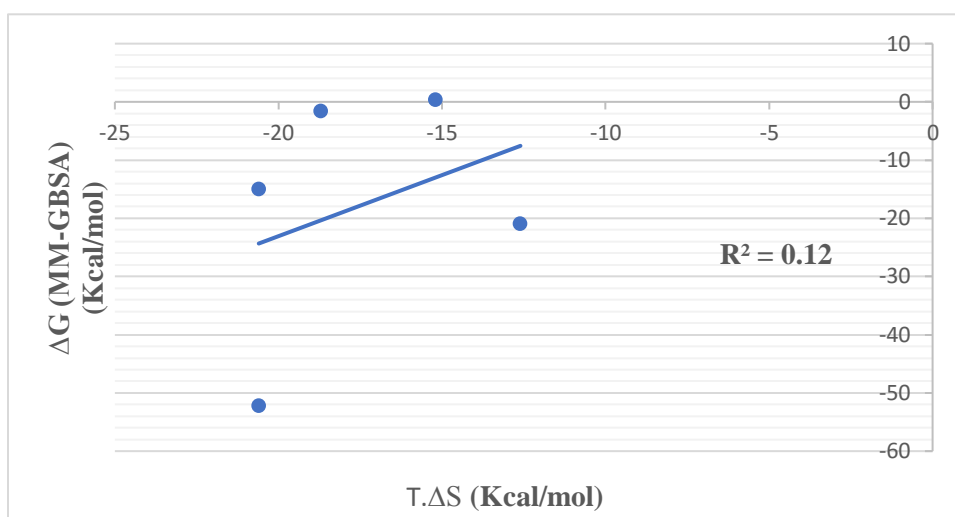


Figure 3.14: Relationship between the difference of Gibbs free energy (ΔG) and the entropic contribution ($T.\Delta S$)

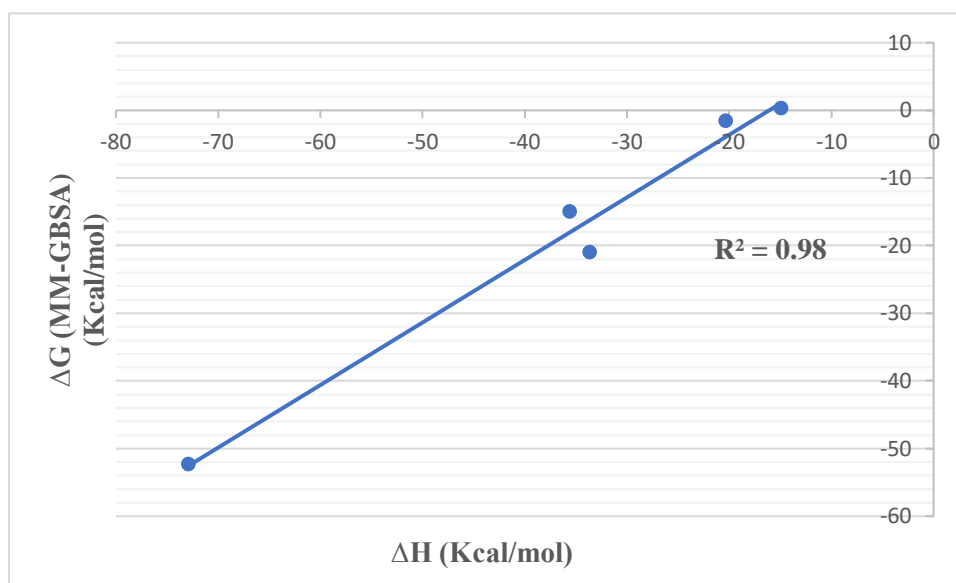


Figure 3.15: Relationship between the difference of Gibbs free energy (ΔG) and the difference of enthalpy (ΔH)

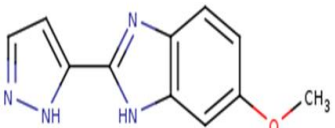
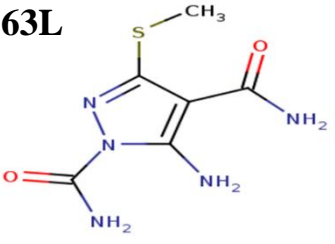
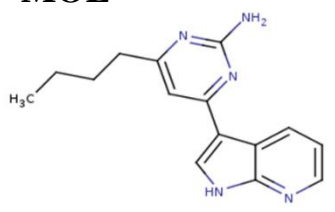
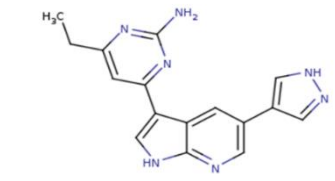
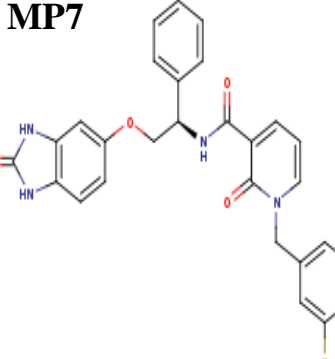
Positive contributions from both enthalpy and entropy are requirements for high affinity of binding. These two aspects of drug association should be optimized in a challenging and perplexing process because enthalpy optimization can frequently be offset by a loss in entropy. Maximizing the enthalpy contribution is difficult due to the formation of favorable H-bonds and van der Waal contacts and this is opposed by the cost of desolvation of incorrectly positioned polar moieties within a molecule.⁶⁶

The previous statement is clearly observed when we try to maximize the number of hydrogen bond interactions in inhibitor (4)-protein complex, conversely, we faced positive contribution of entropy.

The binding free energy of a ligand for its target is a function of enthalpic and entropic contributions as defined by the Gibbs free energy change. This can be parsed into individual contributions of intermolecular van der Waal attractive forces, H-bonding interactions, and repulsive forces like the hydrophobic effect that drive a ligand out of water and into the hydrophobic cavity of a protein.⁶⁶

The negative binding free energy (ΔG_{bind}) of all complexes reflects the favorable interaction between inhibitor-protein complexes in pure water except in the first complex where it gave positive value.

Table 3.7: Thermodynamic parameters of the five protein-inhibitor complexes that calculated at T= 300 K and P= 1 atm

Inhibitor	Experimental		Calculated				
	IC ₅₀ (μ M)	ΔG_{exp} (Kcal/mole)	ΔE_{MM}	ΔG_{sol}	ΔG_{calc} (MM-GBSA) (Kcal/mole)	T ΔS (Kcal/mole)	ΔH (Kcal/mole)
62O 	93	-5.5	-35.9	21.0	0.3 \pm 1.6	-15.2 \pm 3.2	-14.9
63L 	17	-6.5	-56.7	36.4	-1.6 \pm 2.0	-18.7 \pm 2.6	-20.3
MOL 	1.1	-8.1	-65.8	32.2	-21.0 \pm 1.5	-12.6 \pm 7.2	-33.6
61Y 	0.013	-10.8	-58.7	23.1	-15.0 \pm 1.8	-20.6 \pm 3.6	-35.6
MP7 	-	-	-132.0	59.1	-52.3 \pm 2.8	\square -20.6 \pm 3.6	-72.9

3.9 Correlation between IC_{50} and binding free energy

The acceptable IC_{50} value for a ligand to possess a drug-like property is (1-10) nM. According to this parameter which is most critical in determining the drug candidate, we conclude that inhibitor (1), inhibitor (2), inhibitor (3), and inhibitor (4) do not possess a drug-like property ($IC_{50} = 93 \mu\text{M}$, $17 \mu\text{M}$, $1.1 \mu\text{M}$, $0.013 \mu\text{M}$), respectively, because they dissociate and do not stay bound to the enzyme.

These values are correlated with binding free energies of these complexes that calculated by MM-GBSA which are 0.3 Kcal/mol, -1.6 Kcal/mol, -21.0 Kcal/mol, -15.0 Kcal/mol. We noted that IC_{50} becomes lower, binding free energy become larger in negative sign, and become more druggable property.

IC_{50} of Inhibitor (1) is equals $93 \mu\text{M}$, this inhibitor does not possess drug-like property, and this result agree with what we computed, ΔG_{bind} of this inhibitor with PDK-1 kinase is 0.3 Kcal/mol. The positive sign of this value resulted from the formation of only one hydrogen bond interaction.

But if we look about inhibitor (5), we noted that this inhibitor has high value of ΔG_{bind} equals -52.3 Kcal/mol, this high negative value resulted from the formation of six strong hydrogen bond interactions. with no water mediated was present.

But if we compared inhibitor (3) and inhibitor (4) we see the IC_{50} values of inhibitor (3) and inhibitor (4) is 1.1 μM and 0.013 μM respectively. But the binding affinities of these inhibitors are -21.0 Kcal/mol and -15.0 Kcal/mol respectively. This is explained by the fact that the stronger the hydrogen bonds formed between the water molecule and the binding site, more favorable enthalpic contribution occur, and at the same time water molecules become less disordered and more highly restricted (less favorable entropic contribution).⁶⁵

In inhibitor (4)-protein complex there were three water molecules instated in inhibitor (3)-protein complex there were only two water molecules.

As appear in figure 3.16, the IC_{50} values are well correlated with the binding affinities that calculated by MM-GBSA. The coefficient of determination in this case equals 0.55.

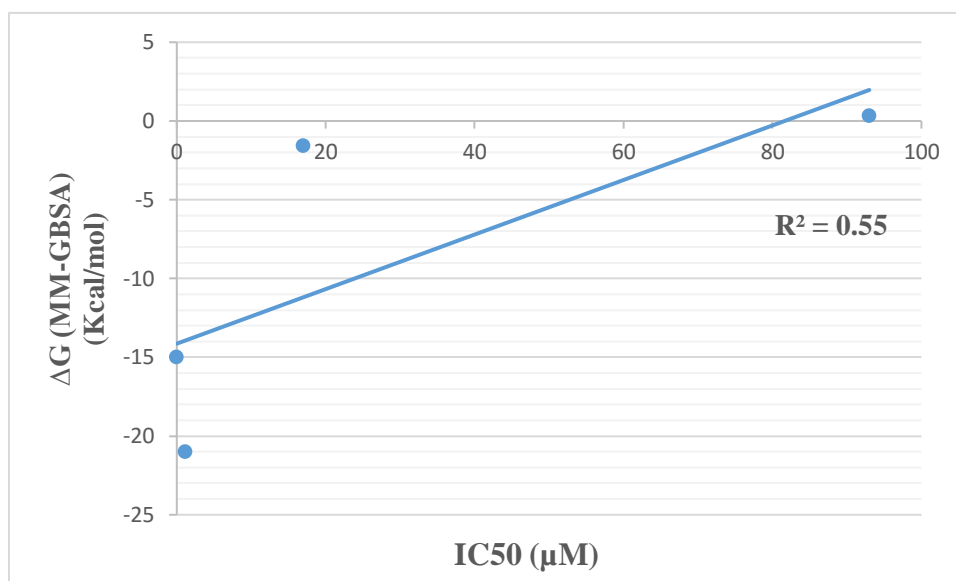


Figure 3.16: Correlation between the IC_{50} values and binding free energies that calculated by MM-GBSA

Whereas, the correlation between the IC_{50} and the binding free energy that calculated by MM-PBSA, is weaker (Figure 3.17). The coefficient of determination in this case equals 0.14.

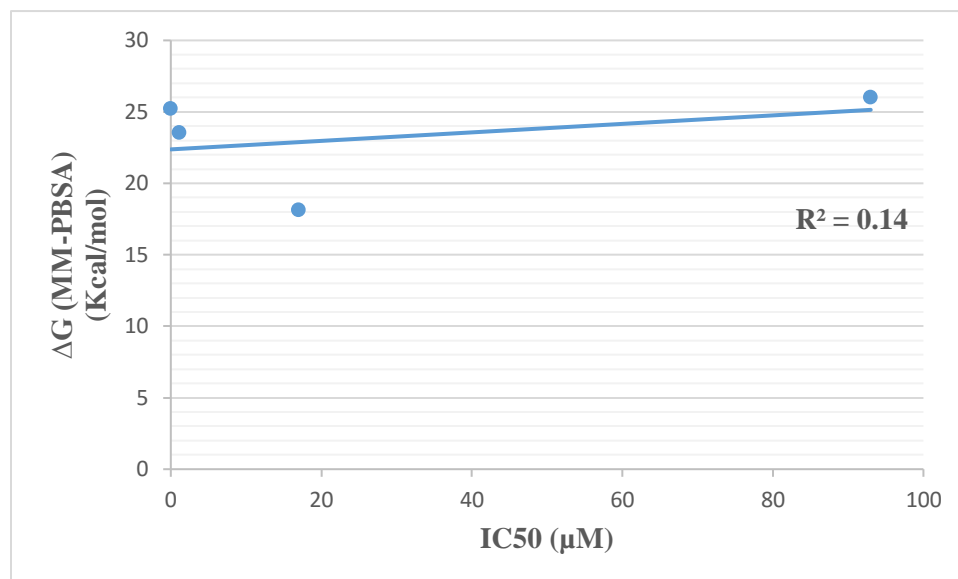


Figure 3.17: Correlation between the IC_{50} values and binding free energies that calculated by MM-PBSA

It is worth noting, that the coefficient of determination is the same with correlation between IC_{50} values and the experimental binding free energies equals 0.55 (Figure 3.18).

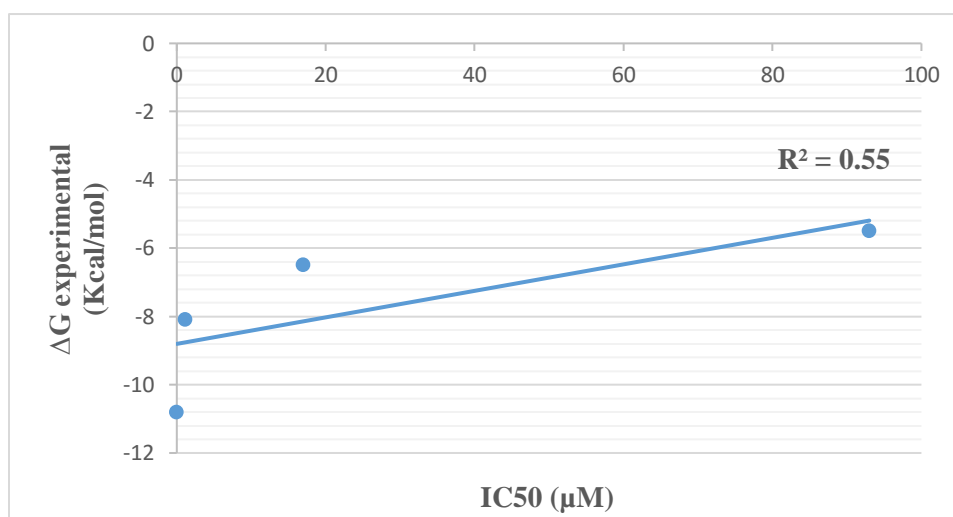


Figure 3.18: Correlation between the IC_{50} values and the experimental binding free energies

3.10 Energies calculated by MM-GBSA and contributing energies

All inhibitors studied in this work except inhibitor (3) share the most prominent binding contributions from the van der Waals (VDW) interactions. VDW values were -42.8 Kcal/mol, -30.7 Kcal/mol, -40.3 Kcal/mol, -76.4 Kcal/mol for inhibitor (1)-kinase complex, inhibitor (2)-kinase complex, inhibitor (4)-kinase complex, and inhibitor (5)-protein complex, respectively (Table 3.8, Figure 3.19).

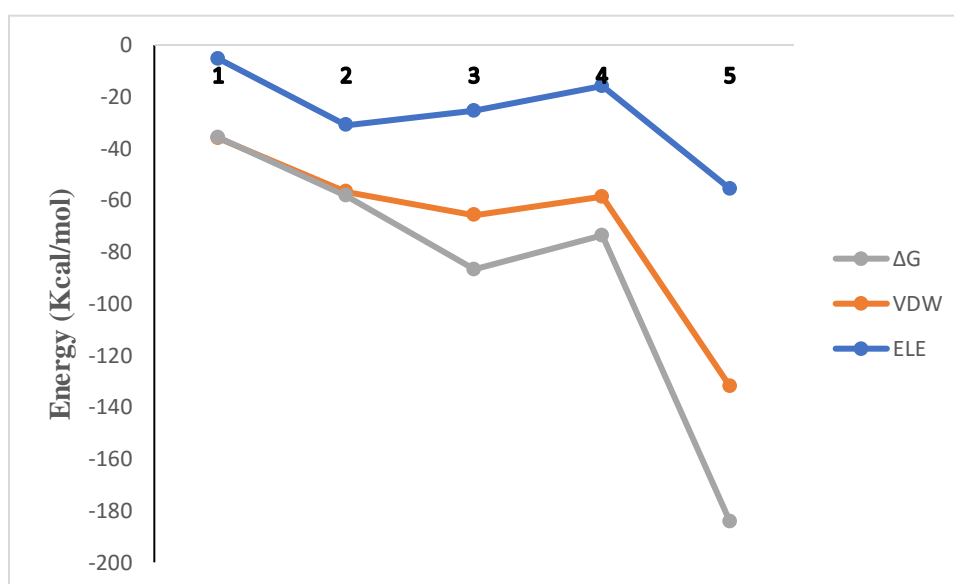
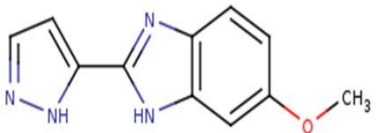
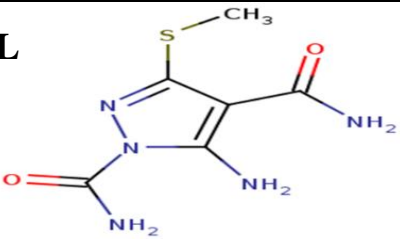
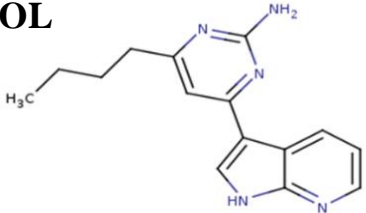
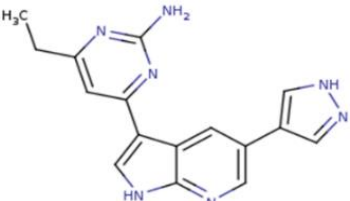
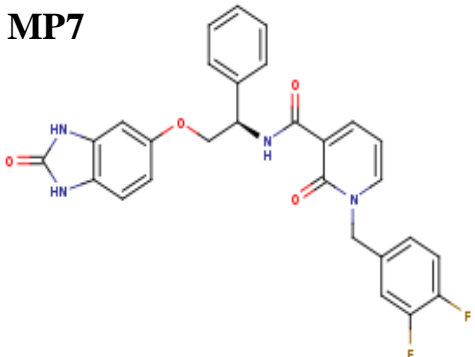


Figure 3.19: Contributions of electrostatic energy and van der Waals energies to the difference of Gibbs free energy (ΔG) of different inhibitor-PDK-1 kinase complexes

Table 3.8: Total binding free energy (ΔG_{total}), van der Waals energy (VDW), electrostatic energy (ELE), solvation free energy (ΔG_{sol}), and binding free energy of inhibitor-protein complex (ΔG_{bind}) that calculated by MM-GBSA. All energies are in unit kcal/mol

Inhibitor	ΔG_{total}	VDW	ELE	ΔG_{sol}	ΔG_{bind} (MM-GBSA)
62O 	-15.0	-30.7	-5.3	21.0	0.3 ± 1.6
63L 	-20.3	-25.7	-31.0	36.4	-1.6 ± 2.0
MOL 	-33.6	-40.3	-25.5	32.2	-21.0 ± 1.5
61Y 	-35.6	-42.8	-15.9	23.1	-15.0 ± 1.8
MP7 	-72.9	-76.4	-55.6	59.1	-52.3 ± 2.8

The binding free energy values are well correlated with van der Waals Energy calculated by molecular mechanics (VDW). The coefficient of determination value in this case equals 0.96 (Figure 3.20).

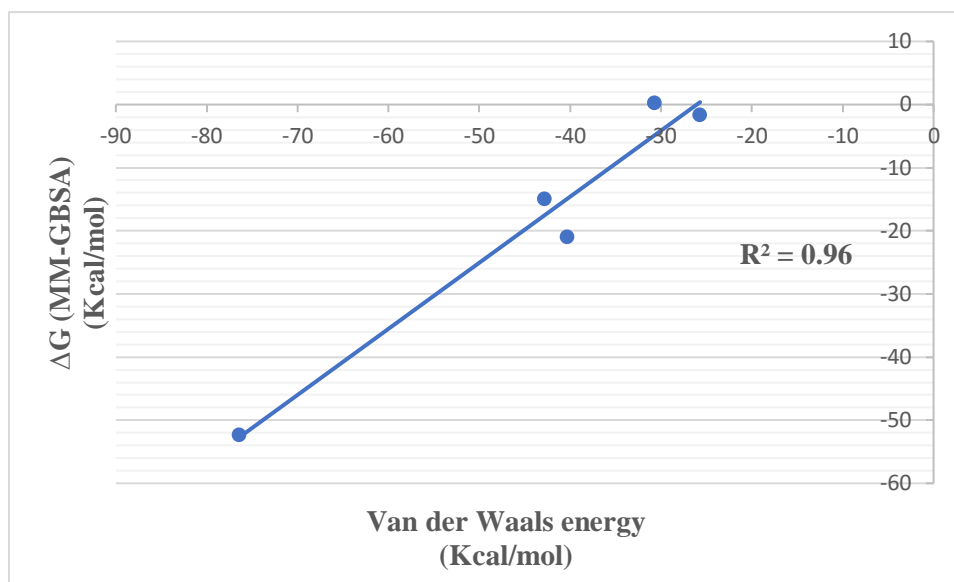


Figure 3.20: Relationship between the difference of Gibbs free energy (ΔG) and the Van der Waals energy

To the contrary, the correlation between the electrostatic energy and the binding free energy, is weaker (Figure 3.21). The coefficient of determination in this case equals 0.70.

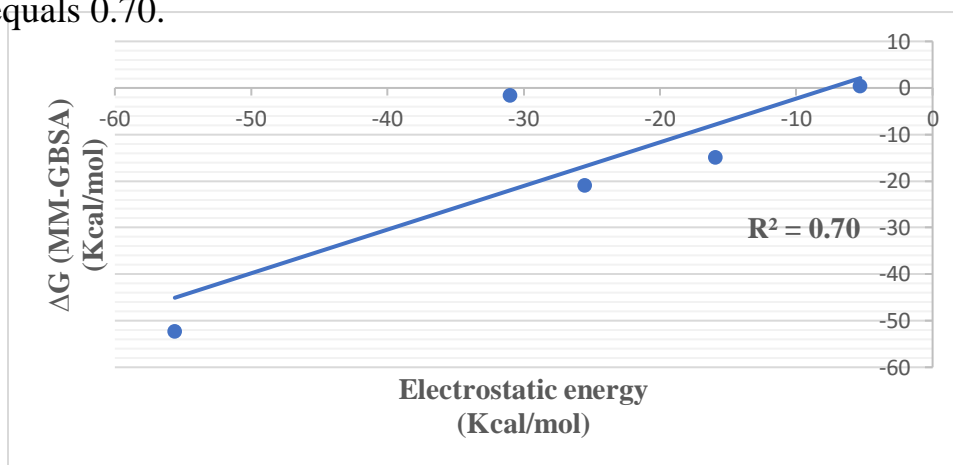


Figure 3.231: Relationship between the difference of Gibbs free energy (ΔG) and the electrostatic energy

3.11 Classification of inhibitors studied

The structure of all inhibitor-protein complexes except inhibitor (5) show a phosphorylated T-loop and are therefore, assumed to be in an active state.¹⁷ According to Traxler model, inhibitors (1-4) bind to the activated (phosphorylated) form of the protein kinase and occupy the ATP binding site with at least a formation of one hydrogen bond with the hinge region. This reflects the fact that these inhibitors belong to traditional pharmacophore model (type I) or classical ATP-competitive inhibitor.⁶⁸

It is worth noting that these inhibitors are reversible ATP-competitive because the type of interaction is mostly hydrogen bonding interaction and no irreversible covalent bond formation.⁶⁹

Inhibitor (5) binds to the inactive kinase conformation (DFG-out) in the PIF/Phosphate pocket of PDK-1 kinase, so this inhibitor is considered as Type II (Deep pocket binder) inhibitor. It is worth noting that this is the first reported example of Type II (DFG-out) kinase inhibitor for AGC kinase.⁶³

Another evidence proved that inhibitor (5) is considered as deep-pocket binder inhibitor Type (II) is the absence of water-mediated hydrogen bond interactions. The presence of water molecules in the binding sites is considered a feature that distinguishes Type (I) from Type (II) inhibitors.

3.12 Analysis of the inhibitors according to Lipinski's Rule of five, Veber Rule and MDDR Rule

The fragment -based approach to calculate the polar surface area (PSA) descriptor, is a free software package. In this study, *Molinspiration* was used to calculate PSA (with other useful molecular descriptors). *SMILES* files are required to process the values.⁷⁰

All inhibitors in this study agreed with the Lipinski's rule of five (ROF), except for inhibitor (2). The number of atoms that donate hydrogen atoms to form hydrogen bonds (HBD) was 6 which is higher than the acceptable value (Fig 3.22).

According to Veber's and MDDR Rules, all values for inhibitors in this study are consistent with these Rules except for inhibitor (2) which has NOR value of one (Fig 3.22). This value is lower than the acceptable value (NOR=3).

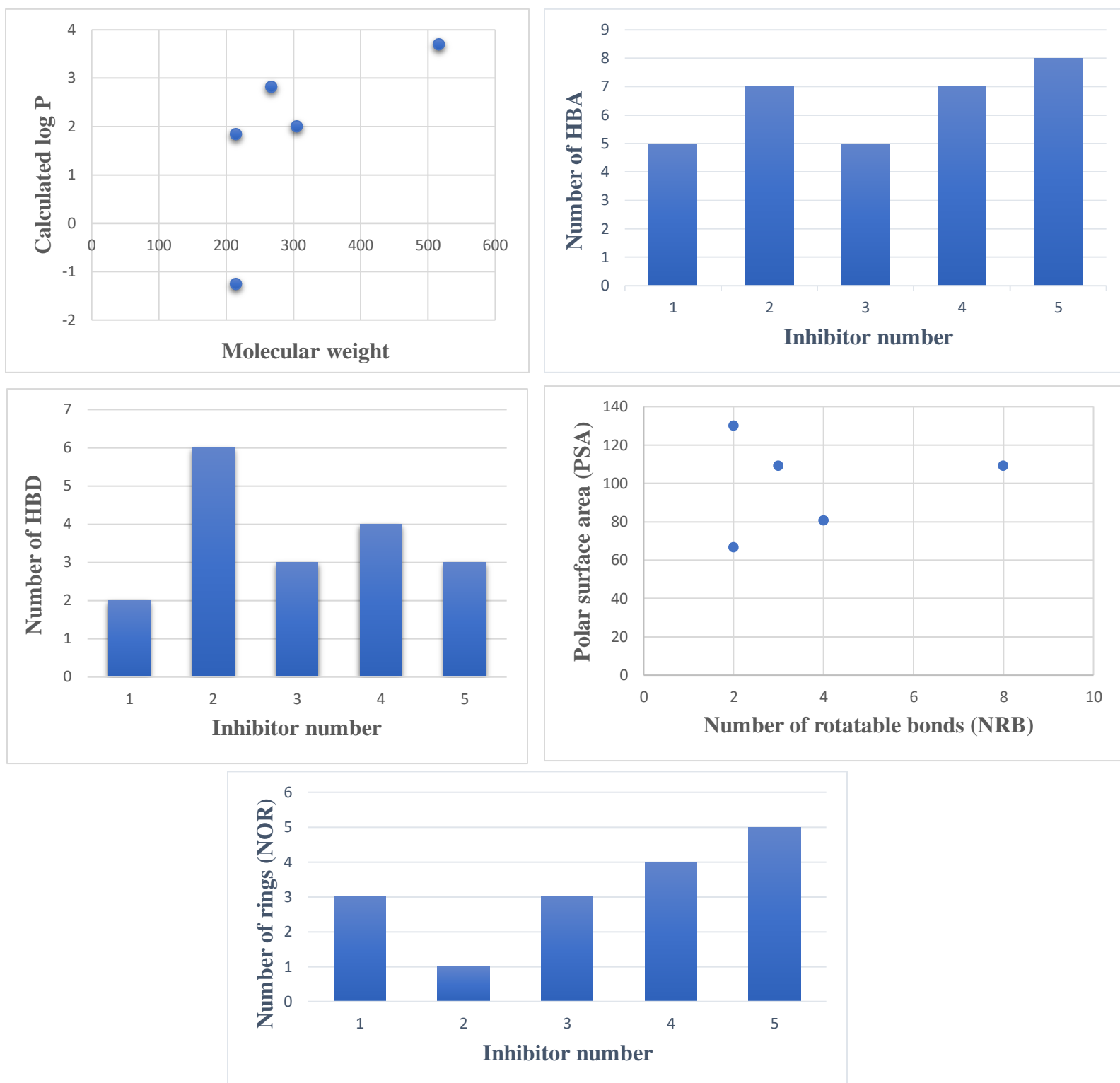
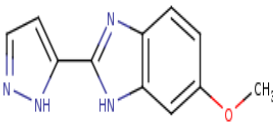
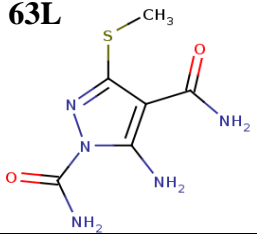
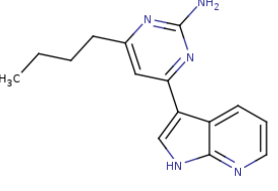
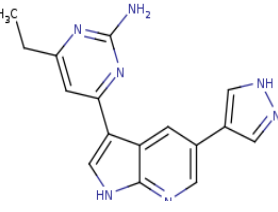
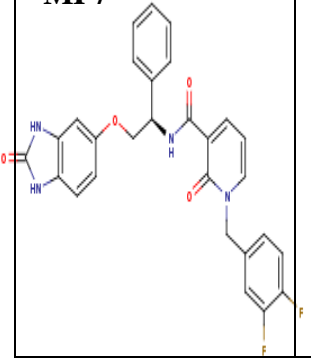


Figure 3.22: Analysis of the inhibitors according to Lipinski's Rule of five, Veber and MDDR Rules

Table 3.9: Analysis of the inhibitors according to Lipinski's Rule of five, Veber and MDDR Rules

Inhibitor	Molecular weight (g/mol)	A ⁷⁰ logP	PSA ⁷⁰ (Å ²)	Num-H acceptor Atoms	Num-H donar Atoms	Num-of rings	Number of Rotatable Bond	Ligand efficiency
62O 	214.23	1.84	66.60	5	2	3	2	0.33
63L 	215.24	-1.26	130.04	7	6	1	2	0.45
MOL 	267.34	2.81	80.49	5	3	3	4	0.45
61 	305.35	2.00	109.17	7	4	4	3	0.47
MP7 	516.50	3.70	108.99	8	3	5	8	0.32

In addition to the previous parameters that determine the drug-like properties, the ligand efficiency is an essential common metric to assess the drug-like quality of a compound⁷¹. This is estimated by relating binding free energy to the number of heavy atoms in a molecule ($LE = -\Delta G / HA$).⁷² Therefore, the resulting ligand efficiency tends to be maximal for small molecules (e.g. fragments) and then steadily decreases as heavier atoms are added. The LE value for a small molecule that inhibit protein-protein interaction is a round 0.24, whereas LE is equal to 0.3 or higher is a desired value.

It is observed that all ligand efficiency values of our inhibitors were higher than 0.3. So we can conclude that all our inhibitors except inhibitor (2) have the drug-like properties when applying Lipinski's Rule of five, Veber Rule and MDDR Rule.

There is a good correlation between the difference of Gibbs free energy (ΔG) calculated by MM-GBSA and the molecular weight, the value of correlation coefficient of determination is $R^2 = 0.94$ (Figure 3.23).

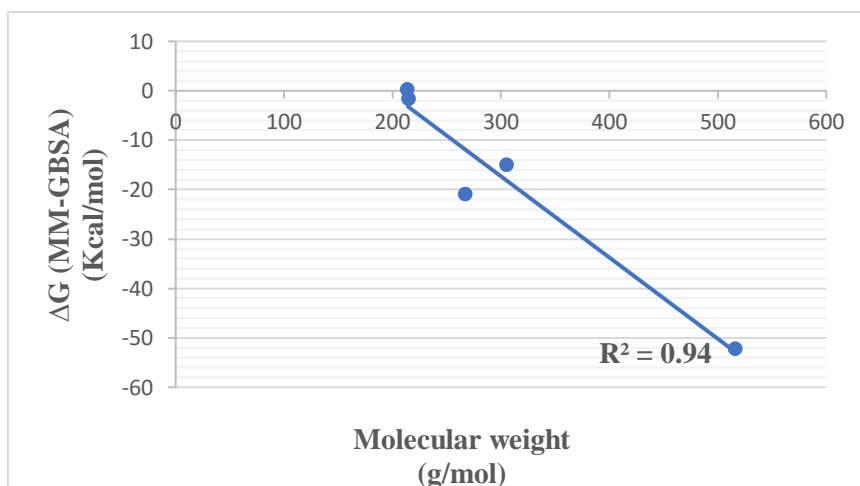


Figure 3.23: Relationship between the difference of Gibbs free energy (ΔG) calculated by MM-GBSA and the molecular weight

Also a good correlation between the difference of Gibbs free energy (ΔG) calculated by MM-GBSA and the lipophilicity property of inhibitor ($\log P$), the value of coefficient of determination is $R^2 = 0.54$ (Figure 3.24).

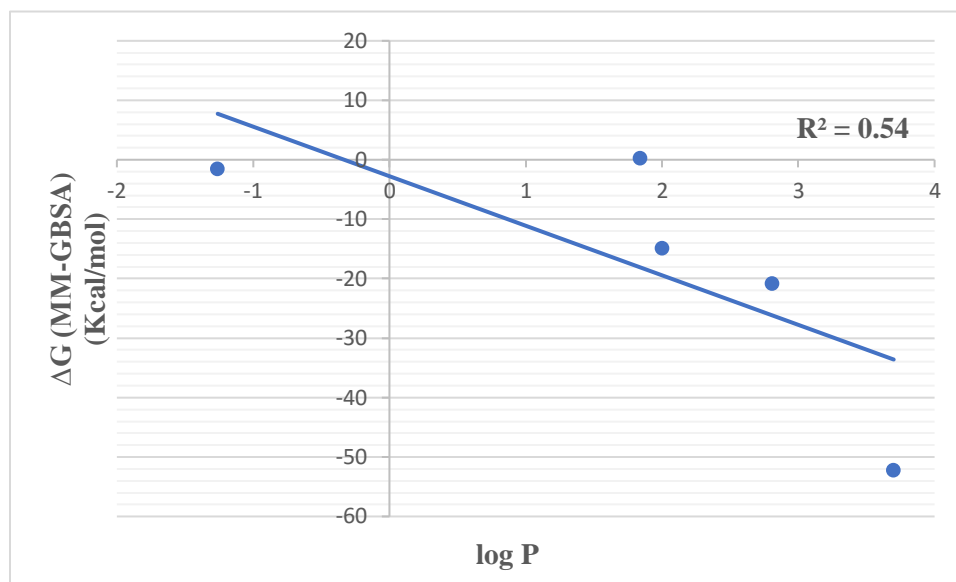


Figure 3.24: Relationship between the difference of Gibbs free energy (ΔG) calculated by MM-GBSA and $\log P$

To the contrary, the correlation between the binding free energy (ΔG) calculated by MM-GBSA and the polar surface area (PSA), is weaker (Figure 3.25).

The coefficient of determination in this case equals 0.02.

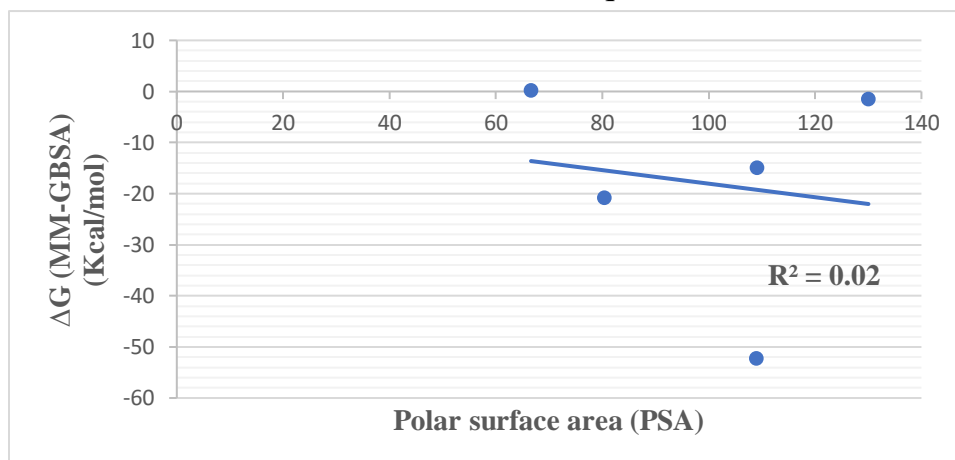


Figure 3.25: Relationship between the difference of Gibbs free energy (ΔG) calculated by MM-GBSA and PSA

3.13 Potency and selectivity of Inhibitor (5)

Inhibitor (5) made six strong hydrogen bonds with the PIF/Phosphate pocket of PDK-1 kinase with no water mediated hydrogen bond interaction; this interaction reflects the high affinity ($\Delta G_{\text{bind}} = -52.3$ Kcal/mol), which indicates high potency of this inhibitor.

The high sequence similarity in the ATP binding pocket between different kinases is a major challenge for developing inhibitors that are specific for one or a small number of kinases.

Inhibitor (5) is consider as type II inhibitors, which occupied PIF/phosphate pocket of PDK-1 kinase. This allosteric site in protein kinase are especially used for developing more selective inhibitors⁷³. This offers a possibility to develop more compounds with higher selectivity more than in the case of classical ATP-competitive inhibitors.⁶⁴

Deep-pocket binder molecules, when used as single substrate, can be classified as substrate-selective PDK-1 inhibitors. When used in combination with ATP-competitive inhibitors they tend to suppress the activation of the downstream kinases.⁷³

4. CONCLUSION

Molecular dynamics simulation was employed to identify an exquisitely potent PDK-1 inhibitor 5 (1-(3,4-difluorobenzyl)-2-oxo-N-((1R)-2-[(2-oxo-2,3-dihydro-1H-benzimidazol-5-yl)oxy]-1-phenylethyl)-1,2-dihydropyridine carboxamide) that uniquely binds to the inactive kinase conformation.

This inhibitor is tightly bound to PDK-1 through five strong hydrogen bonds with the PIF/Phosphate pocket of PDK-1 kinase with no water mediated hydrogen bond interactions. This interaction reflects the high affinity of drug to receptor ($\Delta G_{\text{bind}} = -52.3$ Kcal/mol).

In contrast to compounds 1-4, which are classical ATP-competitive kinase inhibitors (DFG-in) which are 6-methoxy-2-(1H-pyrazol-5-yl)-1H-benzimidazole (inhibitor 1), 4-dicarboxylic acid diamide (inhibitor 2), 4-butyl-6-(1H-pyrrolo[2,3-b]pyridin-3-yl)pyrimidin-2-amine (inhibitor 3), 4-ethyl-6-[5-(1H-pyrazol-4-yl)-1H-pyrrolo[2,3-b]pyridin-3-yl]pyrimidin-2-amine (inhibitor 4).

MM-PBSA and MM-GBSA both methods are used in this work to calculate the binding free energies of PDK-1 kinase with four inhibitors. There is a good correlation between binding free energy which was calculated by MM-GBSA and experimental values of binding free energy which are derived from the experimental

reported IC_{50} values ($R^2=0.55$). To the contrary, the correlation between the binding free energy was calculated by MM-PBSA and experimental values of binding free energy which are derived from the experimental reported IC_{50} values is weaker ($R^2=0.14$). This result agrees with some of the reports that MM-GBSA is considered a better approach than the MM-PBSA in calculating the binding free energies when metals are not involved.

According to IC_{50} values we conclude that inhibitor (1), inhibitor (2), inhibitor (3), and inhibitor (4) do not possess a drug-like property ($IC_{50} = 93 \mu\text{M}$, $17 \mu\text{M}$, $1.1 \mu\text{M}$, $0.013 \mu\text{M}$), respectively, because they dissociate and do not stay bound to the enzyme.

And these values are correlated with binding free energies of these complexes that calculated by MM-GBSA which are 0.3 Kcal/mol , -1.6 Kcal/mol , -21.0 Kcal/mol , -15.0 Kcal/mol , -52.3 Kcal/mol . We noted that IC_{50} become lower, and binding free energy become larger in negative sign, and become more druggable property.

As PDK-1 is a well validated anticancer target, the final results reveal the binding modes between PDK-1 kinase and the five inhibitors which can be used in the future in drug design for cancer treatment. The position of water molecules in the binding sites of inhibitor (2)-kinase and inhibitor (3)-kinase

complexes can be used to design better inhibitors in which the principle lies in the fact that a substituent is added to the ligand that displaces a bound water molecule based on the creation of new inhibitor that includes a structural water mimic.

References

- [1] Hughes, J. P.; Rees, S. S.; Kalindjian, S. B.; Philpott, K. L. *Br. J. Pharmacol.* **2011**, *162* (6), 1239–1249.
- [2] Kapetanovic. I. *Chem Biol Interact.* **2008**, *171*(2), 165–176.
- [3] Drews, J. *Science.* **2000**, *287* (5460), 1960–1964.
- [4] Owens, J. *Nat. Rev. Drug Discov.* **2007**, *6* (2), 99–101.
- [5] Veselovsky, V; Ivanov, S. *Curr. Drug Targets. Infect. Disord.* **2003**, *3* (1), 33–40.
- [6] Sliwoski, G.; Kothiwale, S.; Meiler, J.; Lowe Jr., E. W. *Pharmacol Rev* **2014**, *66* (1), 334–395.
- [7] Wilson, G. L.; Lill, M. A. *Future Med. Chem.* **2011**, *3* (6), 735–750.
- [8] Manning, G. *Science* **2002**, *298* (5600), 1912–1934.
- [9] Hirpara, K. V; Aggarwal, P.; Mukherjee, A. J.; Joshi, N.; Burman, A. C. *Anticancer. Agents Med. Chem.* **2009**, *9* (2), 138–161.
- [10] Shchemelinin, I.; Sefc, L.; Necas, E. *Folia Biol. (Praha).* **2006**, *52* (3), 81–101.
- [11] Giamas, G.; Stebbing, J.; Vorgias, C. E.; Knippschild, U. *Pharmacogenomics* **2007**, *8*, 1005–1016.
- [12] Mikalsen, T.; Gerits, N.; Moens, U. *Biotechnol. Annu. Rev.* **2006**, *12* (6), 153–223.
- [13] Shapiro. C.; Recht. A. *N Engl J Med* **2001**, *344* (26), 1997-2008.

- [14] Garcia, M.; Jemal, A.; Ward, E. M.; Center, M. M.; Hao, Y.; Siegel, R. L.; Thun, M. *American Cancer Society*, **2007**, 18
- [15] Scheid, M. P.; Parsons, M.; Woodgett, J. R. *Mol Cell Biol* **2005**, 25 (6), 2347–2363.
- [16] Mora, A.; Komander, D.; Van Aalten, D. M. F.; Alessi, D. R. *Semin. Cell Dev. Biol.* **2004**, 15 (2), 161–170.
- [17] Biondi, R. M.; Komander, D.; Thomas, C. C.; Lizcano, J. M.; Deak, M.; Alessi, D. R.; Van Aalten, D. M. F. *EMBO J.* **2002**, 21 (16), 4219–4228.
- [18] Vulpetti, A.; Bosotti, R. *Farmaco* **2004**, 59 (10), 759–765.
- [19] Zeng, H.; Cao, R.; Zhang, H. J. *Chem. Inf. Model* **2008**, 48 (9), 1760–1772.
- [20] Miyazawa, K. J. *Biochem.* **2011**, 150 (1), 1–3.
- [21] Bain, J.; Plater, L.; Elliott, M.; Shpiro, N.; Hastie, C. J.; Mclauchlan, H.; Klevernic, I.; Arthur, J. S. C.; Alessi, D. R.; Cohen, P. *Biochem. J* **2007**, 408 (3), 297–315.
- [22] Wucherer-Plietker, M.; Merkul, E.; Müller, T. J. J.; Esdar, C.; Knöchel, T.; Heinrich, T.; Buchstaller, H. P.; Greiner, H.; Dorsch, D.; Finsinger, D.; Calderini, M.; Bruge, D.; Grädler, U. *Bioorganic Med. Chem. Lett.* **2016**, 26 (13), 3073–3080.
- [23] Feldman, R. I. *J. Biol. Chem.* **2005**, 280 (20), 19867–19874.
- [24] Singh, S.; Srivastava, P. *Comput Mol Biosci* **2015**, 5, 20–33.
- [25] Ong, K. and Khoo, H. *Gen. Pharmac* **1997**, 29 (2), 121–126.
- [26] Peifer, C.; Alessi, D. R. *ChemMedChem* **2008**, 3 (12), 1810–1838.
- [27] Blanc, J.; Geney, R.; Menet, C. *Anticancer Agents Med Chem.* **2013**, 13, 731.

- [28] Backes, A. C.; Zech, B.; Felber, B.; Klebl, B.; Müller, G. *Expert Opin. Drug Discov.* **2008**, *3*, 1409-1425.
- [29] Wu, P.; Nielsen, T. E.; Clausen, M. H. *Drug Discov. Today* **2016**, *21* (1), 5–10.
- [30] Leeson, P.; Oncology, H.; Hospital, C. *Nature* **1912**, *481*, 455–456.
- [31] Nguyen, T.; Lee, S.; Wang, H.-K.; Chen, H.-Y.; Wu, Y.-T.; Lin, S.; Kim, D.-W.; Kim, D. *Molecules* **2013**, *18* (12), 15600–15612.
- [32] Lipinski, C. A.; Lombardo, F.; Dominy, B. W.; Feeney, P. J. *Adv. Drug Deliv. Rev.* **1997**, *23*, 3–25.
- [33] Veber, D. F. *J. Med. Chem.* **2002**, *45*, 2615–2623.
- [34] Oprea, T. I. *J. Comput. Aided. Mol. Des.* **2000**, *14* (3), 251–264.
- [35] Swanson, J. M. J.; Henschman, R. H.; McCammon, J. A. *Biophys. J* **2004**, *86* (1), 67–74.
- [36] Lu, N.; Kofke, D. A. *J. Chem. Phys.* **2001**, *115* (15), 6866–6875.
- [37] Synthetic, S. O. F. *Molecular Dynamics - Studies of Synthetic and Biological Macromolecules*; **2012**.
- [38] Miller, B. R.; McGee, T. D.; Swails, J. M.; Homeyer, N.; Gohlke, H.; Roitberg, A. E. *J. Chem. Theory Comput.* **2012**, *8* (9), 3314–3321.
- [39] Homeyer, N.; Gohlke, H. *Mol. Inform.* **2012**, *31* (2), 114–122.
- [40] Honig, B.; Nicholls, A. *Science* **1995**, *268* (5214), 1144–1149.
- [41] Hermansson, A. *Calculating Ligand-Protein Binding Energies from Molecular Dynamics Simulations - Thesis in Physical Chemistry*; **2015**.

- [42] Hou, T.; Wang, J.; Li, Y.; Wang, W. *J. Chem. Inf. Model.* **2011**, *51*, 69–82.
- [43] Casamayor, A. Morrice, A. Alessi, R. *Biochem. J* **1999**, *342* (2), 287.
- [44] Lingeneil, M.; Denschlag, R.; Reichold, R.; Tavan, P. *J. Chem. Theory Comput* **2008**, *4*, 1293–1306.
- [45] Ryckaert, J. P.; Ciccotti, G.; Berendsen, H. J. C. *J. Comput. Phys* **1977**, *23* (3), 327–341.
- [46] Genheden, S.; Kuhn, O.; Mikulskis, P.; Ryde, U. *J. Chem. Inf. Model* **2012**, *52*, 2079-2088.
- [47] Nurisso, A.; Daina, A.; Walker, R. C. A practical introduction to molecular dynamics simulations: applications to homology modeling; **2012**; 857.
- [48] Wang, J.; Wang, W.; Kollman, P. A.; Case, D. A. *J. Mol. Graph. Model.* **2006**, *25* (2), 247–260.
- [49] Costanzi, S.; Tikhonova, I. G.; Harden, T. K.; Jacobson, K. A. *J. Comput. Aided. Mol. Des.* **2009**, *23* (11), 747–754.
- [50] Hou, T.; Wang, J.; Li, Y.; Wang, W. *J. Chem. Inf. Model* **2011**, *51*, 69–82.
- [51] Liu, J.; He, X.; Zhang, J. Z. H. *J. Mol. Model.* **2014**, *20* (10), 2451.
- [52] Zhu, J.; Huang, J. W.; Tseng, P. H.; Yang, Y. T.; Fowble, J.; Shiau, C. W.; Shaw, Y. J.; Kulp, S. K.; Chen, C. S. *Cancer Res.* **2004**, *64* (12), 4309–4318.
- [53] Cheng, Y.; Prusoff, W. H. *Biochem. Pharmacol* **1973**, *22* (23), 3099–3108.
- [54] Alzate-Morales, J. H.; Contreras, R.; Soriano, A.; Tuñon, I.; Silla, E. *Biophys. J.* **2007**, *92* (2), 430–439.
- [55] Kuhn, B.; Mohr, P.; Stahl, M. *J. Med. Chem* **2010**, *53* (6), 2601–2611.

- [56] Furet, P.; Caravatti, G.; Guagnano, V.; Lang, M.; Meyer, T.; Schoepfer, J. *Bioorganic Med. Chem. Lett.* **2008**, *18* (3), 897–900.
- [57] Zhao, B.; Lehr, R.; Smallwood, A. M.; Ho, T. F.; Maley, K.; Randall, T.; Head, M. S.; Koretke, K. K.; Schnackenberg, C. G. *Protein Sci.* **2007**, *16* (12), 2761–2769.
- [58] Medina, J. R.; Blackledge, C. W.; Heerding, D. A.; Campobasso, N.; Ward, P.; Briand, J.; Wright, L.; Axten, J. M. *ACS Med. Chem. Lett.* **2010**, *1* (8), 439–442.
- [59] Levinson, N. M.; Boxer, S. G. *Nat. Chem. Biol.* **2013**, *10* (2), 127–132.
- [60] Dunitz, J. D. *Science*, **1994**, *264*, 670.
- [61] Hamelberg, D.; McCammon, J. A. *J. Am. Chem. Soc.* **2004**, *126* (24), 7683–7689.
- [62] Lam, P. Y. S.; Jadhav, P. K.; Eyermann, C. J.; Hodge, C. N.; Ru, Y.; Bacheler, L. T.; Meek, J. L.; Otto, M. J.; Rayner, M. M.; Wong, Y. N.; Chang, C.; Weber, P. C.; Jackson, D. A.; Sharpe, T. R.; Erickson-viitanen, S. *Science*, **1994**, *263*, 380–384.
- [63] Nagashima, K.; Shumway, S. D.; Sathyanarayanan, S.; Chen, A. H.; Dolinski, B.; Xu, Y.; Keilhack, H.; Nguyen, T.; Wiznerowicz, M.; Li, L.; Lutterbach, B. A.; Chi, A.; Paweletz, C.; Allison, T.; Yan, Y.; Munshi, S. K.; Klippel, A.; Kraus, M.; Bobkova, E. V.; Deshmukh, S.; Xu, Z.; Mueller, U.; Szewczak, A. A.; Pan, B. S.; Richon, V.; Pollock, R.; Blume-Jensen, P.; Northrup, A.; Andersen, J. N. *J. Biol. Chem.* **2011**, *286* (8), 6433–6448.
- [64] Kappe, C. O.; Dallinger, D.; Mannhold, E. R.; Kubinyi, H.; Folkers, G.; Allerton, D. a; Walker, H.; Don, K.; Lira, M. J.; Leurs, S. a. *Protein–Protein Interactions in drug discovery.* **2012**.

- [65] Stroud, R. M.; Finer-Moore. J. Computational and Structural Approaches to Drug Discovery Ligand–Protein Interactions. **2008**.
- [66] Meanwell, N. A. *Chem. Res. Toxicol.* **2016**, *29*, 564–616.
- [67] Barratt, E.; Bingham, R. J.; Warner, D. J.; Laughton, C. A.; Phillips, S. E. V; Homans, S. W. *J. Am. Chem. Soc.* **2005**, *127*, 11827–11834.
- [68] Backes. A.; Zech. B.; Felber. B.; Klebl. B.; Müller. G. *Expert Opin. Drug Discov.* **2008**, *3*, 1409-1425
- [69] Blanc. J.; Geney. R.; Menet. C. *Anti-Cancer Agents in Medicinal Chemistry*, **2013**, *13*, 731-747.
- [70] Ertl, P.; Rohde, B.; Selzer, P. *J. Med. Chem.* **2000**, *43*, 3714-3717.
- [71] Arkin, M.; Tang, Y.; Wells, J. *Chem. Biol.* **2014**, *21*, 1102.
- [72] Schultes. S.; Graaf. C.; Haaksma. E.; Esch. I.; Leurs. R.; Kramer. O. *Drug Discov. Today. Technol.* **2010**, *7*, 157.
- [73] Rettenmaiera, T.; Sadowskyb, J.; Thomsenb, N.; Chenc, S.; Doakb, A.; Arkinc, M.; Wellsb, J. *Proc. Natl. Acad. Sci.* **2014**, *111*, 18590.
- [74] Wang.J.; Wolf. R.; Caldwell. J.; Kollman. P.; Case. D. *J Comput Chem* **2004**, *25*, 1157-1174.
- [75] Jorgensen, W. L.; Chandrasekhar, J.; Madura, J. D.; Impey, R. W.; Klein, M. *L. J. Chem. Phys* **1983**, *79* (2), 926–935.

APPENDICES

APPENDIX A: SEP NON-STANDARD RESIDUE AND INHIBITOR FILES

Input file for force field modification of SEP residue

File 1: SEP_leap.frcmod

From VanBeek et al. Biophys J. (2007) 92, 4168-4178
MASS

BOND

ANGLE

OH-P-OH 45.000 109.500

DIHE

IMPROPER

NONBON

Input file for identification atom types and atom charges of inhibitor (1)

File 2: Inhibitor1.mol2

62O

26 28 1 0 0

SMALL

bcc

@<TRIPOS>ATOM

1 C1	31.4290	24.4900	5.9150	ca	1 62O	-0.035200
2 C2	32.8340	24.3570	5.9830	ca	1 62O	0.031400
3 N3	31.1770	25.7430	5.4030	na	1 62O	-0.283300
4 C4	30.6050	23.4550	6.3540	ca	1 62O	-0.221000
5 N5	33.3580	25.5140	5.4990	nc	1 62O	-0.525100
6 C6	33.3920	23.1590	6.4750	ca	1 62O	-0.035000
7 C7	32.3840	26.3250	5.1600	cd	1 62O	0.468400
8 C8	31.1650	22.2790	6.8370	ca	1 62O	0.150100

Input file for force field modification of inhibitor (1)

File 3: Inhibitor1.frcmod

```
remark goes here
MASS
BOND
ANGLE
DIHE
IMPROPER
ca-ca-ca-na  1.1  180.0  2.0  Using default value
ca-ca-ca-nc  1.1  180.0  2.0  Using default value
ca-cd-na-hn  1.1  180.0  2.0  General improper torsional angle (2 general atom
types)
ca-ca-ca-ha  1.1  180.0  2.0  General improper torsional angle (2 general atom
types)
cd-na-cd-nc  1.1  180.0  2.0  Using default value
ca-ca-ca-os  1.1  180.0  2.0  Using default value
cc-cd-cd-na  1.1  180.0  2.0  Using default value
cc-cd-cc-ha  1.1  180.0  2.0  Using default value
cd-hn-na-nd  1.1  180.0  2.0  General improper torsional angle (2 general atom
types)
cc-h4-cc-nd  1.1  180.0  2.0  Using default value
NONBON
```

APPENDIX B: INPUT FILES FOR SIMULATION

Input file for minimization of water and ion molecules in inhibitor (1) -protein complex

File 1: min.in

```
Minimization of water
&cntrl
  imin=1,maxcyc=1000,ncyc=500,
  cut=10.0,ntb=1,
  ntc=2,ntf=2,
  ntp=100,
  ntr=1, restraintmask=':1-282',
  restraint_wt=2.0
/
Hold protein and ligand fixed
10.0
RES 1-283
END
END
```

Input file for minimization of the whole complex

File 2: min_all.in

Minimization of the whole system

&cntrl

imin=1,maxcyc=1000,ncyc=500,

cut=10.0,ntb=1,

ntc=2,ntf=2,

ntpr=100,

ntr=0,

/

END

Input file for heating the inhibitor (1) -protein complex from 0K to 300K

File 3: eat.in

Heating from 0K to 300K with weak restraints

```
&cntrl
imin=0,irest=0,ntx=1,
nstlim=25000,dt=0.002,
ntc=2,ntf=2,
cut=10.0, ntb=1,
ntpr=500, ntwx=500,
ntt=3, gamma_ln=2.0,
tempi=0.0, temp0=300.0, ig=-1,
ntr=1, restraintmask=':1-282',
restraint_wt=2.0,
nmropt=1
/
&wt TYPE='TEMPO', istep1=0, istep2=25000,
value1=0.1, value2=300.0, /
&wt TYPE='END' /
```


Input file for density equilibration of inhibitor (1) -protein complex

File 4: density.in

```
&cntrl  
  imin=0,irest=1,ntx=5,  
  nstlim=25000,dt=0.002,  
  ntc=2,ntf=2,  
  cut=10.0, ntb=2, ntp=1, taup=1.0,  
  ntr=500, ntwx=500,  
  ntt=3, gamma_ln=2.0,  
  temp0=300.0, ig=-1,  
  ntr=1, restraintmask=':1-282',  
  restraint_wt=2.0,  
/
```

Input file for unrestrained equilibration of inhibitor (1) -protein complex

File 5: equil.in

```
&cntrl  
imin=0,irest=1,ntx=5,  
nstlim=250000,dt=0.002,  
ntc=2,ntf=2,  
cut=10.0, ntb=2, ntp=1, taup=2.0,  
ntpr=1000, ntwx=1000,  
ntt=3, gamma_ln=2.0,  
temp0=300.0, ig=-1,  
/  

```

Input file for unrestrained production of inhibitor (1) -protein complex

File 6: prod.in

```
&cntrl  
imin=0,irest=1,ntx=5,  
nstlim=250000,dt=0.002,  
ntc=2,ntf=2,  
cut=10.0, ntb=2, ntp=1, taup=2.0,  
ntpr=5000, ntwx=5000,  
ntt=3, gamma_ln=2.0,  
temp0=300.0, ig=-1,  
/
```

Input file for running MM-PBSA and MM-GBSA

File 7: mmpbsa.in

Input file for running PB and GB

&general

endframe=50, verbose=1,

entropy=1,

/

&gb

igb=2, saltcon=0.100

/

&pb

istrng=0.100,

/

Input file for running entropy calculations using Nmode

File 8: mmpbsa_nm.in

```
Input file for running entropy calculations using NMode
```

```
&general
```

```
  endframe=50, keep_files=2,
```

```
/
```

```
&nmode
```

```
  nmstartframe=5, nmendframe=45,
```

```
  nminterval=5, nmode_igb=1, nmode_istrng=0.1,
```

```
/
```

Input file for running mass-weighted RMSD measurements

File 9: measure_equil_rmsd.ptraj

```
trajin equil.mdcrd  
reference com_wat.inpcrd  
rms reference out equil.rmsd @CA,C,N 0.1
```

Input file for running conversion from mdcrd file to binpos file

File 10: mdcrd_to_binpos.ptraj

```
trajin prod1.mdcrd
trajin prod2.mdcrd
trajin prod3.mdcrd
trajin prod4.mdcrd
trajout prod.binpos binpos
```

Input file for hydrogen bonding analysis of inhibitor (1) -protein complex

File 11: analyse_hbond.ptraj

```
trajin prod.binpos
```

```
hbond :1-274 out nhb.dat avgout avghb.dat
```


APPENDIX C: OUTPUT FILES

Output file of ΔG_{bind} for inhibitor (1)-protein complex that resulted from MM-GBSA

File 1: MM-GBSA for ΔG_{bind} protein-inhibitor (1) complex

GENERALIZED BORN:

Complex:

Energy Component	Average	Std. Dev.	Std. Err. of Mean
VDWAALS	-2387.1522	18.1991	2.5737
EEL	-19906.0747	28.5435	4.0367
EGB	-4475.4622	20.5100	2.9006
ESURF	88.0450	0.4429	0.0626
G gas	-22293.2270	34.4401	4.8706
G solv	-4387.4172	20.4611	2.8936
TOTAL	-26680.6441	32.3518	4.5752

Receptor:

Energy Component	Average	Std. Dev.	Std. Err. of Mean
VDWAALS	-2354.6887	18.1946	2.5731
EEL	-19888.1698	28.4029	4.0168
EGB	-4477.9034	20.2762	2.8675
ESURF	89.4199	0.4413	0.0624
G gas	-22242.8585	34.5269	4.8828
G solv	-4388.4835	20.2199	2.8595
TOTAL	-26631.3420	32.4518	4.5894

Ligand:

Energy Component	Average	Std. Dev.	Std. Err. of Mean
VDWAALS	-1.8136	0.2344	0.0331
EEL	-12.6183	0.5191	0.0734
EGB	-22.0954	0.4232	0.0598
ESURF	2.1777	0.0136	0.0019
G gas	-14.4319	0.4936	0.0698
G solv	-19.9177	0.4177	0.0591
TOTAL	-34.3496	0.5901	0.0835

Differences (Complex - Receptor - Ligand):

Energy Component	Average	Std. Dev.	Std. Err. of Mean
VDWAALS	-30.6500	1.0904	0.1542
EEL	-5.2866	1.6542	0.2339
EGB	24.5367	1.0683	0.1511
ESURF	-3.5526	0.0346	0.0049
DELTA G gas	-35.9366	1.8382	0.2600
DELTA G solv	20.9841	1.0689	0.1512
DELTA TOTAL	-14.9525	1.6290	0.2304

Output file of ΔG_{bind} for inhibitor (2)-protein complex that resulted from MM-PBSA

File 2: MM-PBSA for ΔG_{bind} protein-inhibitor (1) complex

POISSON BOLTZMANN:

Complex:

Energy Component	Average	Std. Dev.	Std. Err. of Mean
VDWAALS	-2387.1522	18.1991	2.5737
EEL	-19906.0747	28.5435	4.0367
EPB	-4075.2673	19.1133	2.7030
ENPOLAR	2236.9806	3.0541	0.4319
EDISPER	-1309.5224	2.5485	0.3604
G gas	-22293.2270	34.4401	4.8706
G solv	-3147.8090	19.3236	2.7328
TOTAL	-25441.0360	31.8761	4.5080

Receptor:

Energy Component	Average	Std. Dev.	Std. Err. of Mean
VDWAALS	-2354.6887	18.1946	2.5731
EEL	-19888.1698	28.4029	4.0168
EPB	-4083.8299	19.0226	2.6902
ENPOLAR	2231.3477	3.0596	0.4327
EDISPER	-1318.4636	2.5071	0.3546
G gas	-22242.8585	34.5269	4.8828
G solv	-3170.9459	19.3747	2.7400
TOTAL	-25413.8044	31.9662	4.5207

Ligand:

Energy Component	Average	Std. Dev.	Std. Err. of Mean
VDWAALS	-1.8136	0.2344	0.0331
EEL	-12.6183	0.5191	0.0734
EPB	-21.0535	0.3862	0.0546
ENPOLAR	25.0435	0.1278	0.0181
EDISPER	-27.6378	0.1729	0.0245
G gas	-14.4319	0.4936	0.0698
G solv	-23.6478	0.4276	0.0605
TOTAL	-38.0796	0.5793	0.0819

Differences (Complex - Receptor - Ligand):

Energy Component	Average	Std. Dev.	Std. Err. of Mean
VDWAALS	-30.6500	1.0904	0.1542
EEL	-5.2866	1.6542	0.2339
EPB	29.6162	1.0069	0.1424
ENPOLAR	-19.4106	0.2120	0.0300
EDISPER	36.5790	0.3302	0.0467
DELTA G gas	-35.9366	1.8382	0.2600
DELTA G solv	46.7846	1.1997	0.1697
DELTA TOTAL	10.8480	1.6722	0.2365

Output file of ΔG_{bind} for inhibitor (2)-protein complex that resulted from MM-GBSA

File 3: MM-GBSA for ΔG_{bind} protein-inhibitor (2) complex

GENERALIZED BORN:

Complex:			
Energy Component	Average	Std. Dev.	Std. Err. of Mean
VDWAALS	-2382.0840	19.2872	2.7276
EEL	-19827.2949	40.0446	5.6632
EGB	-4408.0595	25.1368	3.5549
ESURF	87.6976	0.4609	0.0652
G gas	-22209.3789	35.4489	5.0132
G solv	-4320.3619	24.9850	3.5334
TOTAL	-26529.7408	27.4538	3.8825
Receptor:			
Energy Component	Average	Std. Dev.	Std. Err. of Mean
VDWAALS	-2357.5888	19.7084	2.7872
EEL	-19954.9192	40.0431	5.6629
EGB	-4425.5261	25.1074	3.5507
ESURF	89.3861	0.4567	0.0646
G gas	-22312.5080	35.2631	4.9869
G solv	-4336.1399	24.9597	3.5298
TOTAL	-26648.6480	27.4911	3.8878
Ligand:			
Energy Component	Average	Std. Dev.	Std. Err. of Mean
VDWAALS	1.2240	1.0341	0.1463
EEL	158.6175	2.1640	0.3060
EGB	-23.0458	0.9649	0.1365
ESURF	2.4317	0.0103	0.0015
G gas	159.8415	2.6065	0.3686
G solv	-20.6142	0.9607	0.1359
TOTAL	139.2273	2.6542	0.3754
Differences (Complex - Receptor - Ligand):			
Energy Component	Average	Std. Dev.	Std. Err. of Mean
VDWAALS	-25.7192	2.1653	0.3062
EEL	-30.9932	3.1003	0.4384
EGB	40.5125	2.1040	0.2976
ESURF	-4.1202	0.0338	0.0048
DELTA G gas	-56.7124	2.9103	0.4116
DELTA G solv	36.3922	2.0901	0.2956
DELTA TOTAL	-20.3201	1.9515	0.2760

Output file of ΔG_{bind} for inhibitor (2)-protein complex that resulted from MM-PBSA

File 4: MM-PBSA for ΔG_{bind} protein-inhibitor (2) complex

POISSON BOLTZMANN:

Complex:

Energy Component	Average	Std. Dev.	Std. Err. of Mean
VDWAALS	-2382.0840	19.2872	2.7276
EEL	-19827.2949	40.0446	5.6632
EPB	-4033.4629	22.8552	3.2322
ENPOLAR	2225.5414	3.0962	0.4379
EDISPER	-1297.4909	2.5382	0.3590
G gas	-22209.3789	35.4489	5.0132
G solv	-3105.4124	22.5362	3.1871
TOTAL	-25314.7913	26.9355	3.8092

Receptor:

Energy Component	Average	Std. Dev.	Std. Err. of Mean
VDWAALS	-2357.5888	19.7084	2.7872
EEL	-19954.9192	40.0431	5.6629
EPB	-4053.8735	22.9975	3.2523
ENPOLAR	2223.0370	3.0854	0.4363
EDISPER	-1307.2618	2.5773	0.3645
G gas	-22312.5080	35.2631	4.9869
G solv	-3138.0983	22.6852	3.2082
TOTAL	-25450.6063	27.0122	3.8201

Ligand:

Energy Component	Average	Std. Dev.	Std. Err. of Mean
VDWAALS	1.2240	1.0341	0.1463
EEL	158.6175	2.1640	0.3060
EPB	-21.0045	0.8966	0.1268
ENPOLAR	21.9338	0.1046	0.0148
EDISPER	-24.3504	0.1600	0.0226
G gas	159.8415	2.6065	0.3686
G solv	-23.4211	0.9001	0.1273
TOTAL	136.4204	2.5309	0.3579

Differences (Complex - Receptor - Ligand):

Energy Component	Average	Std. Dev.	Std. Err. of Mean
VDWAALS	-25.7192	2.1653	0.3062
EEL	-30.9932	3.1003	0.4384
EPB	41.4151	2.2681	0.3208
ENPOLAR	-19.4294	0.2129	0.0301
EDISPER	34.1212	0.3239	0.0458
DELTA G gas	-56.7124	2.9103	0.4116
DELTA G solv	56.1069	2.2933	0.3243
DELTA TOTAL	-0.6054	1.9526	0.2761

Output file of ΔG_{bind} for inhibitor (3)-protein complex that resulted from MM-GBSA

File 5: MM-GBSA for ΔG_{bind} protein-inhibitor (3) complex

GENERALIZED BORN:

Complex:

Energy Component	Average	Std. Dev.	Std. Err. of Mean
VDWAALS	-2413.2870	21.5813	3.0521
EEL	-19820.4055	30.7686	4.3513
EGB	-4419.2772	22.1522	3.1328
ESURF	83.6140	0.5858	0.0828
G gas	-22233.6925	34.3084	4.8519
G solv	-4335.6633	22.0179	3.1138
TOTAL	-26569.3558	30.8426	4.3618

Receptor:

Energy Component	Average	Std. Dev.	Std. Err. of Mean
VDWAALS	-2371.3691	21.3473	3.0190
EEL	-19879.6261	30.4154	4.3014
EGB	-4435.8541	21.8024	3.0833
ESURF	86.0346	0.5906	0.0835
G gas	-22250.9952	34.4450	4.8713
G solv	-4349.8194	21.6557	3.0626
TOTAL	-26600.8147	31.0148	4.3861

Ligand:

Energy Component	Average	Std. Dev.	Std. Err. of Mean
VDWAALS	-1.6425	0.7487	0.1059
EEL	84.7296	1.3193	0.1866
EGB	-21.0097	0.6344	0.0897
ESURF	2.9199	0.0130	0.0018
G gas	83.0871	1.5013	0.2123
G solv	-18.0898	0.6318	0.0893
TOTAL	64.9973	1.8088	0.2558

Differences (Complex - Receptor - Ligand):

Energy Component	Average	Std. Dev.	Std. Err. of Mean
VDWAALS	-40.2754	1.5773	0.2231
EEL	-25.5090	2.5000	0.3536
EGB	37.5866	2.4295	0.3436
ESURF	-5.3405	0.0522	0.0074
DELTA G gas	-65.7844	2.5661	0.3629
DELTA G solv	32.2460	2.4181	0.3420
DELTA TOTAL	-33.5384	1.4634	0.2070

Output file of ΔG_{bind} for inhibitor (3)-protein complex that resulted from MM-PBSA

File 6: MM-PBSA for ΔG_{bind} protein-inhibitor (3) complex

POISSON BOLTZMANN:

Complex:			
Energy Component	Average	Std. Dev.	Std. Err. of Mean
VDWAALS	-2413.2870	21.5813	3.0521
EEL	-19820.4055	30.7686	4.3513
EPB	-3993.3020	21.3042	3.0129
ENPOLAR	2204.6542	4.0279	0.5696
EDISPER	-1269.9511	3.1058	0.4392
G gas	-22233.6925	34.3084	4.8519
G solv	-3058.5989	22.0081	3.1124
TOTAL	-25292.2914	30.6631	4.3364

Receptor:			
Energy Component	Average	Std. Dev.	Std. Err. of Mean
VDWAALS	-2371.3691	21.3473	3.0190
EEL	-19879.6261	30.4154	4.3014
EPB	-4025.4893	21.1439	2.9902
ENPOLAR	2199.6821	4.0331	0.5704
EDISPER	-1287.5893	3.0903	0.4370
G gas	-22250.9952	34.4450	4.8713
G solv	-3113.3965	21.6740	3.0652
TOTAL	-25364.3917	31.0895	4.3967

Ligand:			
Energy Component	Average	Std. Dev.	Std. Err. of Mean
VDWAALS	-1.6425	0.7487	0.1059
EEL	84.7296	1.3193	0.1866
EPB	-19.4857	0.6965	0.0985
ENPOLAR	32.7201	0.1509	0.0213
EDISPER	-35.1051	0.1973	0.0279
G gas	83.0871	1.5013	0.2123
G solv	-21.8707	0.7350	0.1040
TOTAL	61.2164	1.6242	0.2297

Differences (Complex - Receptor - Ligand):			
Energy Component	Average	Std. Dev.	Std. Err. of Mean
VDWAALS	-40.2754	1.5773	0.2231
EEL	-25.5090	2.5000	0.3536
EPB	51.6731	3.3871	0.4790
ENPOLAR	-27.7480	0.2755	0.0390
EDISPER	52.7433	0.3431	0.0485
DELTA G gas	-65.7844	2.5661	0.3629
DELTA G solv	76.6684	3.2720	0.4627

Output file of ΔG_{bind} for inhibitor (4)-protein complex that resulted from MM-GBSA

File 7: MM-GBSA for ΔG_{bind} protein-inhibitor (4) complex

GENERALIZED BORN:

Complex:			
Energy Component	Average	Std. Dev.	Std. Err. of Mean
VDWAALS	-2353.3994	17.5785	2.4860
EEL	-19658.0219	34.9942	4.9489
EGB	-4319.8457	18.9849	2.6849
ESURF	81.1668	0.6750	0.0955
G gas	-22011.4213	37.1507	5.2539
G solv	-4238.6789	18.7732	2.6549
TOTAL	-26250.1002	33.7015	4.7661
Receptor:			
Energy Component	Average	Std. Dev.	Std. Err. of Mean
VDWAALS	-2308.7545	17.7632	2.5121
EEL	-19710.5088	35.4969	5.0200
EGB	-4319.0185	19.2179	2.7178
ESURF	83.4388	0.6664	0.0942
G gas	-22019.2633	37.8085	5.3469
G solv	-4235.5797	18.9902	2.6856
TOTAL	-26254.8430	33.7533	4.7734
Ligand:			
Energy Component	Average	Std. Dev.	Std. Err. of Mean
VDWAALS	-1.8345	0.6602	0.0934
EEL	68.3767	1.3554	0.1917
EGB	-29.0700	0.5917	0.0837
ESURF	2.8460	0.0161	0.0023
G gas	66.5422	1.4134	0.1999
G solv	-26.2240	0.5889	0.0833
TOTAL	40.3182	1.5645	0.2213
Differences (Complex - Receptor - Ligand):			
Energy Component	Average	Std. Dev.	Std. Err. of Mean
VDWAALS	-42.8103	1.8014	0.2548
EEL	-15.8898	3.5751	0.5056
EGB	28.2428	3.3158	0.4689
ESURF	-5.1180	0.0605	0.0086
DELTA G gas	-58.7002	3.1095	0.4397
DELTA G solv	23.1248	3.2962	0.4662
DELTA TOTAL	-35.5753	1.7954	0.2539

Output file of ΔG_{bind} for inhibitor (4)-protein complex that resulted from MM-PBSA

File 8: MM-PBSA for ΔG_{bind} protein-inhibitor (4) complex

POISSON BOLTZMANN:

Complex:			
Energy Component	Average	Std. Dev.	Std. Err. of Mean
VDWAALS	-2353.3994	17.5785	2.4860
EEL	-19658.0219	34.9942	4.9489
EPB	-3927.1281	17.4236	2.4641
ENPOLAR	2158.3678	3.8127	0.5392
EDISPER	-1224.9080	3.1128	0.4402
G gas	-22011.4213	37.1507	5.2539
G solv	-2993.6683	17.1491	2.4252
TOTAL	-25005.0896	31.3041	4.4271
Receptor:			
Energy Component	Average	Std. Dev.	Std. Err. of Mean
VDWAALS	-2308.7545	17.7632	2.5121
EEL	-19710.5088	35.4969	5.0200
EPB	-3936.5249	17.6422	2.4950
ENPOLAR	2151.7913	3.8115	0.5390
EDISPER	-1240.8397	3.1114	0.4400
G gas	-22019.2633	37.8085	5.3469
G solv	-3025.5734	17.3662	2.4559
TOTAL	-25044.8367	31.2005	4.4124
Ligand:			
Energy Component	Average	Std. Dev.	Std. Err. of Mean
VDWAALS	-1.8345	0.6602	0.0934
EEL	68.3767	1.3554	0.1917
EPB	-26.9996	0.6359	0.0899
ENPOLAR	33.9443	0.1751	0.0248
EDISPER	-38.3396	0.1965	0.0278
G gas	66.5422	1.4134	0.1999
G solv	-31.3950	0.7515	0.1063
TOTAL	35.1472	1.3986	0.1978
Differences (Complex - Receptor - Ligand):			
Energy Component	Average	Std. Dev.	Std. Err. of Mean
VDWAALS	-42.8103	1.8014	0.2548
EEL	-15.8898	3.5751	0.5056
EPB	36.3964	3.3776	0.4777
ENPOLAR	-27.3677	0.2681	0.0379
EDISPER	54.2713	0.3780	0.0535
DELTA G gas	-58.7002	3.1095	0.4397
DELTA G solv	63.3000	3.4647	0.4900

Output file of ΔG_{bind} for inhibitor (5)-protein complex that resulted from MM-GBSA

File 9: MM-GBSA for ΔG_{bind} protein-inhibitor (5) complex

GENERALIZED BORN:

Complex:

Energy Component	Average	Std. Dev.	Std. Err. of Mean
VDWAALS	-2334.6961	13.3627	1.8898
EEL	-20111.3512	40.3633	5.7082
EGB	-4065.6798	22.2102	3.1410
ESURF	88.9084	0.4125	0.0583
G gas	-22446.0473	41.1968	5.8261
G solv	-3976.7714	22.1986	3.1394
TOTAL	-26422.8187	31.1430	4.4043

Receptor:

Energy Component	Average	Std. Dev.	Std. Err. of Mean
VDWAALS	-2257.1401	12.9660	1.8337
EEL	-20139.3788	39.9200	5.6455
EGB	-4094.2921	22.2570	3.1476
ESURF	94.0722	0.3976	0.0562
G gas	-22396.5189	41.7082	5.8984
G solv	-4000.2199	22.2518	3.1469
TOTAL	-26396.7388	31.7675	4.4926

Ligand:

Energy Component	Average	Std. Dev.	Std. Err. of Mean
VDWAALS	-1.1075	1.4022	0.1983
EEL	83.6674	1.2794	0.1809
EGB	-40.1660	0.7469	0.1056
ESURF	4.4974	0.0174	0.0025
G gas	82.5599	1.9406	0.2744
G solv	-35.6687	0.7471	0.1056
TOTAL	46.8913	1.9986	0.2826

Differences (Complex - Receptor - Ligand):

Energy Component	Average	Std. Dev.	Std. Err. of Mean
VDWAALS	-76.4485	3.2333	0.4573
EEL	-55.6398	3.1700	0.4483
EGB	68.7784	1.4713	0.2081
ESURF	-9.6612	0.1114	0.0158
DELTA G gas	-132.0884	3.3350	0.4716
DELTA G solv	59.1172	1.4823	0.2096
DELTA TOTAL	-72.9712	2.7883	0.3943

Output file of ΔG_{bind} for inhibitor (5)-protein complex that resulted from MM-PBSA

File 10: MM-PBSA for ΔG_{bind} protein-inhibitor (5) complex

POISSON BOLTZMANN:

Complex:

Energy Component	Average	Std. Dev.	Std. Err. of Mean
VDWAALS	-2334.6961	13.3627	1.8898
EEL	-20111.3512	40.3633	5.7082
EPB	-3542.1323	21.0261	2.9735
ENPOLAR	2238.7802	1.8782	0.2656
EDISPER	-1252.4585	1.7487	0.2473
G gas	-22446.0473	41.1968	5.8261
G solv	-2555.8106	20.6883	2.9258
TOTAL	-25001.8578	32.5969	4.6099

Receptor:

Energy Component	Average	Std. Dev.	Std. Err. of Mean
VDWAALS	-2257.1401	12.9660	1.8337
EEL	-20139.3788	39.9200	5.6455
EPB	-3573.4939	20.9491	2.9626
ENPOLAR	2235.8833	1.8308	0.2589
EDISPER	-1281.1244	1.7811	0.2519
G gas	-22396.5189	41.7082	5.8984
G solv	-2618.7350	20.6246	2.9168
TOTAL	-25015.2538	33.3003	4.7094

Ligand:

Energy Component	Average	Std. Dev.	Std. Err. of Mean
VDWAALS	-1.1075	1.4022	0.1983
EEL	83.6674	1.2794	0.1809
EPB	-37.6917	0.6818	0.0964
ENPOLAR	54.4222	0.1989	0.0281
EDISPER	-53.3586	0.2648	0.0375
G gas	82.5599	1.9406	0.2744
G solv	-36.6281	0.7588	0.1073
TOTAL	45.9319	1.9257	0.2723

Differences (Complex - Receptor - Ligand):

Energy Component	Average	Std. Dev.	Std. Err. of Mean
VDWAALS	-76.4485	3.2333	0.4573
EEL	-55.6398	3.1700	0.4483
EPB	69.0533	1.7267	0.2442
ENPOLAR	-51.5253	0.2645	0.0374
EDISPER	82.0245	0.6233	0.0881
DELTA G gas	-132.0884	3.3350	0.4716
DELTA G solv	99.5525	2.0608	0.2914

Output file of ΔS for inhibitor (1)-protein complex that resulted from Nmode

File 11: Entropic contribution of protein-inhibitor (1) complex

ENTROPY RESULTS (HARMONIC APPROXIMATION) CALCULATED WITH NMODE:

Complex:			
Entropy Term	Average	Std. Dev.	Std. Err. of Mean
Translational	16.9773	0.0000	0.0000
Rotational	17.5628	0.0068	0.0023
Vibrational	3217.1317	3.2815	1.0938
Total	3251.6718	3.2827	1.0942

Receptor:			
Entropy Term	Average	Std. Dev.	Std. Err. of Mean
Translational	16.9713	0.0000	0.0000
Rotational	17.5549	0.0017	0.0006
Vibrational	3199.0826	3.2836	1.0945
Total	3233.6089	3.2845	1.0948

Ligand:			
Entropy Term	Average	Std. Dev.	Std. Err. of Mean
Translational	12.5107	0.0000	0.0000
Rotational	9.6839	0.0000	0.0000
Vibrational	11.0817	0.4783	0.1594
Total	33.2764	0.4783	0.1594

Differences (Complex - Receptor - Ligand):			
Entropy Term	Average	Std. Dev.	Std. Err. of Mean
Translational	-12.5047	0.0000	0.0000
Rotational	-9.6760	0.0062	0.0021
Vibrational	6.9673	3.2004	1.0668
DELTA S total=	-15.2135	3.2025	1.0675

Output file of ΔS for inhibitor (2)-protein complex that resulted from Nmode

File 12: Entropic contribution of protein-inhibitor (2) complex

ENTROPY RESULTS (HARMONIC APPROXIMATION) CALCULATED WITH NMODE:

Complex:			
Entropy Term	Average	Std. Dev.	Std. Err. of Mean
Translational	16.9773	0.0000	0.0000
Rotational	17.5751	0.0023	0.0008
Vibrational	3221.8426	3.0359	1.0120
Total	3256.3949	3.0350	1.0117
Receptor:			
Entropy Term	Average	Std. Dev.	Std. Err. of Mean
Translational	16.9713	0.0000	0.0000
Rotational	17.5723	0.0012	0.0004
Vibrational	3205.1449	2.6761	0.8920
Total	3239.6885	2.6765	0.8922
Ligand:			
Entropy Term	Average	Std. Dev.	Std. Err. of Mean
Translational	12.5148	0.0000	0.0000
Rotational	9.6022	0.0000	0.0000
Vibrational	13.3378	0.4639	0.1546
Total	35.4548	0.4639	0.1546
Differences (Complex - Receptor - Ligand):			
Entropy Term	Average	Std. Dev.	Std. Err. of Mean
Translational	-12.5089	0.0000	0.0000
Rotational	-9.5994	0.0027	0.0009
Vibrational	3.3599	2.6447	0.8816
DELTA S total=	-18.7484	2.6433	0.8811

Output file of ΔS for inhibitor (3)-protein complex that resulted from Nmode

File 13: Entropic contribution of protein-inhibitor (3) complex

ENTROPY RESULTS (HARMONIC APPROXIMATION) CALCULATED WITH NMODE:

Complex:			
Entropy Term	Average	Std. Dev.	Std. Err. of Mean
Translational	16.9734	0.0000	0.0000
Rotational	17.5666	0.0027	0.0009
Vibrational	3205.8049	4.7201	1.5734
Total	3240.3448	4.7214	1.5738

Receptor:			
Entropy Term	Average	Std. Dev.	Std. Err. of Mean
Translational	16.9659	0.0000	0.0000
Rotational	17.5490	0.0113	0.0038
Vibrational	3176.7016	9.3158	3.1053
Total	3211.2167	9.3266	3.1089

Ligand:			
Entropy Term	Average	Std. Dev.	Std. Err. of Mean
Translational	12.7072	0.0000	0.0000
Rotational	10.2694	0.0022	0.0007
Vibrational	18.7394	0.0090	0.0030
Total	41.7160	0.0068	0.0023

Differences (Complex - Receptor - Ligand):			
Entropy Term	Average	Std. Dev.	Std. Err. of Mean
Translational	-12.6997	0.0000	0.0000
Rotational	-10.2518	0.0114	0.0038
Vibrational	10.3639	7.2080	2.4027
DELTA S total=	-12.5878	7.2183	2.4061

Output file of ΔS for inhibitor (4)-protein complex that resulted from Nmode

File 14: Entropic contribution of protein-inhibitor (4) complex

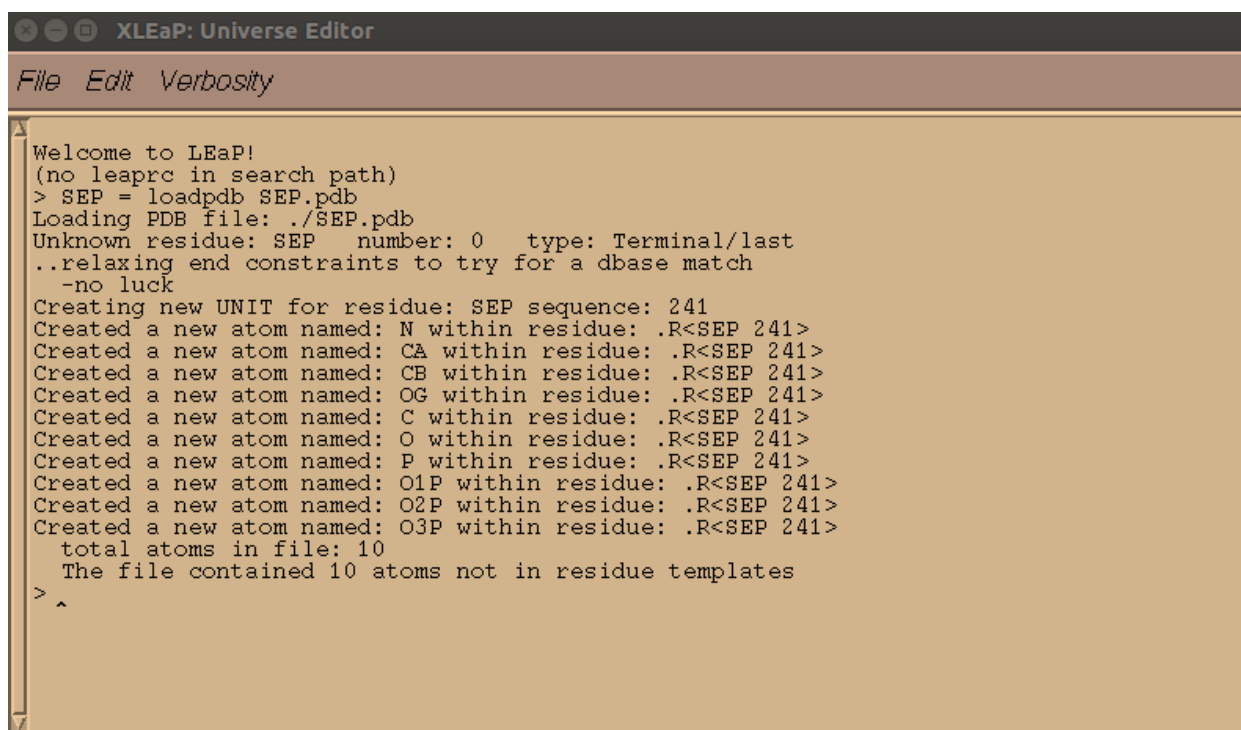
ENTROPY RESULTS (HARMONIC APPROXIMATION) CALCULATED WITH NMODE:

Complex:			
Entropy Term	Average	Std. Dev.	Std. Err. of Mean
Translational	16.9561	0.0000	0.0000
Rotational	17.5128	0.0017	0.0006
Vibrational	3132.5212	4.7875	1.5958
Total	3166.9900	4.7872	1.5957
Receptor:			
Entropy Term	Average	Std. Dev.	Std. Err. of Mean
Translational	16.9474	0.0000	0.0000
Rotational	17.5062	0.0027	0.0009
Vibrational	3108.9020	7.1749	2.3916
Total	3143.3558	7.1748	2.3916
Ligand:			
Entropy Term	Average	Std. Dev.	Std. Err. of Mean
Translational	12.8252	0.0000	0.0000
Rotational	10.4617	0.0001	0.0000
Vibrational	20.9163	0.0024	0.0008
Total	44.2035	0.0026	0.0009
Differences (Complex - Receptor - Ligand):			
Entropy Term	Average	Std. Dev.	Std. Err. of Mean
Translational	-12.8166	0.0000	0.0000
Rotational	-10.4552	0.0026	0.0009
Vibrational	2.7028	3.6238	1.2079
DELTA S total=	-20.5692	3.6237	1.2079

Building a library file for SEP residue

The connectivity information in the pdb file was deleted. Using *xLeap*, atoms are bonded together manually. First, the SEP non-standard residue was loaded (Fig 1)

```
Xleap
SEP = loadpdb SEP.pdb
```



```
XLEaP: Universe Editor
File Edit Verbosity
Welcome to LEaP!
(no leaprc in search path)
> SEP = loadpdb SEP.pdb
Loading PDB file: ./SEP.pdb
Unknown residue: SEP number: 0 type: Terminal/last
..relaxing end constraints to try for a dbase match
-no luck
Creating new UNIT for residue: SEP sequence: 241
Created a new atom named: N within residue: .R<SEP 241>
Created a new atom named: CA within residue: .R<SEP 241>
Created a new atom named: CB within residue: .R<SEP 241>
Created a new atom named: OG within residue: .R<SEP 241>
Created a new atom named: C within residue: .R<SEP 241>
Created a new atom named: O within residue: .R<SEP 241>
Created a new atom named: P within residue: .R<SEP 241>
Created a new atom named: O1P within residue: .R<SEP 241>
Created a new atom named: O2P within residue: .R<SEP 241>
Created a new atom named: O3P within residue: .R<SEP 241>
total atoms in file: 10
The file contained 10 atoms not in residue templates
> ^
```

Figure 1: *XLeap* window shows loading atoms of SEP residue

All atoms of SEP residue were added to the new *UNIT*. It is important to check that *xLeap* "created" the correct atoms. The easiest way is to check for the total number of atoms in the file which should be 10.

The pdb file containing atom coordinates for SEP residue was loaded. *xLeap* does not have necessary SEP parameters and connectivity data, so this information was entered manually.

The SEP residue in *xLeap* was edited (Fig 2) by the command:

```
edit SEP
```

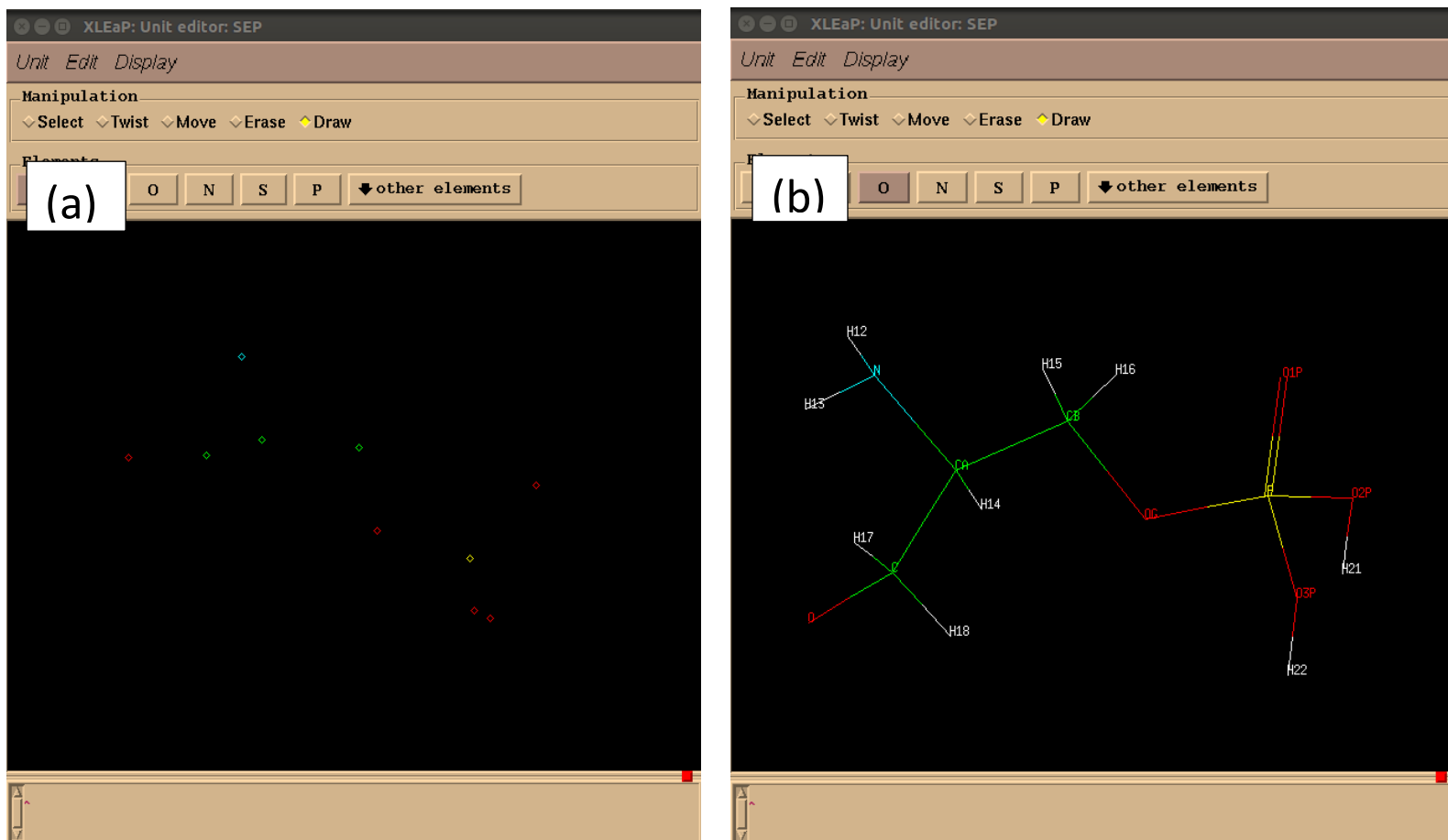
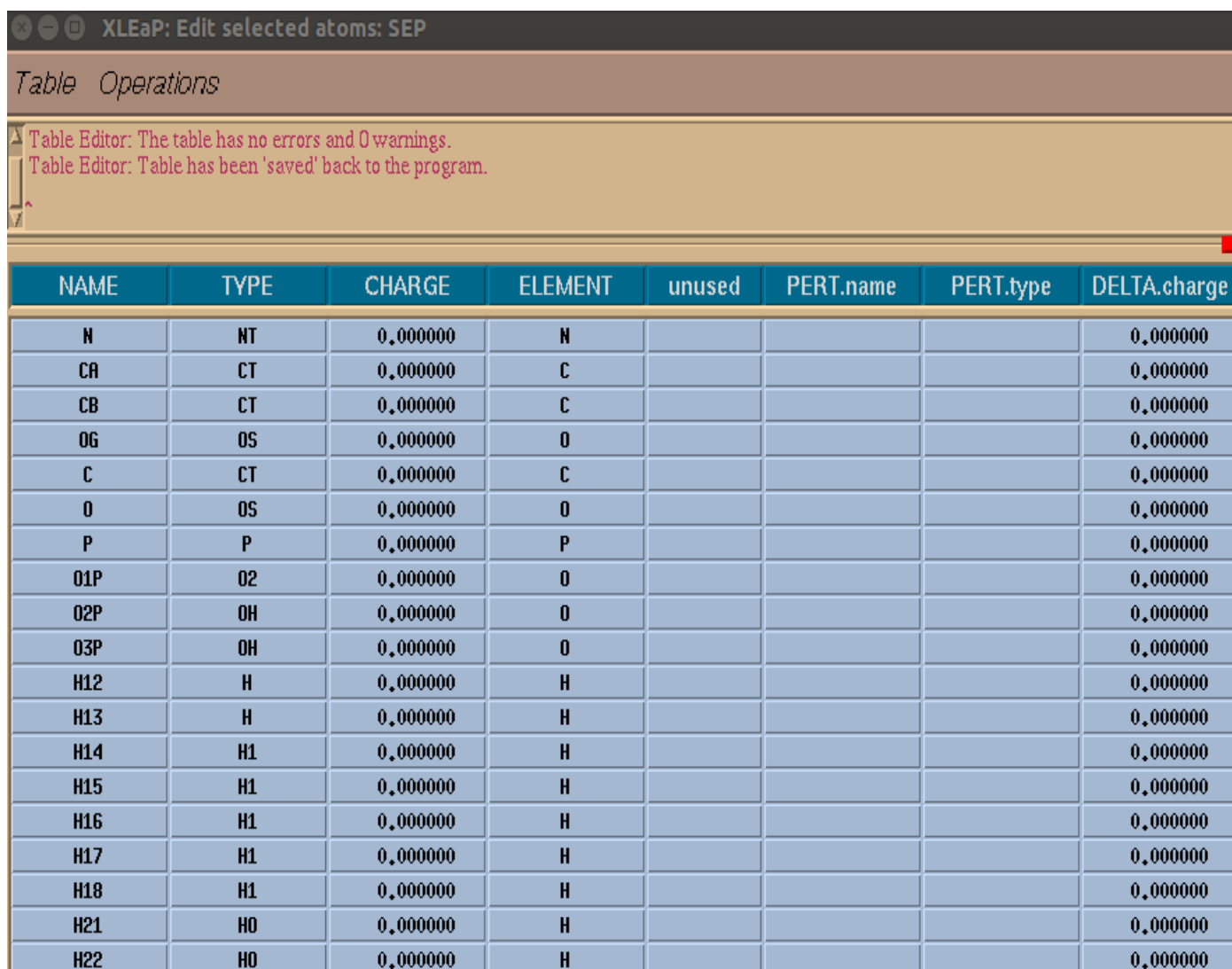


Figure 2: *xLeap* window shows (a) atoms of SEP residue before connecting between them, (b) SEP non-standard residue after connection

Parameters of each atom in SEP residue are given by *parm99.dat* file which lies in *\$AMBERHOME/dat/leap/parm* table given in *xLeap*. The atom types of all SEP atoms were identified by blue table (Table 1).

Table 1: Blue table is given by *XLeap* shows all of atom types in SEP non-standard residue



XLEaP: Edit selected atoms: SEP

Table Operations

Table Editor: The table has no errors and 0 warnings.
Table Editor: Table has been 'saved' back to the program.

NAME	TYPE	CHARGE	ELEMENT	unused	PERT.name	PERT.type	DELTA.charge
N	NT	0.000000	N				0.000000
CA	CT	0.000000	C				0.000000
CB	CT	0.000000	C				0.000000
OG	OS	0.000000	O				0.000000
C	CT	0.000000	C				0.000000
O	OS	0.000000	O				0.000000
P	P	0.000000	P				0.000000
O1P	O2	0.000000	O				0.000000
O2P	OH	0.000000	O				0.000000
O3P	OH	0.000000	O				0.000000
H12	H	0.000000	H				0.000000
H13	H	0.000000	H				0.000000
H14	H1	0.000000	H				0.000000
H15	H1	0.000000	H				0.000000
H16	H1	0.000000	H				0.000000
H17	H1	0.000000	H				0.000000
H18	H1	0.000000	H				0.000000
H21	H0	0.000000	H				0.000000
H22	H0	0.000000	H				0.000000

The O2P and O3P atoms are oxygen atoms in hydroxyl group, so the type of this oxygen is OH in the blue table. But the O1P is oxygen atom in phosphate group, so the type of this atom is O2 according to PARM99.dat¹⁷

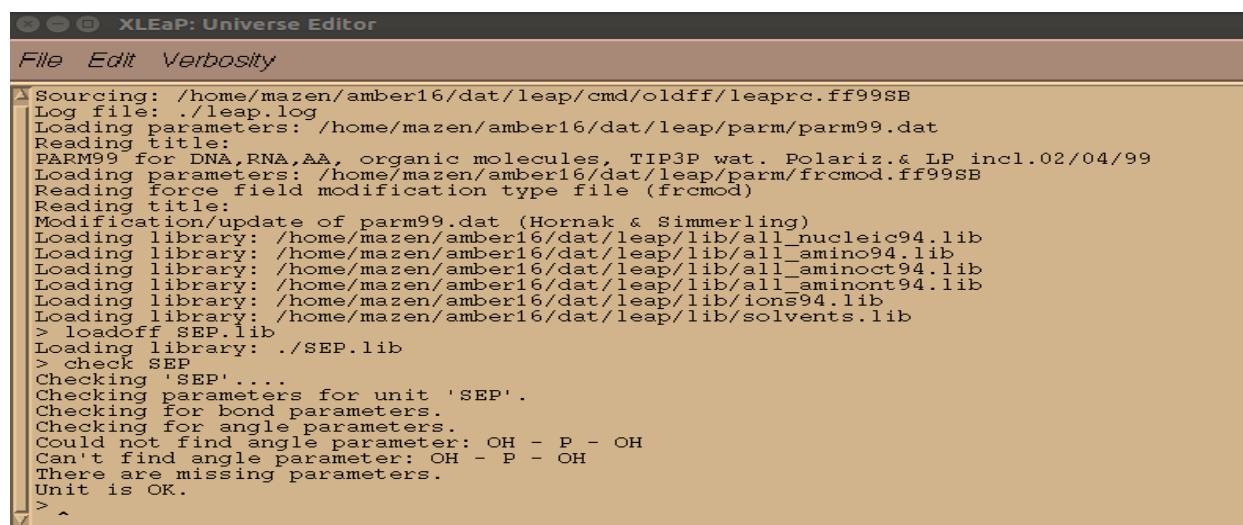
H12 and H13 are connected with nitrogen atom, so these atoms were assigned with an appropriate atom type which is H. HC and H1 were assigned for H in aliphatic bond to Carbon without electron withdrawing group and H in aliphatic bond to Carbon with one electron withdrawing group, respectively.¹⁷

Then library file of SEP was saved which will enable *xLeap* to recognize this residue in the future. This step is very essential to prevent the repetition of all of the previous steps each time. This was done by the following command.

```
Saveoff SEP SEP_leap.lib
Savepdb SEP SEP_leap.pdb
```

The missing bonds and angle parameters of SEP residue were identified by *xLeap*. This was achieved by using the following commands

```
xleap -s -f $AMBERHOME/dat/leap/cmd/oldff/leaprc.ff99SB
loadoff SEP_leap.lib
check SEP
```



```

XLEap: Universe Editor
File Edit Verbosity
^ Sourcing: /home/mazen/amber16/dat/leap/cmd/oldff/leaprc.ff99SB
Log file: ./leap.log
Loading parameters: /home/mazen/amber16/dat/leap/parm/parm99.dat
Reading title:
PARM99 for DNA,RNA,AA, organic molecules, TIP3P wat. Polariz.& LP incl.02/04/99
Loading parameters: /home/mazen/amber16/dat/leap/parm/frcmod.ff99SB
Reading force field modification type file (frcmod)
Reading title:
Modification/update of parm99.dat (Hornak & Simmerling)
Loading library: /home/mazen/amber16/dat/leap/lib/all_nucleic94.lib
Loading library: /home/mazen/amber16/dat/leap/lib/all_aminoc94.lib
Loading library: /home/mazen/amber16/dat/leap/lib/all_aminoc94.lib
Loading library: /home/mazen/amber16/dat/leap/lib/all_aminoc94.lib
Loading library: /home/mazen/amber16/dat/leap/lib/ionS94.lib
Loading library: /home/mazen/amber16/dat/leap/lib/solvents.lib
> loadoff SEP.lib
Loading library: ./SEP.lib
> check SEP
> check SEP
Checking 'SEP'....
Checking parameters for unit 'SEP'.
Checking for bond parameters.
Checking for angle parameters.
Could not find angle parameter: OH - P - OH
Can't find angle parameter: OH - P - OH
There are missing parameters.
Unit is OK.
>
^

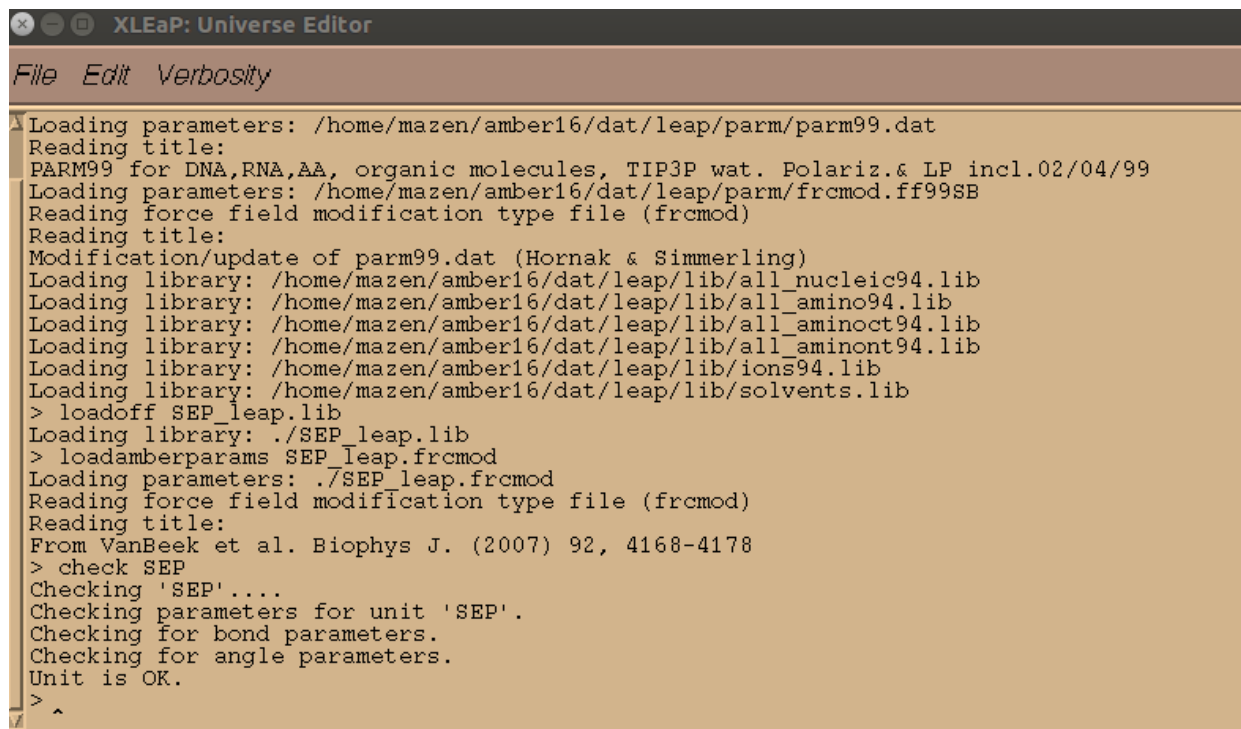
```

Figure 3: XLeap window shows the missing parameters of non-standard residue (SEP)

An *frcmod* file is required to provide all the bonds, angles and dihedral parameters that are not present in the standard FF99SB force field. The only missing parameter in SEP residue is the OH-P-OH angle parameter (Fig 3). So SEP_leap.frcmod file (see Appendix A) was created to define the missing OH-P-OH angle parameter. Then the *frcmod* file of SEP was loaded using this command

```
loadamberparams SEP_leap.frcmod
```

Finally, the SEP residue was successfully built using *xLeap*, by check the residue (UNIT is OK) and by saving it as *prmtop* and *inpcrd* file (Fig 4).



```

XLEaP: Universe Editor
File Edit Verbosity
^ Loading parameters: /home/mazen/amber16/dat/leap/parm/parm99.dat
Reading title:
  PARM99 for DNA,RNA,AA, organic molecules, TIP3P wat. Polariz.& LP incl.02/04/99
Loading parameters: /home/mazen/amber16/dat/leap/parm/frcmod.ff99SB
Reading force field modification type file (frcmod)
Reading title:
Modification/update of parm99.dat (Hornak & Simmerling)
Loading library: /home/mazen/amber16/dat/leap/lib/all_nucleic94.lib
Loading library: /home/mazen/amber16/dat/leap/lib/all_amino94.lib
Loading library: /home/mazen/amber16/dat/leap/lib/all_aminoc94.lib
Loading library: /home/mazen/amber16/dat/leap/lib/all_aminont94.lib
Loading library: /home/mazen/amber16/dat/leap/lib/ions94.lib
Loading library: /home/mazen/amber16/dat/leap/lib/solvents.lib
> loadoff SEP_leap.lib
Loading library: ./SEP_leap.lib
> loadamberparams SEP_leap.frcmod
Loading parameters: ./SEP_leap.frcmod
Reading force field modification type file (frcmod)
Reading title:
From VanBeek et al. Biophys J. (2007) 92, 4168-4178
> check SEP
Checking 'SEP'....
Checking parameters for unit 'SEP'.
Checking for bond parameters.
Checking for angle parameters.
Unit is OK.
> ^

```

Figure 4: *XLeap* window shows that SEP residue successefully built using *xLeap*

Creating *AMBER* input files

The *inpcrd* and *Prmtop* files are the coordinate files and molecular topology/parameter, respectively. These files are necessary for running molecular dynamics simulation of protein-ligand complexes using *Sander*.

Antechamber is designed to be used with the "general AMBER force field (*GAFF*)", and was successfully used in the production of *frcmod* files and *mol2* files of inhibitors. *GAFF* force field covers most pharmaceutical molecules and is

compatible with *AMBER* force fields. *GAFF* is a complete force field and covers all the organic molecules that contain C, N, O, S, P, H, F, Cl, Br and I.⁷⁴

The hydrogenated 6-methoxy-2-(1H-pyrazol-5-yl)-1H-benzimidazole (inhibitor 1) coordinates were done using *Pymol*, then *antechamber* command was used to create the "mol2" file using the following command in terminal:

```
antechamber -i inhibitor1.pdb -fi pdb -o inhibitor1.mol2 -fo mol2 -  
c bcc -s 2
```

This command line produced a number of files in CAPITALS. These files are used by antechamber and are not required here. These files are considered as intermediate files, but *mol2* file of inhibitor1 (see Appendix A) is the most important one because it reveals the definition of our inhibitor (1) residue, including all of the charges and atom types.

To specify any missing parameters (bonds, angles, dihedral angles) before we can create our *prmtop* and *inpcrd* files in *Leap*, we run the *parmchk* command in terminal to test if all the parameters we require are available.

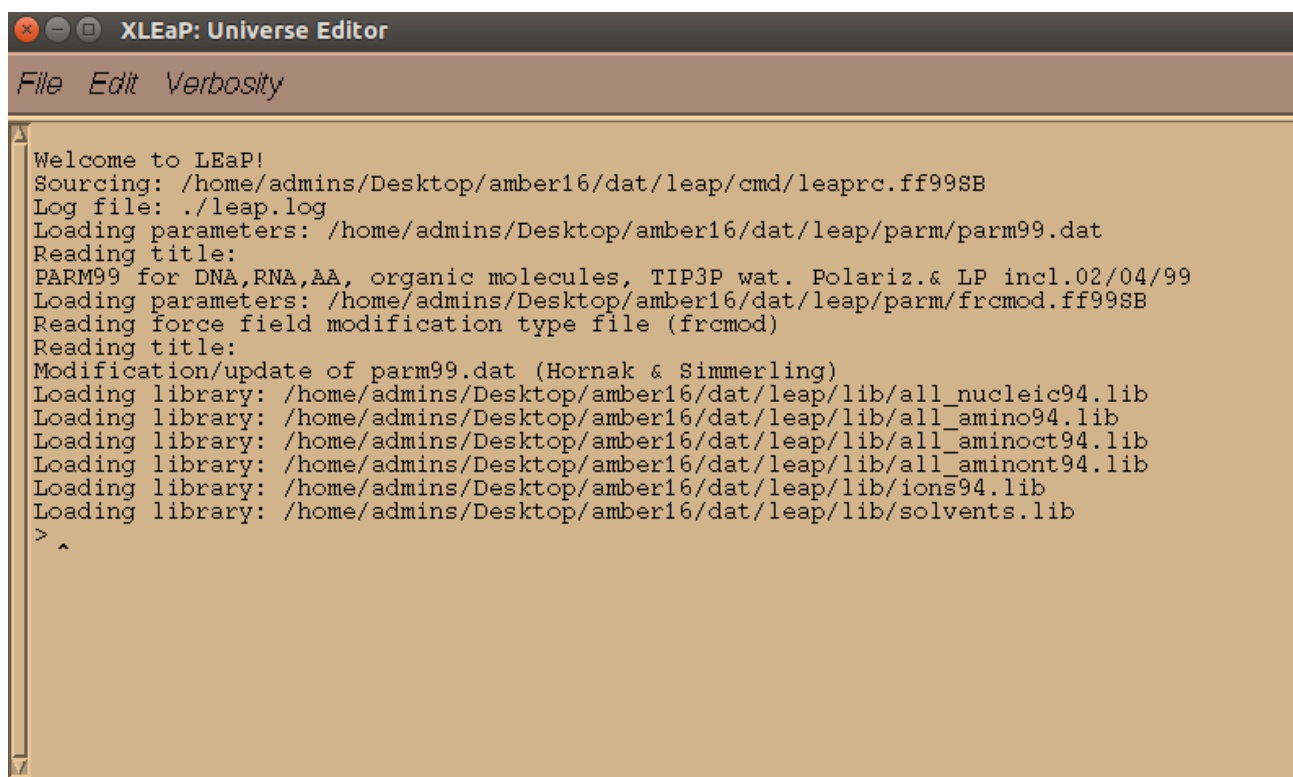
```
parmchk -i inhibitor1.mol2 -f mol2 -o inhibitor1.frcmod
```

Running this command produced a file called *inhibitor1.frcmod* (see Appendix A). This is a parameter file that can be loaded into *xLeap* in order to add missing parameters.

Subsequently, *xLeap* was used to form *prmtop* and *inpcrd* files using the following command was typed in terminal in order to open *xLeap*:

```
xleap -s -f $AMBERHOME/dat/leap/cmd/leaprc.ff99SB
```

This command line starts *xleap* and loads the configuration files needed for *AMBER FF99SB* force field as shown in Figure 5.



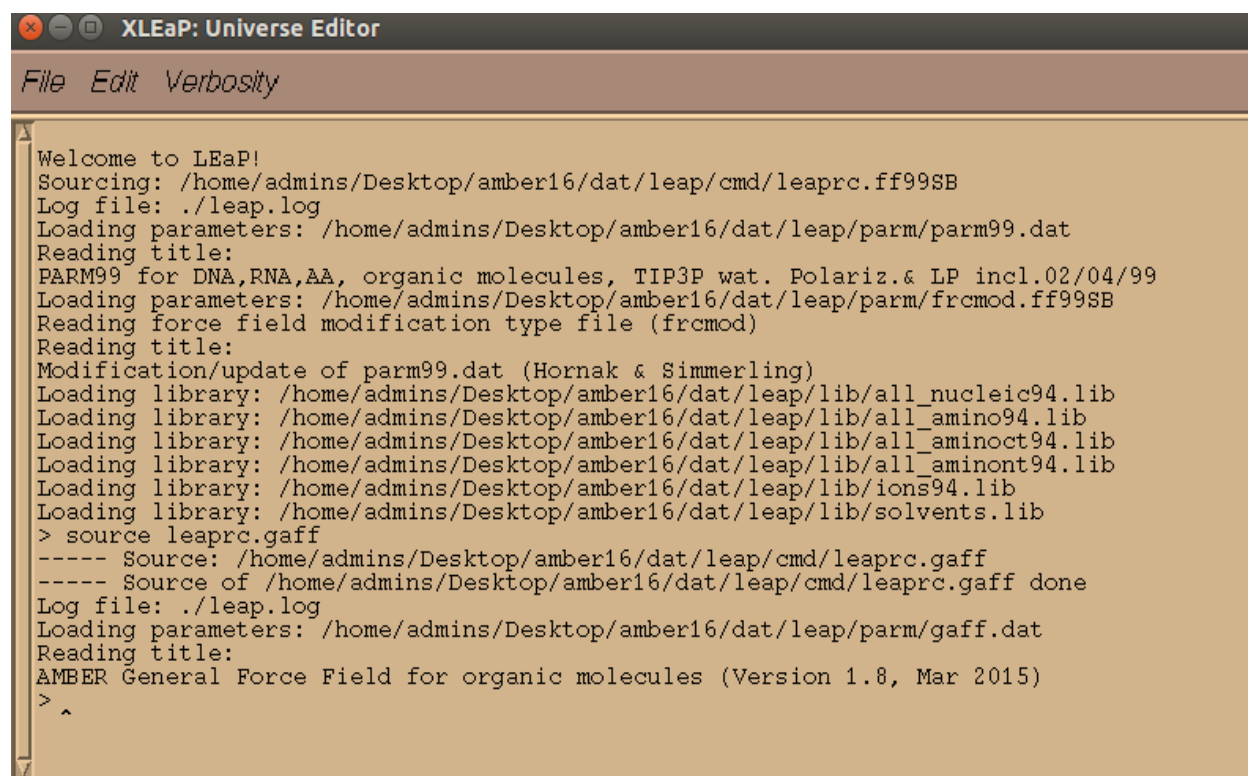
```
XLEaP: Universe Editor
File Edit Verbosity
Welcome to LEaP!
Sourcing: /home/admins/Desktop/amber16/dat/leap/cmd/leaprc.ff99SB
Log file: ./leap.log
Loading parameters: /home/admins/Desktop/amber16/dat/leap/parm/parm99.dat
Reading title:
PARM99 for DNA,RNA,AA, organic molecules, TIP3P wat. Polariz.& LP incl.02/04/99
Loading parameters: /home/admins/Desktop/amber16/dat/leap/parm/frcmod.ff99SB
Reading force field modification type file (frcmod)
Reading title:
Modification/update of parm99.dat (Hornak & Simmerling)
Loading library: /home/admins/Desktop/amber16/dat/leap/lib/all_nucleic94.lib
Loading library: /home/admins/Desktop/amber16/dat/leap/lib/all_amino94.lib
Loading library: /home/admins/Desktop/amber16/dat/leap/lib/all_aminoc94.lib
Loading library: /home/admins/Desktop/amber16/dat/leap/lib/all_aminont94.lib
Loading library: /home/admins/Desktop/amber16/dat/leap/lib/ions94.lib
Loading library: /home/admins/Desktop/amber16/dat/leap/lib/solvents.lib
>
```

Figure 5: *XLeap* window shows FF99SB force field

To ensure that *xLeap* has the *GAFF* force field, it is loaded into *xLeap* by using command line:

```
Source leaprc.gaff
```

xLeap looks like this:



```

XLEaP: Universe Editor
File Edit Verbosity

Welcome to LEaP!
Sourcing: /home/admins/Desktop/amber16/dat/leap/cmd/leaprc.ff99SB
Log file: ./leap.log
Loading parameters: /home/admins/Desktop/amber16/dat/leap/parm/parm99.dat
Reading title:
PARM99 for DNA,RNA,AA, organic molecules, TIP3P wat. Polariz.& LP incl.02/04/99
Loading parameters: /home/admins/Desktop/amber16/dat/leap/parm/frcmod.ff99SB
Reading force field modification type file (frcmod)
Reading title:
Modification/update of parm99.dat (Hornak & Simmerling)
Loading library: /home/admins/Desktop/amber16/dat/leap/lib/all_nucleic94.lib
Loading library: /home/admins/Desktop/amber16/dat/leap/lib/all_amino94.lib
Loading library: /home/admins/Desktop/amber16/dat/leap/lib/all_aminoc94.lib
Loading library: /home/admins/Desktop/amber16/dat/leap/lib/all_aminont94.lib
Loading library: /home/admins/Desktop/amber16/dat/leap/lib/ions94.lib
Loading library: /home/admins/Desktop/amber16/dat/leap/lib/solvents.lib
> source leaprc.gaff
----- Source: /home/admins/Desktop/amber16/dat/leap/cmd/leaprc.gaff
----- Source of /home/admins/Desktop/amber16/dat/leap/cmd/leaprc.gaff done
Log file: ./leap.log
Loading parameters: /home/admins/Desktop/amber16/dat/leap/parm/gaff.dat
Reading title:
AMBER General Force Field for organic molecules (Version 1.8, Mar 2015)
> ^

```

Figure 6: XLeap window shows preparing to load the protein-inhibitor (1) complex X-ray structure

Now inhibitor (1) unit (inhibitor1.mol2) is loaded:

```
620 = loadmol2 inhibitor1.mol2
loadamberparams inhibitor1.frcmod
```

The library file for inhibitor (1) was created, as well as the *prmtop* and *inpcrd*

files using the command lines:

```
saveoff 620 inhibitor1.lib  
saveamberparm 620 inhibitor1.prmtop inhibitor1.inpcrd
```

Inhibitor (1) can be seen (Fig 7 (a)) using edit command:

```
edit 620
```

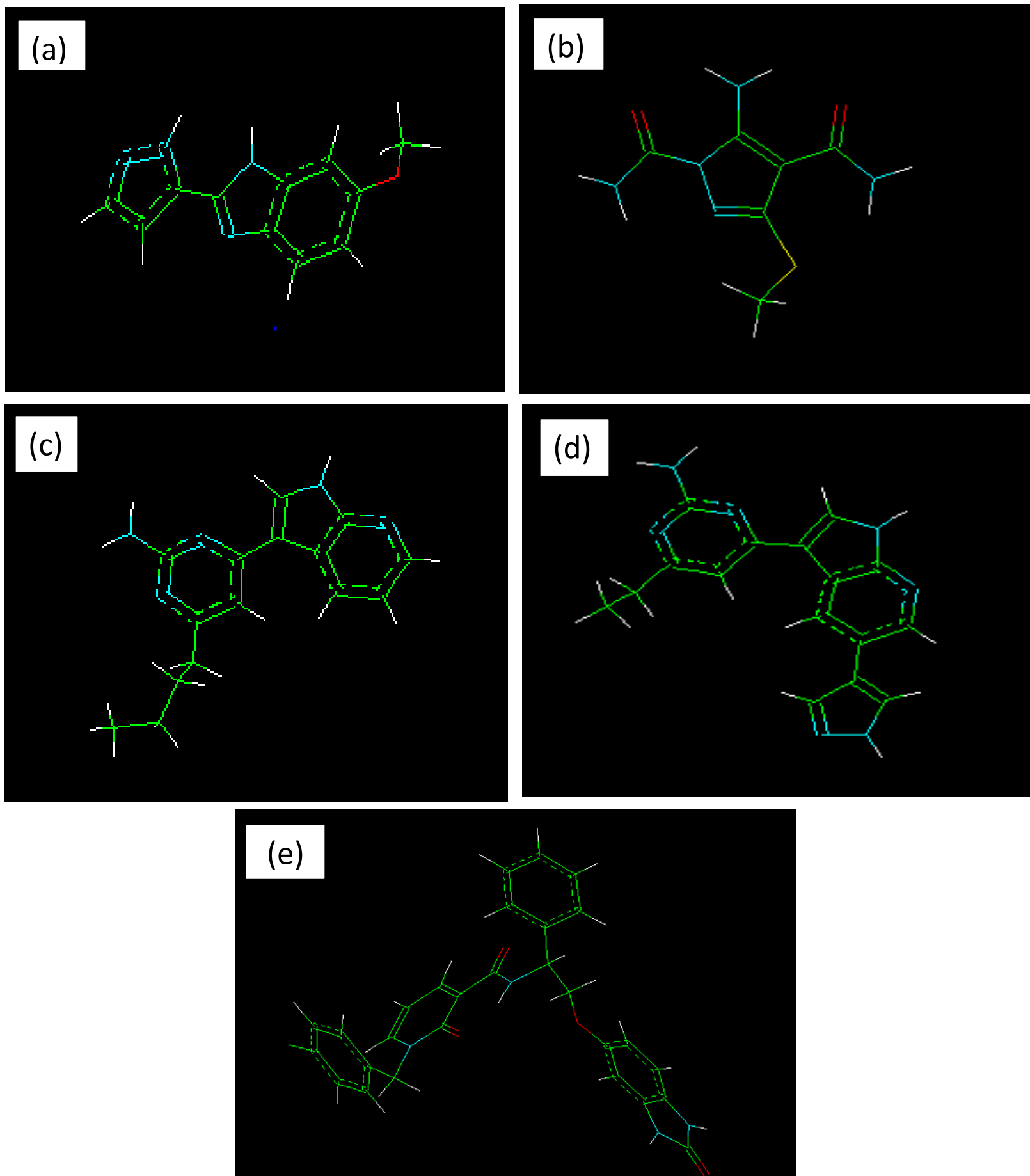



Figure 7: XLeap window showing the graphical representation of (a) inhibitor (1), (b) inhibitor (2), (c) inhibitor (3), (d) inhibitor (4), and (e) inhibitor (5), respectively

Now *xLeap* was ready to load the protein_inhibitor1.pdb file without having any problems. protein_inhibitor (1).pdb file was loaded into xleap after setting it as a new unit called “com” by writing the following commands:

```
Xleap -f $AMBERHOME/dat/leap/cmd/leaprc.ff99SB
Source leaprc.gaff
Loadoff SEP_leap.lib
Loadamberparams SEP_leap.frcmod
620 = loadmol2 620.mol2
Loadamberparams 620.frcmod
Com = loadpdb protein_inhibitor1_dry.pdb
Edit com
```

The *xLeap* window shows the graphical representation of protein_inhibitor1_dry.pdb (Figure 8).

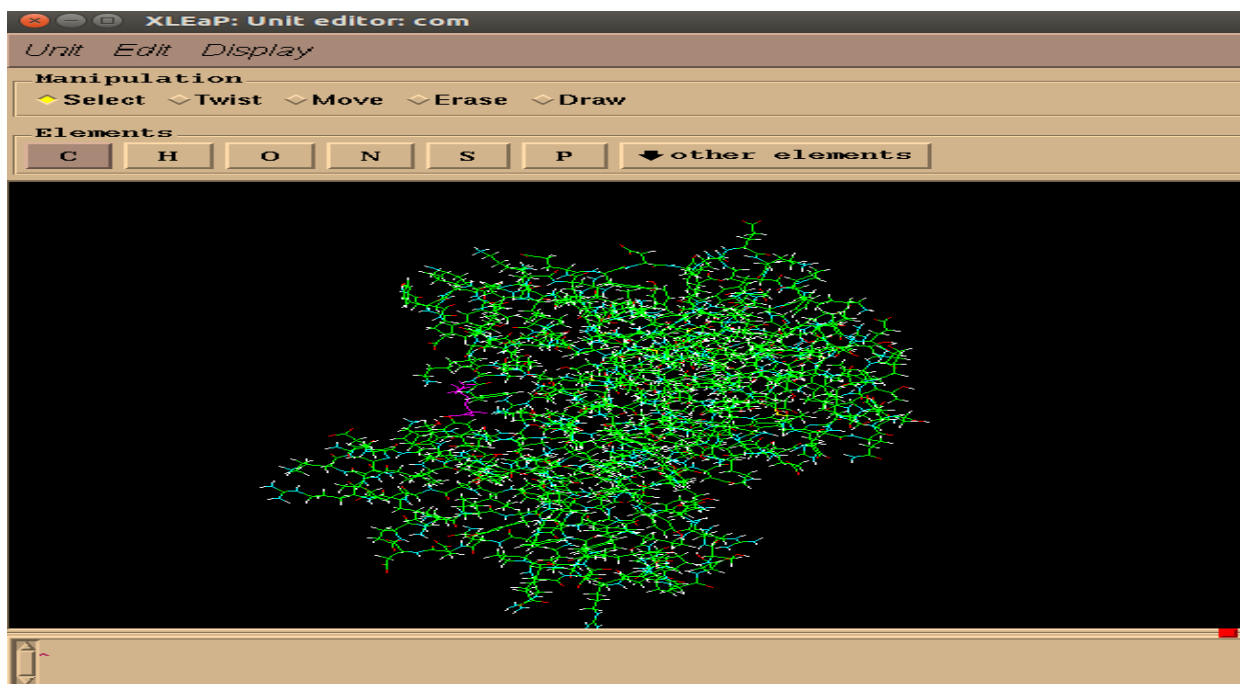


Figure 8: *Xleap* window showing the graphical representation of protein_inhibitor1_dry.pdb

```

set default PBRadii mbondi2
saveamberparm com protein_inhibitor1_dry.prmtop
protein_inhibitor1_dry.inpcrd
saveamberparm 620 inhibitor1.prmtop inhibitor1.inpcrd

```

$\Delta G^0_{\text{nonpolar}}$ was calculated using the default parameters $\gamma = 0.00500 \text{ kcal/ \AA}^2$ and $\beta = 0.0000 \text{ kcal/mol}$ this was achieved using the mbondi2 radius, because this method is effective in the calculation of non-polar solvation energy. The system was neutralized by adding counter ions:

```
charge com
```

Thus, two Cl⁻ atoms were added to neutralize the protein_inhibitor1 complex.

This task was done using the following order:

```
addions com Cl- 0
```

This command line causes a columbic potential on a grid of 1Å resolution and then puts the counter ions simultaneously at the points of lowest/greatest electrostatic potential (Figure 9).

```

XLEaP: Universe Editor
File Edit Verbosity
^ From VanBeek et al. Biophys J. (2007) 92, 4168-4178
> loadoff SEP.lib
Loading library: ./SEP.lib
> com = loadpdb 5hng.pdb
Loading PDB file: ./5hng.pdb
One sided connection. Residue: default_name missing connect0 atom.
One sided connection. Residue: default_name missing connect1 atom.
total atoms in file: 2314
Leap added 2335 missing atoms according to residue templates:
  2335 H / lone pairs
> charge com
Total unperturbed charge:  2.000000
Total perturbed charge:   2.000000
> addions com Cl- 0
2 Cl- ions required to neutralize.
Adding 2 counter ions to "com" using 1A grid
Grid extends from solute vdw + 2.47 to 8.57
Resolution: 1.00 Angstrom.
grid build: 0 sec
(no solvent present)
Calculating grid charges
charges: 14 sec
Placed Cl- in com at (51.08, 42.64, -5.67).
Placed Cl- in com at (32.08, 48.64, 3.33).
Done adding ions.
> ^

```

Figure 9: XLeap editor shows neutralization of the protein_inhibitor1_dry.pdb complex by addition of chlorine ions

Finally, the system was solvated using the following command to add a periodic rectangular box of TIP3P within a distance from the surface of the box to the closest atom of the solute was set to 10 Å in x, y, and z directions (Figure 2.10).⁷⁵

```
solvatebox com TIP3PBOX 10.0
```

The *prmtop* and *inpcrd* files for the solvated system were saved using the

Following commands:

```
saveamberparm com protein_inhibitor1_wat.prmtop
protein_inhibitor1_wat.inpcrd
```

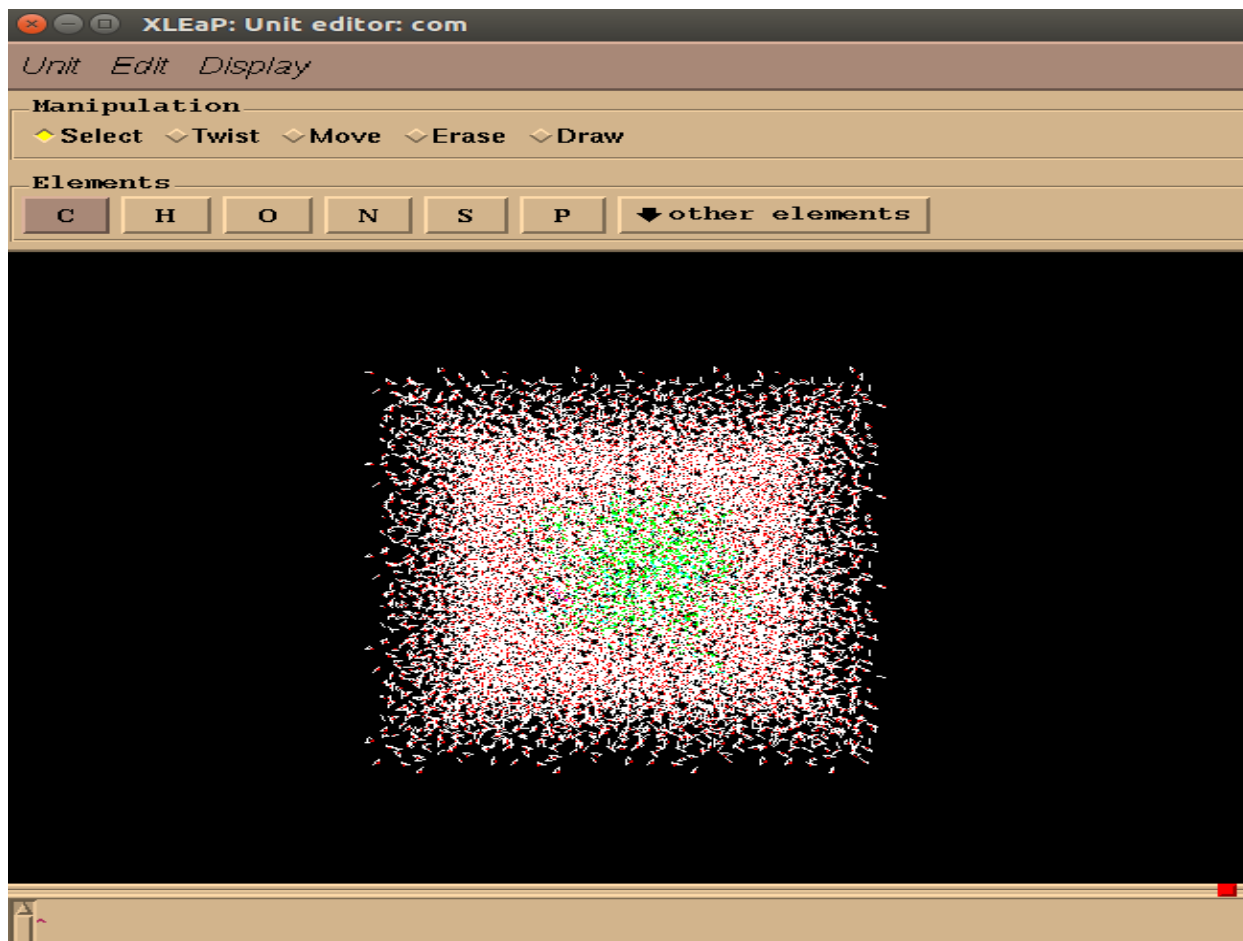


Figure 10: *Xleap* window showing the graphical representation of `protein_inhibitor1_wat.pdb`